THE WATER INSTITUTE

ERDC RESEARCH ACTIVITIES IN SUPPORT OF THE ENGINEERING WITH NATURE® INITIATIVE

Quantifying Climate Change Mitigation Potential of Nature-based Carbon Sequestration and Storage in U.S. Department of Defense (DoD) Lands

SHAWN DOYLE, HOONSHIN JUNG, TOM SEVICK, ABBY LITTMAN, AND TIM CARRUTHERS

Prepared for and funded by the U.S. Army Engineer Research and Development Center in support of the Engineering With Nature® Initiative

May 2024

ABOUT THE WATER INSTITUTE

The Water Institute is an independent, non-profit, applied research institution advancing science and developing integrated methods to solve complex environmental and societal challenges. We believe in and strive for more resilient and equitable communities, sustainable environments, and thriving economies. For more information, visit www.thewaterinstitute.org.

DISCLAIMER

Any opinions, findings and conclusions or recommendations expressed in this material are those of the authors and do not necessarily reflect the views of the U.S. Army Engineer Research and Development Center.

SUGGESTED CITATION

Doyle, S., H. Jung, T. Sevick, A. Littman, and T. Carruthers (2024). Quantifying Climate Change Mitigation Potential of Nature-based Carbon Sequestration and Storage in U.S. Department of Defense (DoD) Lands. The Water Institute. Prepared for and funded by the U.S. Army Engineer Research and Development Center in support of the Engineering With Nature® Initiative. Baton Rouge, LA.

PREFACE

This report was developed by The Water Institute (the Institute) for the U.S. Army Corps of Engineers (USACE) Engineer Research and Development Center's (ERDC) Engineering With Nature® (EWN) Initiative.

The EWN Initiative works toward better integration and alignment of traditional infrastructure approaches with nature-based solutions (NBS). This document is produced as part of a collaborative effort between the Institute and ERDC to develop an analytical framework to quantify the climate change mitigation potential of nature-based carbon capture and storage of U.S. Department of Defense lands.

Questions about this research should be directed to the project lead and Director of Coastal Ecology Research at the Institute, Tim Carruthers (tcarruthers@thewaterinstitute.org).

ACKNOWLEDGEMENTS

This project was funded by the U.S. Army Corps of Engineers Engineering With Nature Initiative. This report was reviewed by Alyssa Dausman and reviewed, edited, and formatted by Charley Cameron of the Institute. Dexter Ellis developed and improved figures throughout the document. The authors are grateful to Jean Cowan, Senior Project Manager at the Institute, for supporting the final stages of report development and overseeing report review and revisions. Partners outside of the Institute include Ben Kocar (US Army Engineer Research and Development Center), who provided essential support and input throughout the project.

This material is based upon work supported by the USACE Engineering With Nature® Program under contract number W912HZ22C0026.

TABLE OF CONTENTS

LIST OF FIGURES

LIST OF TABLES

LIST OF ACRONYMS

Acronym	Term
AFB	Air Force Base
AGB	Aboveground biomass
ANPP	Aboveground net primary productivity
CPRA	Coastal Protection and Restoration Authority
DoD	U.S. Department of Defense
ERDC	Engineer Research and Development Center
GHG	Greenhouse gas
IPCC	Intergovernmental Panel on Climate Change
LCMAP	Land Cover Monitoring Assessment and Projection
NECB	Net ecosystem carbon balance
NEE	Net ecosystem exchange
NFCMS	National Forest Carbon Monitoring System
NLCD	National Land Cover Database
NOAA	National Oceanic and Atmospheric Administration
SA	Soil carbon accumulation rate
USACE	U.S. Army Corps of Engineers
USGS	U.S. Geological Survey

UNIT TABLE

Abbreviation	Term
CO_2e	carbon dioxide equivalent
ha	hectare
MMT	million metric tons
Mg	megagram
t	metric ton
yr	year

INTRODUCTION

The U.S. Department of Defense (DoD) is the largest institutional producer of greenhouse gases (GHG) in the world (Crawford, 2019). In response to Executive Order 14008 (Administration of Joseph R. Biden, Jr., 2021), DoD is tackling the climate change crisis with climate change adaptation and climate change mitigation by reducing GHG emissions. The DoD operates on more than 25 million acres of land and water and nearly 5,000 sites in different regions, climates, and landscapes in the U.S., U.S. territories, affiliated states, and around the world. Encompassing large areas of diverse landscapes across the globe, DoD installations represent not just strategic assets but also significant ecological resources. Optimizing land management on these installations presents an opportunity to achieve multiple objectives: enhancing natural carbon sequestration, bolstering installation resilience and readiness, and supporting biodiversity conservation.

The U.S. Army Corps of Engineers, Engineer Research and Development Center (USACE ERDC; Larson et al., 2017) has highlighted the potential for DoD lands to sequester carbon that could contribute to achieving “carbon neutral” status for DoD facilities and installations. They also state that “while a significant body of literature and products (including predictive models) exist for carbon accounting, due to the highly variable and unique nature of DoD lands and land uses, the applicability of these models for DoD lands is currently unknown.”

The National Oceanic and Atmospheric Administration (NOAA) and Restore America’s Estuaries (Restore America’s Estuaries, 2016) also identified DoD land as ideal for quantifying climate benefits of carbon sequestration and storage, and have recommended the development of “a database of blue carbon storage, sequestration and emission factors that can support landscape-level carbon accounting on coastal lands.” There is presently no estimate of the climate mitigation potential across DoD lands and installations.

An efficient and accurate approach is thus needed to quantify the natural carbon capture and storage potential of DoD lands. This information will guide DoD efforts towards installation climate change mitigation, resilience, and mission readiness. Meeting these objectives will enable DoD lands to be used as a model for quantifying natural carbon capture and storage potential more broadly in federal lands. Once quantified, the potential for transfer into monetary and/or non-monetary benefits, including credit in governmental agency projects as potential mitigation banks can be investigated. These objectives will also enable natural carbon capture and storage potential to support holistic, sustainable, and resilient management (including conservation and restoration) of DoD lands to inform adaptation actions of water resources and environmental challenges including flood-risk management.

The analytical framework described in this report (Figure 1) was designed to quantify landscape-scale carbon fluxes within DoD installations and help inform evidence-based strategies to maximize carbon storage across a variety of ecosystems. To develop the approach and assess transferability across diverse landscapes, the installations were used as case studies; Fort Moore, Scott Air Force Base, and Tyndall Air Force Base (Figure 1). This included the development of a database of carbon fluxes of various habitats (Appendix A and Appendix B) and evaluation of GIS datasets to assess the total area of various habitats

(Appendix C). Together, the information provided by this framework and associated databases can help empower DoD land managers to make informed decisions that balance environmental and operational objectives.

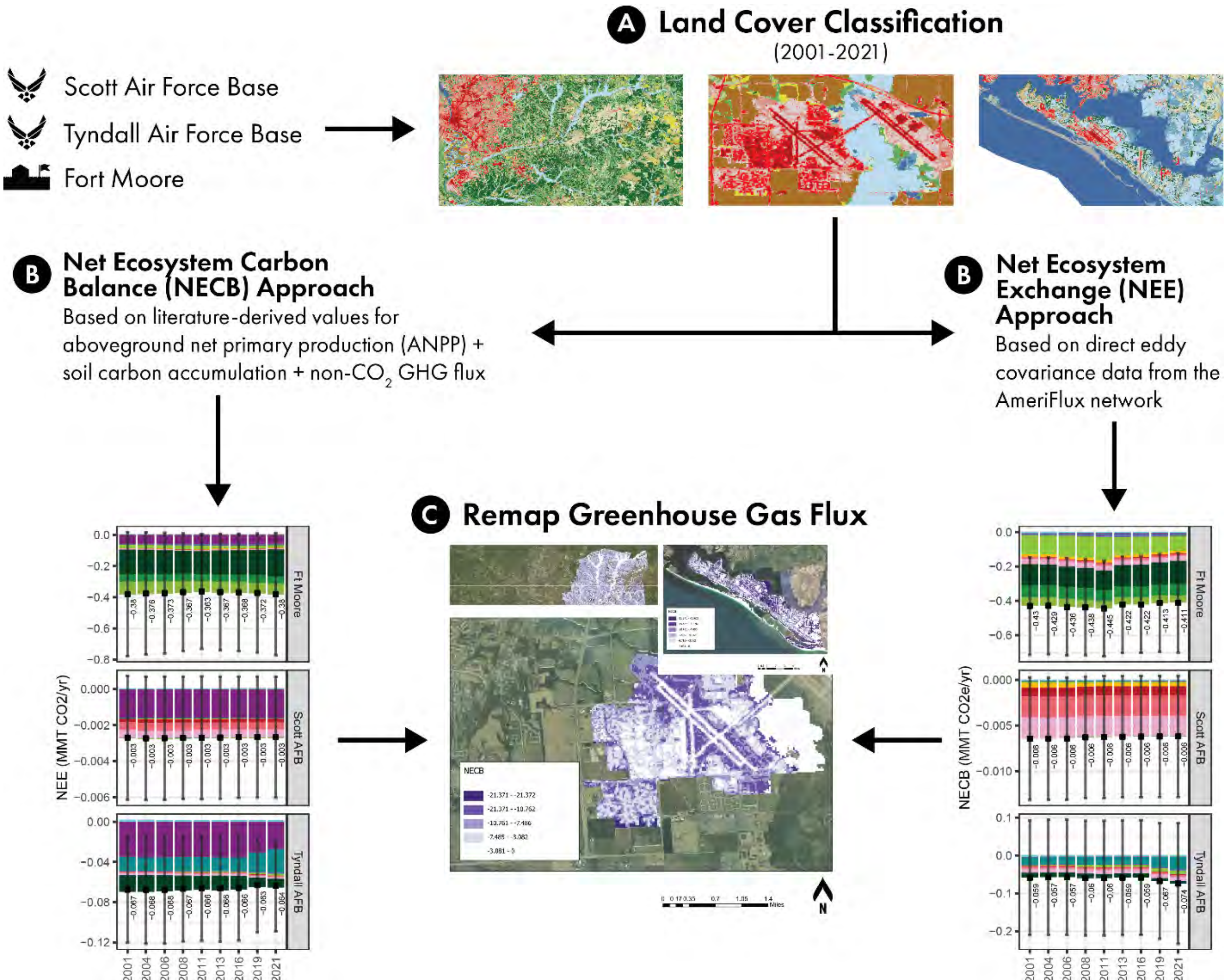

Figure 1. Overview of analysis framework

METHODS

SITE DESCRIPTIONS

Three DoD bases were selected to pilot the analytical framework: Fort Moore (Figure 2A), Scott Air Force Base (AFB; Figure 2B), and Tyndall AFB (Figure 2C). Scott AFB is in St. Clair County, Illinois approximately 17 miles east-southeast of downtown St. Louis. Tyndall AFB is located on the Gulf of Mexico coast in Bay County, Florida, 12 miles east of Panama City. Fort Moore is located near Columbus, Georgia, adjacent to the Alabama-Georgia border.

Figure 2. DoD sites used for this study. (A) Fort Moore, Georgia; (B) Scott AFB, Illinois; (C) Tyndall AFB, Florida.

LAND COVER ANALYSIS

For each DoD site, base boundaries were defined using geospatial polygons compiled by the Defense Installation Spatial Data Infrastructure Program. Land cover classifications across each base were imported from the U.S. Geological Survey (USGS) National Land Cover Database (NLCD), which provides nationwide data on land cover and land cover change at a resolution of 30 m (Table 1). The NLCD classifies land into 21 cover types, including forests, shrublands, grasslands, wetlands, and developed areas (Figure 3; Table 2).

Table 1. Datasets for finding area of land cover classes for DoD sites.

Dataset Name	Dataset Description	Location
DoD Sites Boundaries	Feature Layer (polygons)	Real Property (osd.mil)
NLCD Land Cover (CONUS [Conterminous U.S.]) All Years	Single band raster images	https://www.mrlc.gov/data/nlcd-land-cover-conus-all-years

Rasterized land cover data from the NLCD was clipped to DoD site boundaries and subsequently transformed to simplified polygon vector data layers in ArcGIS Pro (Environmental Systems Research Institute). The coordinate system was set to *USA_Contiguous_Albers_Equal_Area_Conic_USGS_version*, and the desired sites were extracted using the *Export Features* function. The area (ha) of each land cover class was then aggregated across each DoD site and summed.

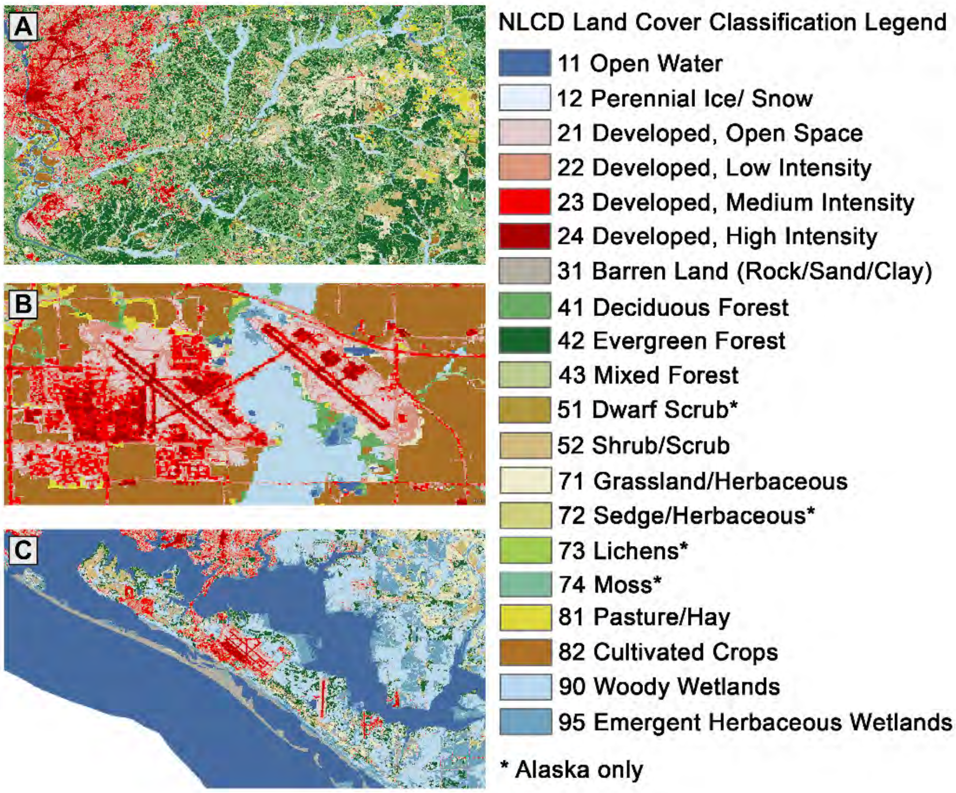

Figure 3. Example of NLCD classifications from 2019. (A) Fort Moore; (B) Scott AFB; (C) Tyndall AFB. Land cover classifications are described in Table 2.

Table 2. NLCD land cover class definitions (from: https://www.mrlc.gov/data/legends/national-land-cover-database-class-legend-and-description).

Habitat	Classification Description
Open Water	Areas of open water, generally with less than 25% cover of vegetation or soil.
Perennial Ice/Snow	Areas characterized by a perennial cover of ice and/or snow, generally greater than 25% of total cover.
Developed, Open Space	Areas with a mixture of some constructed materials, but mostly vegetation in the form of lawn grasses. Impervious surfaces account for less than 20% of total cover. These areas most commonly include large-lot single-family housing units, parks, golf courses, and vegetation planted in developed settings for recreation, erosion control, or aesthetic purposes.
Developed, Low Intensity	Areas with a mixture of constructed materials and vegetation. Impervious surfaces account for 20% to 49% percent of total cover. These areas most commonly include single-family housing units.
Developed, Medium Intensity	Areas with a mixture of constructed materials and vegetation. Impervious surfaces account for 50% to 79% of the total cover. These areas most commonly include single-family housing units.
Developed, High Intensity	Highly developed areas where people reside or work in high numbers. Examples include apartment complexes, row houses and commercial/industrial. Impervious surfaces account for 80% to 100% of the total cover.

Habitat	Classification Description
Barren Land	Areas of bedrock, desert pavement, scarps, talus, slides, volcanic material, glacial debris, sand dunes, strip mines, gravel pits and other accumulations of earthen material. Generally, vegetation accounts for less than 15% of total cover.
Deciduous Forest	Areas dominated by trees generally greater than 5 meters tall, and greater than 20% of total vegetation cover. More than 75% of the tree species shed foliage simultaneously in response to seasonal change.
Evergreen Forest	Areas dominated by trees generally greater than 5 meters tall, and greater than 20% of total vegetation cover. More than 75% of the tree species maintain their leaves all year. Canopy is never without green foliage.
Mixed Forest	Areas dominated by trees generally greater than 5 meters tall, and greater than 20% of total vegetation cover. Neither deciduous nor evergreen species are greater than 75% of total tree cover.
Shrub/Scrub	Areas dominated by shrubs; less than 5 meters tall with shrub canopy typically greater than 20% of total vegetation. This class includes true shrubs, young trees in an early successional stage or trees stunted from environmental conditions.
Herbaceous/Grassland	Areas dominated by graminoid or herbaceous vegetation, generally greater than 80% of total vegetation. These areas are not subject to intensive management such as tilling but can be utilized for grazing.
Hay/Pasture	Areas of grasses, legumes, or grass-legume mixtures planted for livestock grazing or the production of seed or hay crops, typically on a perennial cycle. Pasture/hay vegetation accounts for greater than 20% of total vegetation.
Cultivated Crops	Areas used to produce annual crops, such as corn, soybeans, vegetables, tobacco, cotton, and perennial woody crops such as orchards and vineyards. Crop vegetation accounts for greater than 20% of total vegetation. This class also includes all land being actively tilled.
Woody Wetlands	Areas where forest or shrubland vegetation accounts for greater than 20% of vegetative cover and the soil or substrate is periodically saturated with or covered with water.
Emergent Herbaceous Wetlands	Areas where perennial herbaceous vegetation accounts for greater than 80% of vegetative cover and the soil or substrate is periodically saturated with or covered with water

NET ECOSYSTEM CARBON BALANCE (NECB)

Calculations

NECB represents the overall ecosystem carbon flux balance from all sources and sinks, including physical, biological, geological, and anthropogenic processes (Chapin et al., 2006). By definition, a positive NECB represents a net carbon flux to the atmosphere (i.e., a carbon source) while a negative NECB represents a net carbon flux into the soil and flora (i.e., a carbon sink). The NECB of each base (in t CO_2e yr^{-1}) was calculated using a modified method (Eq. 1 and Eq. 2) described by Baustian et al. (2023):

$$\mathrm{NECB}_i = (\mathrm{ANPP}_i + \mathrm{SA}_i + \mathrm{GHG}_i) \times \mathrm{area}_i \quad (1)$$

$$\mathrm{NECB}_{\mathrm{base}} = \sum_{i=1}^{16} \mathrm{NECB}_i \quad (2)$$

Where $\boldsymbol{i}$ represents the 16 possible NLCD habitat classification types (Table 2) and ANPP, SA, GHG, and area are as follows:

- **Aboveground Net Primary Productivity ($ANPP_i$):** The average live aboveground plant biomass produced within one year (t CO_2e ha^{-1} yr^{-1}) in habitat $\boldsymbol{i}$. Equivalent to the total amount of carbon fixed through photosynthesis after accounting for carbon released by plants via autotrophic respiration.
- **Soil Carbon Accumulation Rate (SA_i):** The average net amount of carbon (t CO_2e ha^{-1} yr^{-1}) which accumulates in soils and sediments each year in habitat $\boldsymbol{i}$. Equivalent to the amount of carbon that is fixed by plant roots and stored in soils each year while also accounting for the accumulation of dead belowground biomass, aboveground litter, and captured allochthonous carbon (Troxler et al., 2013).
- **Greenhouse Gas Fluxes (GHG_i):** The average annual flux of the non-CO_2 greenhouse gases CH_4 and N_2O (t CO_2e ha^{-1} yr^{-1}) in habitat $\boldsymbol{i}$. CO_2 is excluded because CO_2 balance is already accounted for in ANPP and soil accumulation rates.
- **$area_i$:** The total area (ha) of habitat $\boldsymbol{i}$ on the base

NECB uncertainty was calculated using Eq. 3 and Eq. 4 by combining the uncertainties of ANPP, SA, and GHG following the Intergovernmental Panel on Climate Change (IPCC) good practice guidance for uncertainty management in greenhouse gas inventories (Penman et al., 2000).

$$\mathrm{U}_i = \frac{\sqrt{\left(\sigma_{\mathrm{ANPP}_i}{}^2 + \sigma_{\mathrm{SA}_i}{}^2 + \sigma_{\mathrm{GHG}_i}{}^2\right) \times \mathrm{area}_i{}^2}}{\left(\left|\mu_{\mathrm{ANPP}_i}\right| + \left|\mu_{\mathrm{SA}_i}\right| + \left|\mu_{\mathrm{GHG}_i}\right|\right) \times \mathrm{area}_i} \tag{3}$$

$$\text{Uncertainty Base NECB } (\%) = \sqrt{\textstyle\sum_{i=1}^{16} \mathrm{U}_i^2} * 100 \tag{4}$$

Where $\mathbf{U}_i$ is the relative NECB uncertainty for each habitat $\boldsymbol{i}$, and $\boldsymbol{\sigma}$ and $\boldsymbol{\mu}$ are the sample standard deviation and mean, respectively, of the literature-derived values for ANPP, SA, and GHG.

Estimation of ANPP, SA, and GHG

ANPP rates, SA rates, and GHG fluxes were assumed to be spatially uniform within each habitat type and were estimated for each habitat type (Table 3) using a comprehensive literature review (Appendix A).

Table 3. ANPP rates, SA rates, non-CO_2 GHG fluxes (mean ± sd) for each of the 16 NLCD habitat types. All values are t CO_2e ha^{-1} yr^{-1}.

Habitat	ANPP	SA	GHG
Open Water	-3.67 ± 3.30	-7.28 ± 4.88	0.19 ± 0.21
Perennial Ice/Snow	0.00 ± 0.00	0.00 ± 0.00	0.24 ± 0.11
Developed, Open Space	-10.3 ± 9.29	-1.42 ± 1.28	0.00 ± 0.00
Developed, Low Intensity	-6.58 ± 5.92	-0.91 ± 0.82	0.00 ± 0.00
Developed, Medium Intensity	-2.71 ± 2.44	-0.37 ± 0.34	0.00 ± 0.00
Developed, High Intensity	0.00 ± 0.00	0.00 ± 0.00	0.00 ± 0.00
Barren Land	0.00 ± 0.00	0.00 ± 0.00	0.00 ± 0.00
Deciduous Forest	-2.90 ± 1.46	-1.06 ± 1.91	0.12 ± 0.27
Evergreen Forest	-4.81 ± 3.73	-0.79 ± 2.35	0.12 ± 0.27
Mixed Forest	-3.86 ± 2.83	-0.97 ± 2.17	0.12 ± 0.27
Shrub/Scrub	-3.26 ± 0.70	-0.45 ± 0.36	-0.03 ± 0.05
Herbaceous/Grassland	-12.9 ± 4.36	-1.78 ± 1.13	-0.01 ± 0.01
Hay/Pasture	-18.56 ± 6.89	-2.84 ± 1.27	0.03 ± 0.00
Cultivated Crops	0.00 ± 0.00	-1.44 ± 1.04	0.07 ± 0.00
Woody Wetlands	-16.1 ± 7.28	-8.85 ± 3.94	24.58 ± 24.07
Emergent Herbaceous Wetlands	-33.84 ± 19.34	-7.19 ± 4.22	25.4 ± 34.04

Reliable data for SA rates in developed areas (e.g., single-family housing units, parks, golf courses, commercial properties, etc.) were not available and were thus estimated by assuming developed areas consisted of various mixes of lawn grass and impervious surfaces. As such, developed areas were modeled as various proportions of undeveloped grasslands. SA rates in open, low, and medium developed habitats were estimated at 80%, 51%, and 21% of the corresponding grassland habitat rate, respectively while rates in highly developed habitats were assumed to be zero.

As described in the 2019 refinement to the *2006 IPCC Guidelines for National Greenhouse Gas Inventories* (Eggleston et al., 2006), accurate estimates emissions of non-CO_2 GHG fluxes (N_2O and CH_4) in developed areas are a known knowledge gap. Hence, GHG fluxes in developed areas were set to zero for this study.

ANPP Estimation for Forest Habitats

Among the three bases, forests were a predominant habitat: forests and woody habitats constituted over 74% and 48% of the total land area at Fort Moore and Tyndall AFB, respectively, while at Scott AFB, forested habitats rank as the most extensive habitat (15.1%) after developed areas. Hence, in addition to the literature review, carbon stock/flux data from the Global Forest Watch (Global Forest Watch, 2002) and National Forest Carbon Monitoring System (NFCMS) databases (Williams et al., 2021; Table 4) were used to supplement estimates of forest ANPP rates at the three study sites (Appendix B).

Table 4. List of carbon stocks and fluxes for forest habitat

Source	Organization	Spatial Resolution	Carbon flux or stock	
World Forest Map	Global Forest Watch	30 m	Fluxes	Forest carbon removal (Mg CO_2/ha), Forest carbon emissions (Mg CO_2/ha), Forest carbon net flux (Mg CO_2/ha)
Forest Carbon Stocks and Fluxes from the NFCMS, Conterminous USA	NASA	30 m	Stock/Fluxes	Aboveground biomass (AGB), total live biomass, total ecosystem carbon, aboveground coarse woody debris (CWD), and net ecosystem productivity (NEP)

NET ECOSYSTEM EXCHANGE (NEE)

Calculations

NEE is a measure of the net exchange of carbon between the atmosphere and ecosystem carbon pools, including above- and below-ground biomass, soil organic matter, and dead organic matter. NEE is calculated as the difference between the carbon uptake by photosynthesis and the carbon loss by respiration and other processes. A positive NEE represents a net carbon flux to the atmosphere (i.e., a carbon source) while a negative NEE represents a net carbon flux into the physical environment (i.e., a carbon sink).

NEE rates across each base (t CO_2e yr^{-1}) were calculated using Eq. 5 and Eq. 6,

$$\mathrm{NEE}_i = \mu_{\mathrm{NEE}_i} \times \mathrm{area}_i \qquad (5)$$

$$\mathrm{NEE}_{\mathrm{base}} = \sum_{i=1}^{16} \mathrm{NEE}_i \qquad (6)$$

Where ***i*** represents the 16 possible NLCD habitat classification types (Table 2) and **μ** is the mean NEE rates (t CO_2e ha^{-1} yr^{-1}) derived from FLUXNET (Pastorello et al., 2020). Following the IPCC method described above for NECB uncertainty (Penman et al. 2000), NEE uncertainty was calculated similarly using Eq. 7 and Eq. 8 by combining NEE uncertainties of all habitats across each base.

$$\mathrm{U}i = \frac{\sigma_{\mathrm{NEE}_i} \times \mathrm{area}_i}{\left|\mu_{\mathrm{NEE}_i}\right| \times \mathrm{area}_i} \qquad (7)$$

$$\text{Uncertainty Base NEE (\%)} = \sqrt{\sum_{i=1}^{16} \mathrm{U}_i^2} * 100 \qquad (8)$$

Where $\mathbf{U}_i$ is the relative uncertainty of NEE for each habitat ***i***, and **σ** is the sample standard deviation of measured NEE rates.

Eddy-Covariance Measurements of NEE

Directly measured NEE rates were downloaded and collated from the AmeriFlux network’s FLUXNET and BASE databases, a comprehensive repository of carbon, water, and energy flux measurements from various ecosystems across the Americas. The databases provide continuous measurements of Net Ecosystem Exchange (NEE), among other variables, which were used to calculate NEE rates for different land cover types. FLUXNET-based NEE rates for each NLCD land cover type were aggregated by averaging the yearly NEE measurements from all sites falling within that land cover type (Table 5). Developed areas were assumed to primarily be various mixtures of lawn grasses and impervious surfaces and thus NEE rates for developed areas were estimated using proportions of the FLUXNET data products for undeveloped grasslands.

Table 5. NEE rates (average ± sd) for each NLCD habitat classification based on AmeriFlux network data. Units for values are t CO_2e ha^{-1} yr^{-1}.

Habitat	NEE	AmeriFlux FLUXNET datasets used
Open water	6.13 ± 0.46	Water Bodies sites
Perennial ice/snow	-3.07 ± 2.4	Snow and Ice sites
Developed, open space	-2.19 ± 8.1	Grassland sites @ 80%
Developed, low intensity	-1.39 ± 6.54	Grassland sites @ 51%
Developed, medium intensity	-0.57 ± 3.82	Grassland sites @ 21%
Developed, high intensity	0.00 ± 0.00	Assumed to be negligible
Barren land	-0.01 ± 0.09	BASE sites: US-A03 and US-A10
Deciduous forest	-6.15 ± 15.36	Deciduous Needleleaf and Deciduous Broadleaf sites
Evergreen forest	-7.03 ± 11.09	Evergreen Needleleaf Forest sites
Mixed forest	-3.4 ± 15.19	Mixed Forest sites
Shrub/scrub	-1.59 ± 3.75	Open Shrubland sites
Grassland/herbaceous	-2.73 ± 10.12	Grassland sites
Hay/Pasture	0.16 ± 12.81	Pasture sites: US-Snf, US-xAE, US-xSR, US-xCL, US-xNQ, and US-Jo1
Cultivated crops	-6.48 ± 18.18	Cropland sites
Woody wetlands	-9.34 ± 12.46	Forested wetland sites: US-Orv and US-NC4.
Herbaceous wetlands	-11.15 ± 12.58	Herbaceous wetland sites: US-EDN, US-HB1, US-KS3, US-Myb, US-OWC, US-Sne, US-Tw1, US-Tw5, and US-xDS

RESULTS

Two different approaches were used to quantify carbon fluxes by habitat across Fort Moore, Scott AFB, and Tyndall AFB. The first method calculated carbon flux as a NECB and used a comprehensive literature review to estimate the habitat-scale net carbon flux from aboveground net primary production, soil carbon accumulation, and non-CO_2 GHG emissions. The second method calculated carbon flux as a NEE rate, and instead relied on direct measurements of CO_2 exchange from each habitat type using the eddy covariance method. Both approaches utilized habitat land cover classifications from the NLCD.

NLCD land cover classifications for 2001 to 2021 are detailed in Appendix C. There were site-specific differences in the similarity of calculated NECB and NEE at each of the three DoD installations (Figure 4). For Tyndall AFB, both approaches estimated similar overall carbon sequestration rates between -0.06 and -0.07 MMT CO_2e/year, although uncertainty with the NEE approach was approximately three-fold lower on average. In contrast, the NECB and NEE approaches for Fort Moore differed by ~13%, representing a moderate difference of 0.06 MMT CO_2e/year, and average uncertainty with the NECB approach (± 0.28 MMT CO_2e/year) was lower than the NEE approach (± 0.38 MMT CO_2e/year). The largest differences were observed at Scott AFB, where the NECB approach estimated natural carbon sequestration rates and uncertainties approximately two-fold larger than those predicted via NEE. However, this represented a difference of less than 0.01 MMT CO_2e/year in absolute terms due to the relatively small land area at Scott AFB.

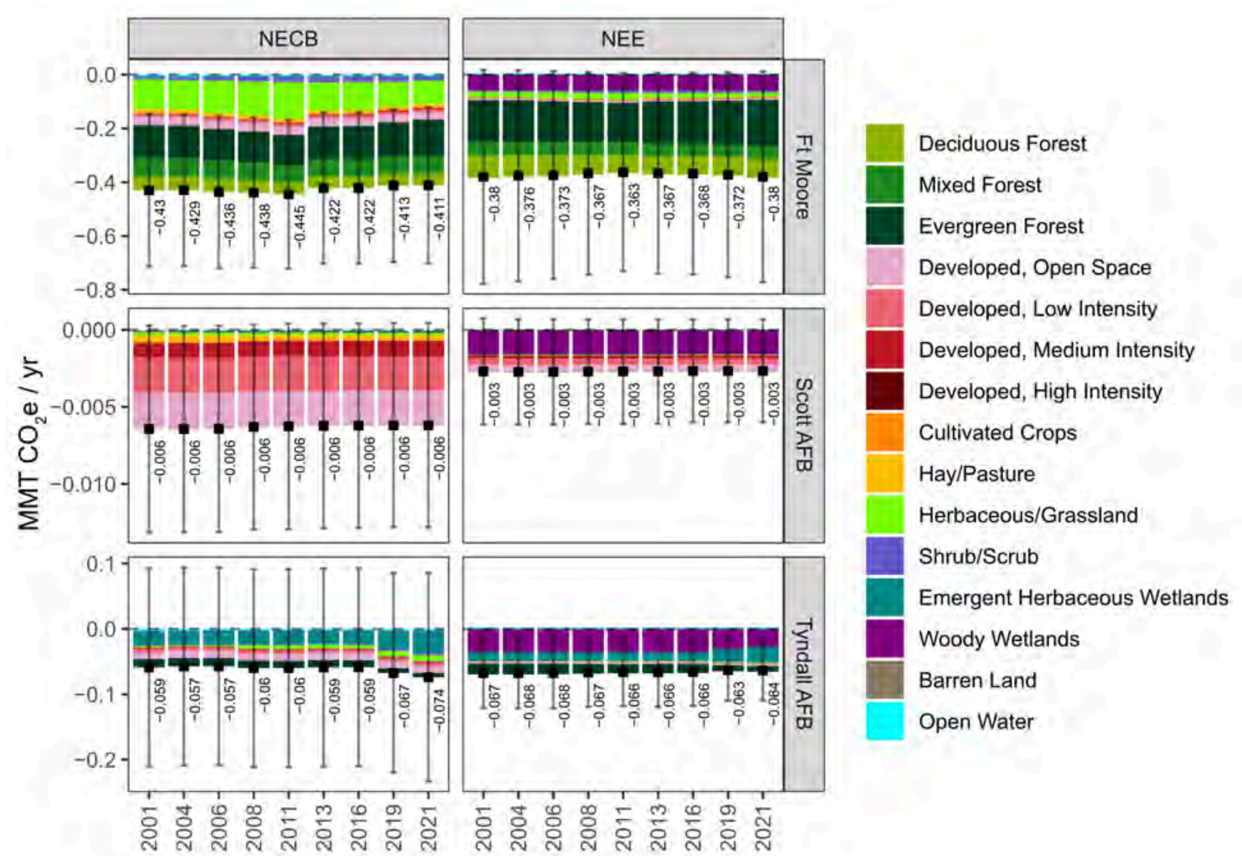

Figure 4. Net ecosystem carbon balance by habitat for Fort Moore, Scott AFB, and Tyndall AFB. Error bars denote the percent uncertainty of NECB summed across all habitats at each base. MMT = million metric tonnes. Negative values indicate net carbon storage while positive values indicate net release to the atmosphere.

All installations were quantified as being a net annual sink for GHG over the twenty-year period of analysis using both the NECB and NEE approach. It is important to note that some habitats within each installation may reach an equilibrium point where annual carbon sequestration becomes saturated and is balanced by decomposition, resulting in no additional storage (Gulde et al., 2008). This equilibrium is ultimately dictated by the decay rate of the most stable carbon pool, which is in turn influenced by various factors including soil texture, mineralogy, nutrient availability, and past and current management practices. Climate also plays a role, with factors like soil temperature and moisture affecting decomposition rates. Equilibrium state is also strongly affected by the extensity, magnitude, and frequency of disturbances like fire (Wardle et al., 2003), drought, nitrogen deposition (Luo & Weng, 2011) or erosion (Polyakov & Lal, 2004), which can partially reset the current equilibrium state for decades or centuries. Furthermore, the total carbon storage potential of a habitat at equilibrium can also change over time as long-term changes in weathering patterns alter the stability of humic compounds. As such, it is challenging to definitively determine whether a site is currently at carbon equilibrium. Indeed, although equilibrium state can be estimated using direct field measurements of soil carbon stocks and decay rates, these field measurements need to be conducted for several decades to infer if a site is near equilibrium because any changes in current carbon stocks or decay rates may only reflect inter-annual variance (Wutzler & Reichstein, 2007) Therefore, while these results show net negative carbon fluxes for each over the study period, further investigation would be needed to determine the multi-decadal stability and total potential of this storage at each site.

FORT MOORE

Fort Moore, the largest DoD site piloted under this framework (~73,500 ha) had a mean installation-wide carbon sequestration rate between -0.43 (NECB) and -0.37 (NEE) MMT CO_2e/year. Using the NECB approach, the highest ANPP and SA rates within Fort Moore were observed in mesic hardwood forests located in lowland areas alongside clearwater creeks, drains, and ponds (Figure 5). However, because these lowland areas are classified as woody wetlands in the NLCD, the NECB approach assumes them to also have elevated GHG rates. These floodplain and seepage forests thus contribute minimally to the overall natural carbon sequestration capacity of Fort Moore under an NECB framework, despite their elevated ANPP and SA rates. In contrast, most of the annual net carbon sequestration across Fort Moore is driven by extensive areas of well-drained pine, pine-hardwood, or grassland dominated uplands.

SCOTT AFB

Scott AFB, due to its small size (~1,200 ha), has the lowest average carbon sequestration rate overall (NECB: -0.006 MMT CO_2e/year, NEE: -0.003 MMT CO_2e/year). Most natural carbon sequestration at Scott AFB is driven by tree growth (i.e., ANPP) and soil carbon accumulation within a riparian forest (woody wetland NLCD classification) located on the eastern boundary of the base (Figure 6). However, this forest is located in a lowland area within the Silver Creek floodplain and is identified as a woody wetland in the NLCD. Thus, the ANPP and SA carbon sinks within this forest were potentially offset by large non-CO_2 GHG emissions during periods of inundation which promote methane production. However, this is based on broad assumptions, and methane production in freshwater, woody wetlands is highly variable and difficult to predict accurately (Rosentreter et al., 2021). These periods of elevated emissions likely fluctuate in magnitude, contributing significantly to uncertainty in carbon flux calculations. For example, in Scott AFB's overall NECB, 52% of the uncertainty stems from carbon flux within this forest, with 89% of that uncertainty specifically linked to methane emissions (Table 7). Given the small spatial extent of Scott AFB and the fact that this ~168 ha forest alone represents over 14% of total base’s land cover, the overall carbon flux from this base may intermittently shift from net negative to net positive during periods of high GHG emissions from this forest.

TYNDALL AFB

Tyndall AFB (~11,800 ha) natural habitats consist primarily of tidal wetlands and coastal longleaf pine forests and had an average base-wide carbon sequestration rate of -0.06 MMT CO_2e/year (NECB) and -0.07 MMT CO_2e/year (NEE). Unlike Scott AFB and Fort Moore, natural carbon sequestration at Tyndall was driven by very high ANPP and SA rates present in emergent herbaceous wetlands (-33.8 and -7.2 t CO_2e ha^{-1} y^{-1}, respectively). While some of the sequestration capacity of these wetlands was offset by non-CO_2 GHG emissions, these wetlands remain overall carbon sinks for Tyndall AFB (Figure 7). In addition, non-CO_2 GHG emissions from these wetlands are likely overestimated as NLCD does not differentiate between fresh, intermediate, brackish, and saline wetlands. Sulfate from seawater inhibits methane production, therefore GHG rates from Tyndall’s herbaceous wetland habitats are expected to be low, given their proximity to the Gulf of Mexico. As a result, NECB rates for Tyndall AFB are likely more negative (stronger sinks) than estimated under this framework.

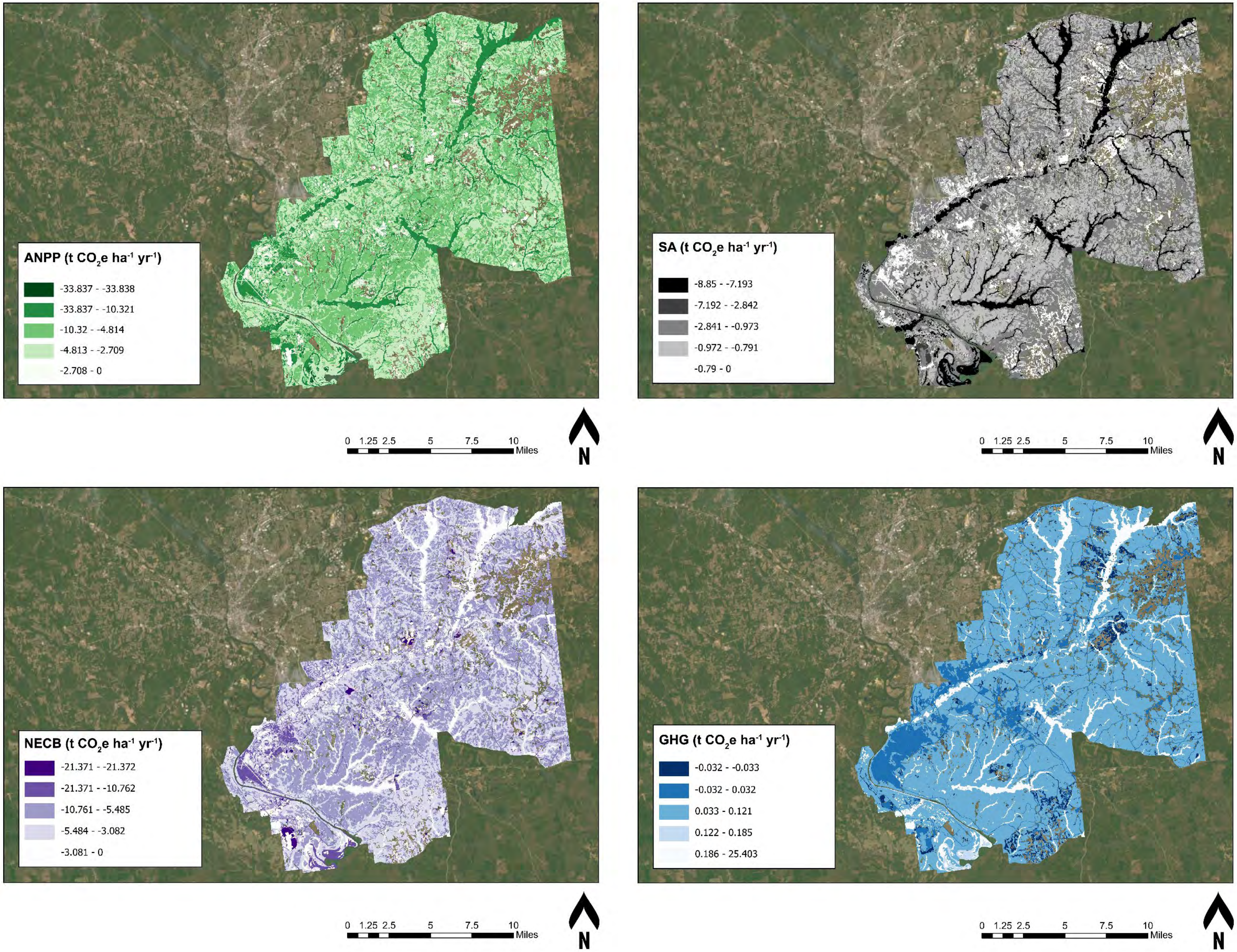

Figure 5. ANPP, SA, GHG, and NECB rates for Fort Moore in 2021.

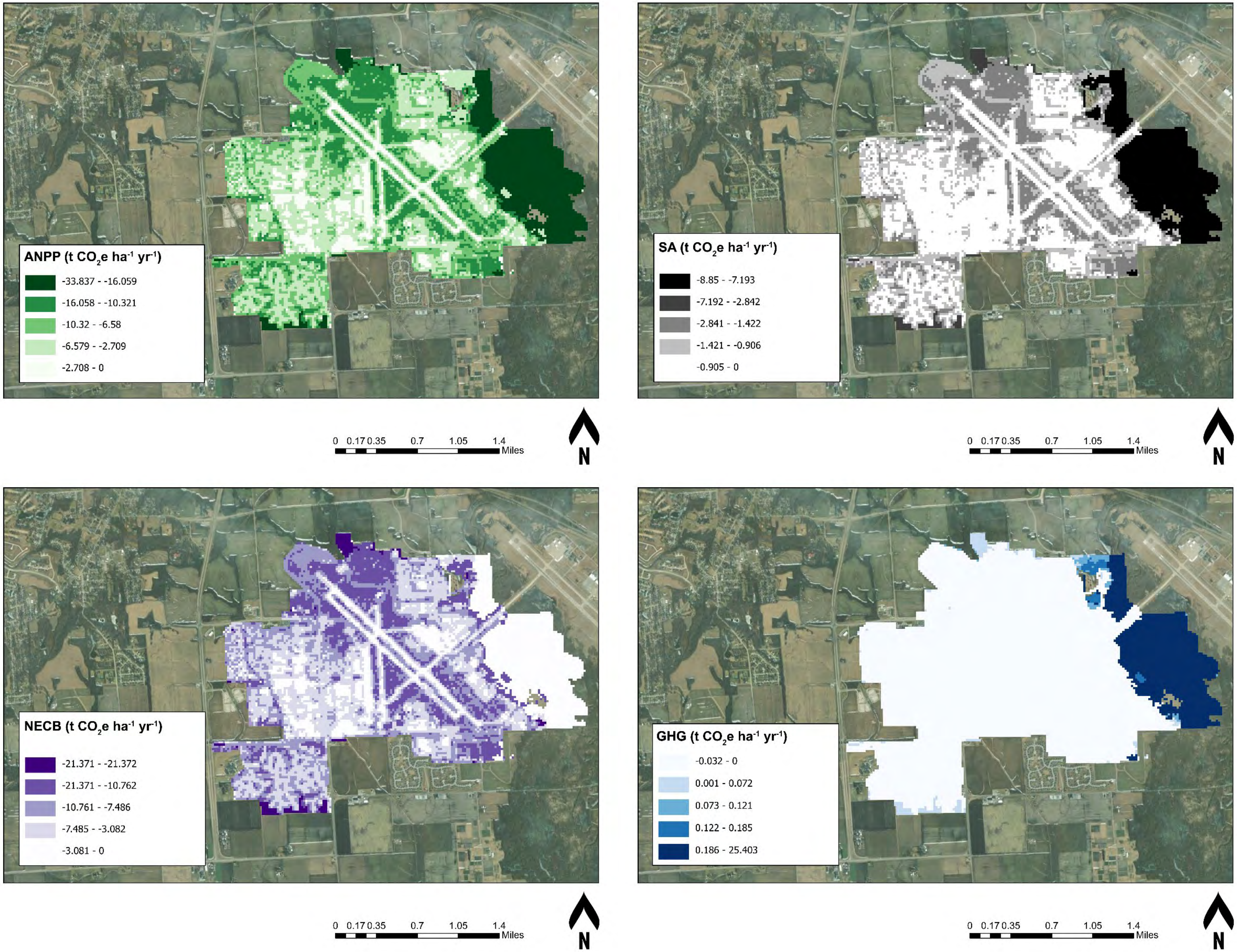

Figure 6. ANPP, SA, GHG, and NECB rates for Scott AFB in 2021.

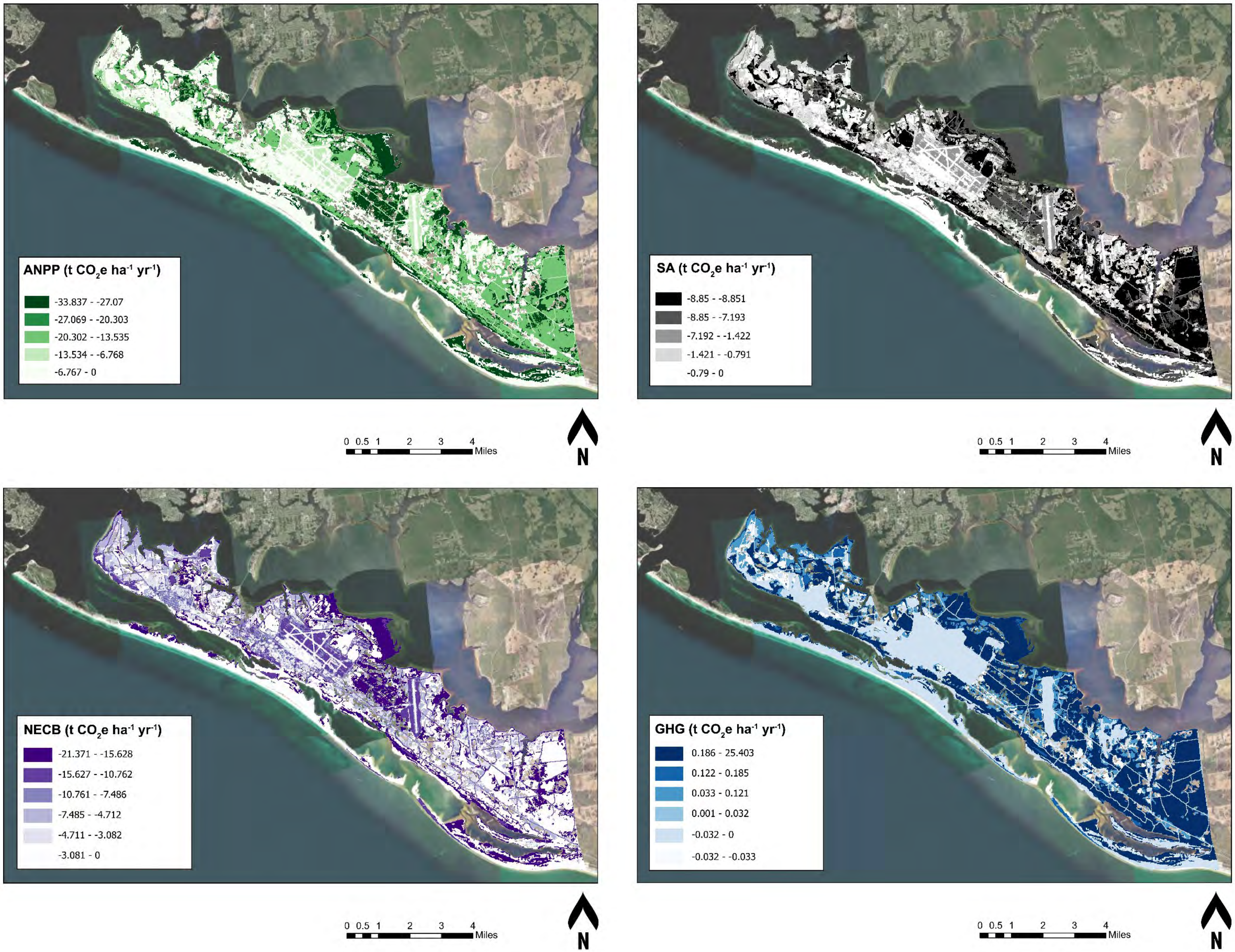

Figure 7. ANPP, SA, GHG, and NECB rates for Tyndall AFB in 2021

Table 6. The proportion of base-wide carbon flux uncertainty from each habitat at Fort Moore.

Habitat	% of base area	Relative NECB uncertainty (%)	Relative NEE uncertainty (%)
Evergreen Forest	30.3	24.0	28.5
Mixed Forest	19.0	12.5	24.5
Deciduous Forest	16.3	7.4	21.3
Herbaceous/Grassland	10.2	7.0	8.8
Woody Wetlands	8.6	37.9	9.1
Shrub/Scrub	4.4	0.6	1.4
Developed, Open Space	3.4	4.5	2.4
Developed, Low Intensity	2.2	1.9	1.2
Developed, Medium Intensity	1.5	0.5	0.5
Hay/Pasture	0.9	0.9	1.0
Open Water	0.8	0.9	0.0
Barren Land	0.8	0.0	0.0
Cultivated Crops	0.6	0.1	1.0
Developed, High Intensity	0.6	0.0	0.0
Emergent Herbaceous Wetlands	0.3	1.9	0.3

Table 7. The proportion of base-wide carbon flux uncertainty from each habitat at Scott AFB.

Habitat	% of base area	Relative NECB uncertainty (%)	Relative NEE uncertainty (%)
Developed, Medium Intensity	27.6	7.9	16.6
Developed, Low Intensity	25.8	17.9	26.5
Developed, Open Space	16.3	17.7	20.7
Woody Wetlands	14.3	52.0	28.1
Developed, High Intensity	11.4	0.0	0.0
Hay/Pasture	1.6	1.4	3.3
Herbaceous/Grassland	0.8	0.4	1.2
Open Water	0.6	0.5	0.0
Deciduous Forest	0.5	0.2	1.3
Emergent Herbaceous Wetlands	0.3	1.9	0.6
Cultivated Crops	0.3	0.0	0.9
Mixed Forest	0.3	0.2	0.7
Shrub/Scrub	0.0	0.0	0.0

Table 8. The proportion of base-wide carbon flux uncertainty from each habitat at Tyndall AFB.

Habitat	% of base area	Relative NECB uncertainty (%)	Relative NEE uncertainty (%)
Woody Wetlands	31.3	53.3	43.4
Evergreen Forest	17.1	5.2	21.0
Emergent Herbaceous Wetlands	11.9	32.8	16.7
Barren Land	11.8	0.0	0.1
Developed, Open Space	8.1	4.1	7.3
Developed, Low Intensity	6.2	2.0	4.5
Developed, Medium Intensity	4.1	0.5	1.7
Shrub/Scrub	3.3	0.2	1.4
Herbaceous/Grassland	3.1	0.8	3.6
Open Water	2.6	1.0	0.1
Developed, High Intensity	1.8	0.0	0.0
Hay/Pasture	0.1	0.0	0.1
Deciduous Forest	0.0	0.0	0.0
Mixed Forest	0.0	0.0	0.0

DISCUSSION

Quantification of the carbon sequestration potential of DoD lands is required for informed climate mitigation strategies. This report explores two approaches to quantify carbon fluxes across the diverse range of habitats found on DoD lands: a literature-based method using NECB and a measurement-based approach using NEE via eddy covariance towers. Outputs from both approaches demonstrate that lands within Fort Moore, Scott AFB, and Tyndall AFB all acted as net carbon sinks over a 20-year period.

Large differences in net carbon flux between the three studied installations were observed. Over the 20-year study period, the mean total flux at Fort Moore was approximately -0.4 MMT CO_2e per year, about 100-fold higher than Scott AFB (-0.004 MMT CO_2e per year) and about 6-fold higher than Tyndall AFB (-0.06 MMT CO_2e per year). These differences largely reflect the difference in land area extent of each base. On a per hectare difference, the calculated carbon fluxes using both approaches were comparable (Figure 8).

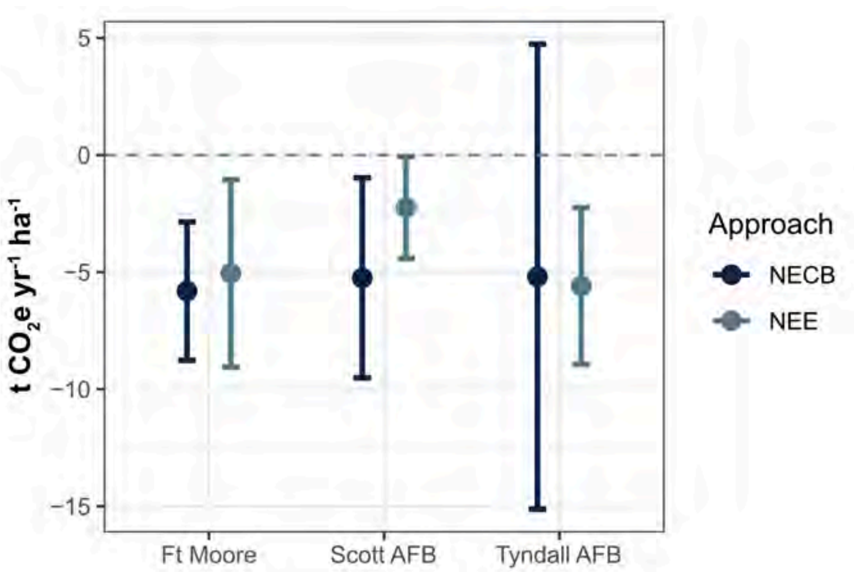

Figure 8. NECB and NEE rates for Fort Moore, Scott AFB, and Tyndall AFB were comparable on a per hectare basis. Error bars denote 95% confidence intervals.

Both the NECB and NEE approaches piloted in this framework offer insights into carbon flux dynamics at each base, though each approach has different strengths and weaknesses (Table 9). The NECB approach leverages existing data, providing a cost-effective means for initial evaluations and installation-wide assessments of carbon dynamics. However, it includes uncertainties and assumptions that arise from aggregating point measurements from these source studies into an average annual rate or flux. For example, measurements in the source studies likely do not reflect conditions for the entire habitat over the course of a year. In contrast, the NEE approach relies on highly accurate, localized carbon flux measurements from the AmeriFlux network of eddy covariance towers. While the precision of eddy covariance measurements is unmatched for the areas surrounding the deployed towers, carbon flux is known to be highly spatially variable and so, at larger spatial scales, these remain proxy estimates that likely differ from specific habitats on each base. Additionally, only a small minority of eddy covariance towers in the AmeriFlux network are equipped to measure methane and thus AmeriFlux NEE measurements are based on CO_2 flux alone. This creates a discrepancy between the two approaches within wetland habitats where CH_4 and N_2O emissions may be high and partially offset CO_2 sinks. For example, this discrepancy in non-CO2 GHG accounting is responsible for a substantial amount of the difference between the NECB and NEE estimates for Scott AFB: the estimated carbon flux for the woody wetland habitats located in the Silver Creek floodplain are much more negative under the NEE approach (Figure 4).

Table 9. Strengths and weaknesses of the two carbon flux quantification approaches detailed in this framework.

Approach	Strengths	Weaknesses
NECB (Net Ecosystem Carbon Balance)	Leverages existing data, making it cost-effective. Suitable for regional assessments and initial evaluations. Decomposes carbon flux into ANPP, SA, and GHG, providing further insight into specific sources and/or sinks on each base.	Inherits uncertainties and potential biases from underlying datasets. Inherent accuracies from scaling up from localized studies. Significant uncertainty in some habitats, especially wetlands. NLCD classifications do not differentiate between wetland types, which differ significantly in overall carbon flux.
NEE (Net Ecosystem Exchange)	Utilizes highly accurate, localized measurements for each habitat type. Data available at multiple timescales (hourly, daily, weekly, etc.), enabling increased temporal resolution (e.g., seasonal).	Based only on CO_2 flux; estimates likely underestimated in habitats with high non-CO_2 GHG emissions (e.g., CH_4 emissions in wetlands). High uncertainty around habitat types that are poorly represented (e.g., developed areas) in the AmeriFlux network. Requires extrapolating tower measurements from habitat proxies that are similar but not identical to the target study area. Does not identify source of carbon flux (e.g., plant growth vs soil carbon accumulation). NLCD classifications do not differentiate between wetland types, which differ significantly in overall carbon flux.

Both the NECB and NEE frameworks described here have several limitations. Both approaches intrinsically aim to decompose carbon fluxes into distinct habitat categories identified through the NLCD. Intra-habitat variability is thus difficult to capture with either approach. This is especially the case for wetland habitats for which the various subtypes (i.e., fresh, intermediate, brackish, and saline) are known to have high variation in carbon flux potential (Luo et al., 2019). Likewise, data on carbon flux is largely lacking for developed areas, both in the literature and in the AmeriFlux network—which currently possesses only eight stations reporting data in developed areas (although all are provided only through the BASE pipeline, and do not report NEE). This limitation is less important for estimates at Fort Moore, where developed areas all together represent only 7.7% of the bases total area. However, the lack of data on urban and suburban carbon fluxes is more pressing for Tyndall AFB and Scott AFB, where all developed areas represent 20.2% and 81.1% of each bases total area, respectively.

ALTERNATIVE HABITAT CLASSIFICATIONS

The recent emergence of the Land Cover Monitoring Assessment and Projection (LCMAP) database (Brown et al., 2020) alongside the well-established NLCD presents both opportunities and challenges for land use/land cover analyses. NLCD boasts a long history and standardized methodology, offering consistent high-resolution data from 2001 to 2021 for long-term trend analysis (Homer et al., 2020). However, its 2-to-3-year update cycle limits its ability to capture rapid land surface changes. LCMAP, meanwhile, represents a new generation of land cover mapping that offers annual updates from 1985 to 2021 with the same nominal 30-m spatial resolution as the NLCD, but uses a land cover scheme with only eight land cover classes (Table 10)—as opposed to the 16 land cover classes provided by the NLCD. Thus, NLCD has better thematic detail (i.e., habitat classifications) and is ideal for studying spatial patterns (such as the framework detailed in this report). On the other hand, LCMAP excels at capturing land use changes in the year they occur and its larger historical period (37 years), which may be more useful to modeling the impacts of disturbances at each base or building predictive machine learning based carbon flux models that require a more extensive training set than can be offered by the NLCD. Ultimately, leveraging both databases, along with careful consideration of their strengths and limitations, can offer a more comprehensive understanding of land-use dynamics at each base.

Table 10. LCMAP land cover class definitions.

Habitat	Classification description
Developed	Areas of intensive use with much of the land covered with structures (e.g., high density residential, commercial, industrial, or transportation), or less intensive uses where the land cover matrix includes vegetation, bare ground, and structures (e.g., low density residential, recreational facilities, cemeteries, transportation/utility corridors, etc.), including any land functionally related to the developed or built-up activity.
Cropland	Land in either a vegetated or unvegetated state used in production of food, fiber, and fuels. This includes cultivated and uncultivated croplands, hay lands, orchards, vineyards, and confined livestock operations. Forest plantations are considered as Tree Cover class regardless of the use of the wood products.
Grass/Shrub	Land predominantly covered with shrubs and perennial or annual natural and domesticated grasses (e.g., pasture), forbs, or other forms of herbaceous vegetation. The grass and shrub cover must comprise at least 10% of the area and tree cover is less than 10% of the area.
Tree Cover	Tree-covered land where the tree cover density is greater than 10%. Cleared or harvested trees (i.e., clearcuts) will be mapped according to current cover (e.g., Barren, Grass/Shrub).
Water	Areas covered with water, such as streams, canals, lakes, reservoirs, bays, or oceans.
Wetland	Lands where water saturation is the determining factor in soil characteristics, vegetation types, and animal communities. Wetlands are comprised of mosaics of water, bare soil, and herbaceous or wooded vegetated cover.
Ice/Snow	Land where accumulated snow and ice does not completely melt during the summer period (i.e., perennial ice/snow).
Barren	Land comprised of natural occurrences of soils, sand, or rocks where less than 10% of the area is vegetated.

CONCLUSIONS

The framework presented in this report allows one to rapidly estimate landscape-scale net carbon flux across a wide range of habitat types on DoD installations. Two quantification approaches—a literature-based NECB and eddy-covariance based NEE approach—were detailed and applied to three DoD installations of varying sizes and with different ecosystem representations. The estimated relative uncertainty of these two approaches varied between ± 62% and ± 265%. All three installations were quantified as being a net annual sink for GHG over two decades, although determining both if and when these annual sink rates saturate the total carbon storage potential of each base will require long-term on-site monitoring.

Both quantification approaches used solely publicly available data and could therefore be applied to all facilities in the U.S. (the current extent of the NLCD). However, applying this framework at DoD bases located outside the U.S. would require the use of an alternative land classification approach, such as the WorldCover database (Zanaga et al., 2022), which uses Sentinel-1 and Sentinel-2 data to supply a global map of land cover. Compared to the NLCD, WorldCover provides higher spatial resolution (10 m), but is only available for 2020 and 2021, has a lower overall landcover accuracy of ~75% (versus ~90.3% for NLCD in 2019), and has only 11 habitat classifications. Due to its higher accuracy and better thematic resolution in developed areas (i.e., open, low-, medium-, and high-intensity), the use of the NLCD approach is recommended for DoD facilities located within the contiguous U.S., Alaska, or Hawaii. For facilities located in other countries or overseas U.S. insular areas (e.g., Guam), the WorldCover database provides an acceptable drop-in substitute.

Beyond quantifying net carbon fluxes across an entire DoD installation, the methodologies detailed in this framework will be useful for future planning and decision-making efforts by the DoD and/or USACE regarding landscape-scale GHG fluxes. Although the uncertainties around estimated net carbon fluxes remain large in many cases, this framework nonetheless represents a desktop approach that can rapidly identify locations within DoD installations where natural carbon sequestration rates are high without the need for expensive and laborious field surveys. Furthermore, this framework can also help identify locations where carbon flux uncertainties are large, and thus help land managers easily identify specific sites where investment in on-site monitoring would provide the most impact in reducing carbon flux uncertainties (Table 11). For installations where the uncertainty of non-CO_2 GHG fluxes is dominant (e.g., due to the presence of large expanses of wetlands), this might involve deploying mobile or fixed-point flux towers within habitats where the uncertainty for these emissions is high. For example, at Scott AFB, almost a third of the entire installation's net carbon flux uncertainty is due to potential methane emissions from the forest located within the Silver Creek floodplain (Table 11). Targeted field campaigns in these locations would provide more localized data on methane and nitrous oxide exchange, reducing uncertainty for more accurate carbon flux accounting. Alternatively, at DoD sites that contain large areas of development relative to installation size (e.g., Scott AFB), or extensive expanses of forested lands (e.g., Fort Moore), then ANPP may also represent a significant level of uncertainty. At these sites, high-resolution remote sensing with advanced spectral analysis of satellite or drone imagery could reveal variations in vegetation health and productivity and improve ANPP estimates.

Table 11. The five largest sources of uncertainty in net carbon flux estimates at Ft. Moore, Scott AFB, and Tyndall AFB.

Installation	Habitat	Parameter	Relative uncertainty (%)
Ft Moore	Woody Wetlands	GHG	25.8%
	Evergreen Forest	ANPP	14.1%
	Evergreen Forest	SA	8.9%
	Woody Wetlands	ANPP	7.8%
	Mixed Forest	ANPP	6.7%
Scott AFB	Woody Wetlands	GHG	35.4%
	Developed, Low Intensity	ANPP	15.7%
	Developed, Open Space	ANPP	15.5%
	Woody Wetlands	ANPP	10.7%
	Developed, Medium Intensity	ANPP	6.9%
Tyndall AFB	Woody Wetlands	GHG	36.2%
	Emergent Herbaceous Wetlands	GHG	19.4%
	Emergent Herbaceous Wetlands	ANPP	11.0%
	Woody Wetlands	ANPP	11.0%
	Woody Wetlands	SA	5.9%

Lastly, following draft guidance from the White House Office of Management and Budget that recommends the inclusion of GHG effects in assessing changes in ecosystem services in cost-benefit analyses (Office of Information and Regulatory Affairs & Office of Management and Budget, 2023), this framework could also serve as a valuable tool to quantify additional carbon benefits of USACE civil works, military construction, and environmental projects. This may also support USACE study teams in meeting new Agency Specific Procedures to meet the requirements in the draft Principles, Requirements, and Guidelines (USACE, 2024) for including and evaluating the public benefits of nature-based alternatives in that it provides a tool for evaluating and quantifying carbon benefits of such features. Furthermore, this framework could aid efforts to include GHG flux quantification as a criterion for project prioritization or facility planning, ensuring that environmental considerations are included in strategic planning efforts by the DoD. This framework, therefore, not only serves as a baseline for current and future environmental impact assessments but also paves the way for a more sustainable and informed approach to managing DoD lands and projects in the future.

REFERENCES

Administration of Joseph R. Biden, Jr. (2021). *Executive Order 14008: Tackling the Climate Crisis at Home and Abroad*.

Baustian, M. M., Liu, B., Moss, L. C., Dausman, A., & Pahl, J. W. (2023). Climate Change Mitigation Potential of Louisiana's Coastal Area: Current Estimates and Future Projections. *Ecological Application*.

Brown, J. F., Tollerud, H. J., Barber, C. P., Zhou, Q., Dwyer, J. L., Vogelmann, J. E., Loveland, T. R., Woodcock, C. E., Stehman, S. V., Zhu, Z., & others. (2020). Lessons learned implementing an operational continuous United States national land change monitoring capability: The Land Change Monitoring, Assessment, and Projection (LCMAP) approach. *Remote Sensing of Environment*, *238*, 111356. https://doi.org/10/ggwd75

Chapin, F. S., Woodwell, G. M., Randerson, J. T., Rastetter, E. B., Lovett, G. M., Baldocchi, D. D., Clark, D. A., Harmon, M. E., Schimel, D. S., Valentini, R., Wirth, C., Aber, J. D., Cole, J. J., Goulden, M. L., Harden, J. W., Heimann, M., Howarth, R. W., Matson, P. A., McGuire, A. D., … Schulze, E.-D. (2006). Reconciling carbon-cycle concepts, terminology, and methods. *Ecosystems*, *9*(7), 1041–1050. https://doi.org/10.1007/s10021-005-0105-7

Crawford, N. C. (2019). *Pentagon fuel use, climate change, and the costs of war*. Watson Institute, Brown University.

Eggleston, H., Buendia, L., Miwa, K., Ngara, T., & Tanabe, K. (2006). *2006 IPCC guidelines for national greenhouse gas inventories*.

Global Forest Watch. (2002). Global forest watch. *World Resources Institute, Washington, DC Available from http://www.globalforestwatch.org (Accessed August 2023)*.

Gulde, S., Chung, H., Amelung, W., Chang, C., & Six, J. (2008). Soil carbon saturation controls labile and stable carbon pool dynamics. *Soil Science Society of America Journal*, *72*(3), 605–612. https://doi.org/10/bmdvt8

Homer, C., Dewitz, J., Jin, S., Xian, G., Costello, C., Danielson, P., Gass, L., Funk, M., Wickham, J., Stehman, S., Auch, R., & Riitters, K. (2020). Conterminous United States land cover change patterns 2001–2016 from the 2016 National Land Cover Database. *ISPRS Journal of Photogrammetry and Remote Sensing*, *162*, 184–199. https://doi.org/10/ghz3bp

Larson, S. L., Busby, R. R., Martin, W. A., Medina, V. F., Seman, P. M., Hiemstra, C. A., Mishra, U., & Larson, T. (2017). *Sustainable carbon dioxide sequestration as soil carbon to achieve carbon neutral status for DoD lands* [Report]. Environmental Laboratory (U.S.). https://erdc-library.erdc.dren.mil/jspui/handle/11681/25406

Luo, M., Huang, J.-F., Zhu, W.-F., & Tong, C. (2019). Impacts of increasing salinity and inundation on rates and pathways of organic carbon mineralization in tidal wetlands: A review. *Hydrobiologia*, *827*(1), 31–49. https://doi.org/10.1007/s10750-017-3416-8

Luo, Y., & Weng, E. (2011). Dynamic disequilibrium of the terrestrial carbon cycle under global change. *Trends in Ecology & Evolution*, *26*(2), 96–104. https://doi.org/10.1016/j.tree.2010.11.003

Office of Information and Regulatory Affairs & Office of Management and Budget. (2023). *Guidance for assessing changes in environmental and ecosystem services in benefit-cost analysis* [Draft for Public Review]. https://www.whitehouse.gov/wp-content/uploads/2023/08/DraftESGuidance.pdf

Pastorello, G., Trotta, C., Canfora, E., Chu, H., Christianson, D., Cheah, Y.-W., Poindexter, C., Chen, J., Elbashandy, A., Humphrey, M., Isaac, P., Polidori, D., Ribeca, A., van Ingen, C., Zhang, L., Amiro, B., Ammann, C., Arain, M. A., ArdÃ¶, J., … Papale, D. (2020). The FLUXNET2015 dataset and the ONEFlux processing pipeline for eddy covariance data. *Scientific Data*, *7*(1), 225. https://doi.org/10/gg4hq7

Penman, J., Kruger, D., Galbally, I., Hiraishi, T., Nyenzi, B., Emmanuel, S., Buendia, L., Hoppaus, R., Martinsen, T., Meijer, J., & others. (2000). *Good practice guidance and uncertainty management in national greenhouse gas inventories*.

Polyakov, V., & Lal, R. (2004). Modeling soil organic matter dynamics as affected by soil water erosion. *Environment International*, *30*(4), 547–556. https://doi.org/10/dvn5p7

Restore America's Estuaries. (2016). *Recommendations from the Blue Carbon National Working Group. Based on a workshop convened by Restore America's Estuaries and NOAA's Office of Habitat Conservation held May 20-21, 2015.*

Rosentreter, J. A., Borges, A. V., Deemer, B. R., Holgerson, M. A., Liu, S., Song, C., Melack, J., Raymond, P. A., Duarte, C. M., Allen, G. H., Olefeldt, D., Poulter, B., Battin, T. I., & Eyre, B. D. (2021). Half of global methane emissions come from highly variable aquatic ecosystem sources. *Nature Geoscience*, *14*(4), 225–230. https://doi.org/10/gjnqn2

Troxler, T. G., Gaiser, E., Barr, J., Fuentes, J. D., Jaffé, R., Childers, D. L., Collado-Vides, L., Rivera-Monroy, V. H., Castañeda-Moya, E., Anderson, W., Chambers, R., Chen, M., Coronado-Molina, C., Davis, S. E., Engel, V., Fitz, C., Fourqurean, J. W., Frankovich, T., Kominoski, J. S., … Whelan, K. (2013). Integrated carbon budget models for the Everglades terrestrial-coastal-oceanic gradient: Current status and needs for inter-site comparisons. *Oceanography*, *26*(3), 98–107. https://doi.org/10/grpfkv

USACE. (2024). *Draft Environmental Assessment and Finding of No Significant Impact. Proposed Rule: 33 CFR 234, Corps of Engineers Agency Specific Procedures for Principles, Requirements and Guidelines Applicable to Actions Involving Investment in Water Resources*.

Wardle, D. A., Hörnberg, G., Zackrisson, O., Kalela-Brundin, M., & Coomes, D. A. (2003). Long-term effects of wildfire on ecosystem properties across an island area gradient. *Science*, *300*(5621), 972–975. https://doi.org/10/dpn9m2

Williams, C. A., Hasler, N., Gu, H., & Zhou, Y. (2021). *Forest Carbon Stocks and Fluxes from the NFCMS, Conterminous USA, 1990-2010*. ORNL Distributed Active Archive Center. https://doi.org/10.3334/ORNLDAAC/1829

Wutzler, T., & Reichstein, M. (2007). Soils apart from equilibrium - consequences for soil carbon balance modelling. *Biogeosciences*, *4*(1), 125–136. https://doi.org/10/dgxk25

Zanaga, D., Van De Kerchove, R., Daems, D., De Keersmaecker, W., Brockmann, C., Kirches, G., Wevers, J., Cartus, O., Santoro, M., Fritz, S., & others. (2022). *ESA WorldCover 10 m 2021 v200*.

APPENDICES

APPENDIX A. LOOKUP TABLE FOR ANNUAL NET PRIMARY PRODUCTIVITY, SEDIMENT ACCRETION, AND NON-CO_2 GREENHOUSE GAS FLUX

Through comprehensive literature reviews, aboveground net primary productivity (ANPP), sediment/soil accumulation rate, and non-CO_2 greenhouse gas (GHG) flux across a total of 16 habitats represented in the three DoD sites were collected and compiled for this study.

A.1 ABOVEGROUND NET PRIMARY PRODUCTIVITY (ANPP)

Table A-1. Aboveground net primary productivity values obtained from published literature.

Habitat	Notes	AG primary productivity rates (tonne CO_2e ha^{-1} yr^{-1})	References
Open Water (All types of water)	Phytoplankton growth (Louisiana)	-3.67	(Day, 1973)
Perennial Ice/Snow	Snow: *Digitaria eriantharyo, Digitaria erianthaonite* algae; Ice: *Digitaria erianthayanoba, Digitaria erianthateria algae*	-0.004	(Anesio et al., 2009)
Developed, Open Space	Uses ANPP values from Herbaceous/Grassland habitats, reduced by 20%	-10.321	-
Developed, Low Intensity	Uses ANPP values from Herbaceous/Grassland habitats, reduced by 49%	-6.580	-
Developed, Medium Intensity	Uses ANPP values from Herbaceous/Grassland habitats, reduced by 79%	-2.709	-
Developed, High Intensity	ANPP assumed to be zero.	0.000	-
Barren Land	ANPP assumed to be zero.	0.000	-
Deciduous Forest	Elm/Ash/Cottonwood	-2.905	National Forest Carbon Monitoring System. See Table B-1.
Evergreen Forest	Loblolly/Shortlear Pine	-4.814	National Forest Carbon Monitoring System. See Table B-1.
Mixed Forest	Average of Deciduous and Evergreen	-3.860	National Forest Carbon Monitoring System. See Table B-1.
Shrub/Scrub	United Kingdom – mean (control/draught/warming temperature treatment)	-0.73 (-0.77-/-0.67/-0.76)	(Reinsch et al., 2017)

Habitat	Notes	AG primary productivity rates (tonne CO_2e ha^{-1} yr^{-1})	References
	The Netherlands – mean (control/draught/warming temperature treatment)	-1.15 (-1.36/-0.83/-1.27)	
	Denmark-Mols- mean (control/draught/warming temperature treatment)	-1.00 (-1.13/-0.77/-1.11)	
	Denmark-Brandbjerg – mean (control/draught/warming temperature treatment)	-1.86 (-1.83/-1.84/-1.90)	
	Hungary – mean (control/draught/warming temperature treatment)	-0.32 (-0.31/-0.26/-0.39)	
	Spain – mean (control/draught/warming temperature treatment)	-0.71 (-0.74/-0.61/-0.77)	
	Italy – mean (control/draught/warming temperature treatment)	-0.45 (-0.53/-0.29/-0.54)	
Herbaceous/Grassland	Alpine meadow	-10.129	(Sun et al., 2023)
	Annual grassland	-13.405	
	Arid grassland	-20.304	
	Basin grassland	-5.358	
	Burned prairie	-11.561	
	Chihuahuan Desert grassland	-13.710	
	Cool season meadow	-19.818	
	Desert grassland	-4.032	
	Desert steppe	-3.077	
	Dry grassland	-2.386	
	Dry meadow	-5.505	
	Grassland	-11.177	
	Invaded prairie	-34.388	
	Meadow	-8.242	
	Mediterranean grassland	-17.704	
	Mesic grassland, historic tallgrass prairie	-13.151	
	Mesic tallgrass prairie	-15.598	
	Mixed-grass prairie	-11.081	
	Mountain grassland	-10.143	
	Native savanna	-11.377	
	Piedmont grassland	-12.698	
	Prairie	-13.638	
	Remnant prairie	-21.139	

Habitat	Notes	AG primary productivity rates (tonne CO_2e ha^{-1} yr^{-1})	References
	Restored prairie	-26.130	
	Semiarid shortgrass steppe	-4.386	
	Shortgrass prairie	-7.783	
	Shortgrass steppe	-3.895	
	Subalpine meadow	-7.982	
	Subhumid mixed-grass prairie	-12.998	
	Subtropical savanna	-14.680	
	Switchgrass field	-28.964	
	Tallgrass prairie	-16.636	
	Temperate grassland	-8.950	
	Temperate sand prairie	-13.065	
	Wet meadow	-16.454	
Hay/Pasture	*Pancium maximum*	-31.20	(Murray et al., 2016)
	Pancium maximum	-24.59	
	Cenchrus ciliaris, Pancium maximum, Panicum coloratum	-21.29	
	Cenchrus ciliaris	-30.09	
	Chloris Gayana, Barachiaris brizantha	-31.56	
	Pancium maximum	-28.26	
	Pancium maximum, Chloris Gayana, Setaria anceps	-13.58	
	Pancium maximum	-16.15	
	Cenchrus ciliaris, Pancium maximum, Chloris Gayana, Panicum coloratum, Barachiaris brizantha	-19.45	
	Cenchrus ciliaris	-6.97	
	Cenchrus ciliaris, Pancium maximum, Chloris Gayana, Panicum coloratum	-11.38	
	Cenchrus ciliaris	-16.15	
	Cenchrus ciliaris	-10.28	
	Cenchrus ciliaris, Pancium maximum, Chloris Gayana, Panicum coloratum	-16.52	
	Cenchrus ciliaris, Pancium maximum, Chloris Gayana, Panicum coloratum	-24.59	
	Chloris Gayana, Panicum coloratum, Digitaria eriantha	-17.25	
	Schizachyrium scoparium, Pappophorum caespitosum	-18.72	
	Digitaria eriantha	-9.54	
	Botriocloa sp.	-20.55	

Habitat	Notes	AG primary productivity rates (tonne CO_2e ha^{-1} yr^{-1})	References
	Pancicum coloratum, Eragrostis curvula, Tetrachine dregei	-13.58	
	Pancicum coloratum	-19.08	
	Eragrostis curvula, Botriocloa sp.	-25.69	
	Digitaria eriantha, Panicum coloratum, Eragrostis curvula, Sorgum almun	-13.58	
	Eragrostis curvula	-16.88	
	Digitaria eriantha	-12.85	
	Digitaria eriantha, Eragrostis curvula	-12.85	
Cultivated Crops	For annual crops, increase in biomass stocks in a single year were assumed equal to biomass losses from harvest and mortality in that same year – thus there was no net accumulation of biomass carbon stocks	0.000	
Woody Wetlands	Forest wetlands, *Taxodium distichum, Nyssa aquatica, Nyssa sylvatica, Acer rubrum, Fraxinus caroliniana*	-16.680	(Brantley et al., 2008)
	Forest wetlands	-29.826	(Cardoch et al., 2002)
	Swamp, *T. distichum–Nyssa aquatica*	-3.551	(Hoeppner et al., 2008)
	Swamp Forest, bald cypress (*Taxodium distichum*)	-15.689	(Middleton & McKee, 2004)
	Swamp Forest, bald cypress-water tupelo	-25.995	(Conner & Day, 1976)
	Bottomland hardwood, *Acer rubrum* var. drummon *Nyssa aquatica*	-18.827	
	Forest wetlands	-22.295	(Elder & Cairns, 1982)
	Forest wetlands	-14.285	(Conner et al., 1993)
	Bottomland hardwood	-26.160	(Day et al., 1977)
	Cypress Tupelo	-18.827	
	Swamp Forest	-16.688	(Conner & Day, 1987)
	Maurepas Swamp, bald cypress (*Taxodium distichum*) and water tupelo (*Nyssa aquatica*) or the complex branching structure of shrubs such as wax myrtle (*Morella cerifera*)	-13.129	(G. Shaffer et al., 2016)
	Swamp forest, bald cypress-water tupelo (*Taxodium distichum-Nyssa aquatica*) swamps	-12.172	(Shaffer et al. 2009)

Habitat	Notes	AG primary productivity rates (tonne CO_2e ha^{-1} yr^{-1})	References
	Swamp forest, water tupelo (Nyssa aquatica), swamp black gum (Nyssa biflora and d baldcypress (Taxodium distichum)	-16.639	(Brantley et al., 2008)
	Cypress-tupelo swamp	-9.909	(Edwards et al. 2019)
	full-canopy, *Taxodium distichum/ Nyssa aquatica* L.	-6.973	
	intermediate, *Taxodium distichum/ Nyssa aquatica* L.	-5.138	
	open-canopy, *Taxodium distichum/ Nyssa aquatica* L.	-2.936	
	VB1-2, *Taxodium distichum/Diospyros virginiana*	-12.485	(Megonigal et al., 1997)
	VB3-4, *Taxodium distichum/Fraxinus* spp.	-16.854	
	VB5-6, *Quercus* spp./*Fraxinus* spp. Celtis laevigata	-18.456	
	BB-Nat1 and 2, *Nyssa aquatica/Taxodium distichum*	-13.840	
	BB-Imp1, *Fraxinus* spp./*Celtis laevigata*	-3.336	
	BB-Imp2, *Liriodendron styraciflua/Fraxinus* spp.	-14.764	
	PR1-2, *Liquidambar styraciflua*	-18.596	
	PR3-4, *Carya aquatica*	-22.650	
	PR5-6, *Liquidambar styraciflua*	-16.837	
	Bottomland hardwood, Bald cypress-water tupelo	-28.620	
	Baldcypress-water tupelo	-25.037	(Conner & Day, 1976)
	Natural flooding, Bald cypress-water tupelo	-19.256	(Cramer et al., 1981)
	Permanently flooded, Bald cypress-water tupelo	-14.632	(Conner et al., 1993)
	controlled flooding, Bald cypress-water tupelo	-29.380	(Conner, 1994)
	Roma Swamp, cypress (*Taxodium distichum*), water tupelo (*Nyssa aquatica*),	-18.020	(Day et al., 2006)
	Baldcypress	-10.107	(Hillmann et al., 2019)
	Water tupelo	-13.592	(Hillmann et al., 2020)
	Water	-5.929	(Shaffer et al. 2009)

Habitat	Notes	AG primary productivity rates (tonne CO_2e ha^{-1} yr^{-1})	References
Emergent Herbaceous Wetlands	Fresh Herbaceous Marsh	-25.595	(Pezeshki & DeLaune, 1991)
	Fresh Herbaceous Marsh	-16.331	(Stagg et al., 2016)
	Fresh Herbaceous Marsh	-13.601	(Day et al., 2013)
	Fresh Herbaceous Marsh	-9.359	(DeLaune et al. 2016)
	Fresh Herbaceous Marsh	-15.598	
	Fresh Herbaceous Marsh	-31.429	(Cardoch et al., 2002)
	Fresh Herbaceous Marsh	-46.793	(Cardoch et al., 2002)
	Fresh Herbaceous Marsh	-22.616	(Feijtel et al., 1985)
	Fresh Herbaceous Marsh	-18.556	(White & Simmons, 1988)
	Intermediate Herbaceous Marsh	-27.218	(Graham & Mendelssohn, 2010)
	Intermediate Herbaceous Marsh	-35.874	(Sasser and Gosselink 1984)
	Intermediate Herbaceous Marsh	-23.412	(Hopkinson et al., 1978)
	Intermediate Herbaceous Marsh	-36.030	(Hopkinson et al., 1980)
	Intermediate Herbaceous Marsh	-16.471	(Stagg et al., 2016)
	Intermediate Herbaceous Marsh	-19.388	(Graham & Mendelssohn, 2010)
	Intermediate Herbaceous Marsh	-15.034	(White & Simmons, 1988)
	Intermediate Herbaceous Marsh	-19.871	(Sasser et al. 2018)
	Intermediate Herbaceous Marsh	-25.284	
	Intermediate Herbaceous Marsh	-22.913	
	Brackish Herbaceous Marsh	-65.829	(Feijtel et al., 1985)
	Brackish Herbaceous Marsh	-66.060	(Sasser and Gosselink 1984)
	Brackish Herbaceous Marsh	-55.573	(Flynn et al., 1999)
	Brackish Herbaceous Marsh	-21.106	
	Brackish Herbaceous Marsh	-99.800	(Hopkinson et al., 1978)
	Brackish Herbaceous Marsh	-22.378	
	Brackish Herbaceous Marsh	-19.124	(Day et al., 2013)
	Brackish Herbaceous Marsh	-68.686	(Hopkinson et al., 1980)
	Brackish Herbaceous Marsh	-57.183	(Cramer et al., 1981)
	Brackish Herbaceous Marsh	-70.676	

Habitat	Notes	AG primary productivity rates (tonne CO_2e ha^{-1} yr^{-1})	References
	Brackish Herbaceous Marsh	-24.558	(Stagg et al., 2016)
	Brackish Herbaceous Marsh	-60.726	(Pezeshki & DeLaune, 1991)
	Brackish Herbaceous Marsh	-10.338	(Nyman et al., 1995)
	Brackish Herbaceous Marsh	-16.061	(Delaune & Smith, 1984)
	Brackish Herbaceous Marsh	-55.672	(Sasser et al. 2018)
	Brackish Herbaceous Marsh	-69.512	
	Brackish Herbaceous Marsh	-36.234	(White et al., 1978)
	Brackish Herbaceous Marsh	-36.234	
	Brackish Herbaceous Marsh	-18.497	(White & Simmons, 1988)
	Brackish Herbaceous Marsh	-55.738	(Cardoch et al., 2002)
	Saline Wetland	-29.558	(Kaswadji et al., 1990)
	Saline Wetland	-19.426	
	Saline Wetland	-13.114	
	Saline Wetland	-66.028	(Pham, 2014)
	Saline Wetland	31.846	
	Saline Wetland	-17.075	
	Saline Wetland	-59.218	(Snedden et al. 2015)
	Saline Wetland	-39.453	(Sasser and Gosselink 1984)
	Saline Wetland	-21.304	
	Saline Wetland	-28.737	(Darby & Turner, 2008)
	Saline Wetland	-53.908	(Hopkinson et al., 1978)
	Saline Wetland	-51.083	
	Saline Wetland	-21.794	(Hopkinson et al., 1980)
	Saline Wetland	-17.722	(Day et al., 2013)
	Saline Wetland	-31.688	(Pezeshki & DeLaune, 1991)
	Saline Wetland	-58.121	
	Saline Wetland	-16.318	(Stagg et al., 2016)
	Saline Wetland	-19.063	(Kirby & Gosselink, 1976)
	Saline Wetland	-13.343	(Stagg & Mendelssohn, 2011)
	Saline Wetland	-41.110	(Edwards and Mills 2005)
	Saline Wetland	-18.369	(White et al., 1978)
	Saline Wetland	-30.915	

Habitat	Notes	AG primary productivity rates (tonne CO_2e ha^{-1} yr^{-1})	References
	Saline Wetland	-23.245	
	Saline Wetland	-39.673	(Sasser et al. 2018)
	Saline Wetland	-28.295	
	Saline Wetland	-38.805	(Cardoch et al., 2002)
	Saline Wetland	-32.746	(Feijtel et al., 1985)

A.2 SEDIMENT/SOIL CARBON ACCUMULATION RATE

Table A-2. Sediment/Soil carbon accumulation rates obtained through literature reviews.

Habitat	Notes	Sediment/Soil Carbon Accumulation rates (tonne CO_2e ha^{-1} yr^{-1})	References
Open Water	Fresh and Intermediate	-2.2	(Stow et al., 1985)
	Fresh and Intermediate	-2.2	(Smith, DeLaune, and Patrick 1983)
	Fresh and Intermediate	-3.3	(Scaroni, 2011)
	Fresh and Intermediate	-6.9	(Hillmann et al., 2020)
	Fresh and Intermediate	-11.3	
	Brackish	-16.3	
	Saline	-8.7	(Smith, DeLaune, and Patrick 1983)
	Saline	-7.3	(Hillmann et al., 2020)
Perennial Ice/Snow	Soil carbon accumulation assumed to be negligible.	0.0	-
Developed, Open Space	Assumed 80% of Herbaceous/Grassland habitats	-1.399	-
Developed, Low Intensity	Assumed 51% of Herbaceous/Grassland habitats	-0.892	-
Developed, Medium Intensity	Assumed 21%of Herbaceous/Grassland habitats	-0.367	-
Developed, High Intensity	Soil carbon accumulation assumed to be negligible.	0.00	-
Barren Land	Soil carbon accumulation assumed to be negligible.	0.00	-
Deciduous Forest	Heshui, Gansu, China	-0.039	(Hou et al., 2020)
	Heshui, Gansu, China	-0.138	
	Heshui, Gansu, China	-0.482	
	Nanxiaohe watershed, China	-0.093	

Habitat	Notes	Sediment/Soil Carbon Accumulation rates (tonne CO_2e ha^{-1} yr^{-1})	References
	Nanxiaohe watershed, China	-0.108	
	Nanxiaohe watershed, China	-0.637	
	Ansai county, Shaanxi, China	-0.830	
	Yongshou County, Shaanxi, China	-0.284	
	Ansai county, Shaanxi, China	-0.307	
	Yongshou County, Shaanxi, China	-0.734	
	Yongshou County, Shaanxi, China	-2.444	
	Ansai County, China	-2.680	
	Ansai, Shaanxi, China	-1.489	
	Ansai county, China	-1.536	
	Ansai county, China	-1.744	
	Ansai, Shaanxi, China	-1.929	
	Ansai County, northern Shaanxi, China	-0.555	
	Ansai County, northern Shaanxi, China	-0.565	
	Ansai County, northern Shaanxi, China	-0.685	
	Ansai County, northern Shaanxi, China	-0.747	
	Ansai County, northern Shaanxi, China	-1.455	
	Ansai County, northern Shaanxi, China	-2.337	
	Saskatchewan, Canada	+0.142	
	Ansai County, northern Shaanxi, China	-0.575	
	Ansai County, northern Shaanxi, China	-0.585	
	Ansai County, northern Shaanxi, China	-0.709	
	Ansai County, northern Shaanxi, China	-0.752	
	Ansai County, northern Shaanxi, China	-1.477	
	Saskatchewan, Canada	-1.728	
	Ansai County, northern Shaanxi, China	-2.219	
	Saskatchewan, Canada	-2.607	
	Ningxia, China	+1.563	
	Ningxia, China	+1.559	
	Krasnoyarsk, Siberia	+0.980	
	Ansai, Shaanxi, China	-0.051	
	Ansai, Shaanxi, China	-0.062	
	Ansai, Shaanxi, China	-0.128	
	Ansai, Shaanxi, China	-0.141	
	Fuxian County, Shaanxi, China	-0.221	
	Ansai county, China	-0.283	
	Fuxian County, Shaanxi, China	-0.322	
	Ansai county, China	-0.378	
	Ansai, Shaanxi, China	-0.380	
	Ansai county, China	-0.405	

Habitat	Notes	Sediment/Soil Carbon Accumulation rates (tonne CO_2e ha^{-1} yr^{-1})	References
	Ansai county, China	-0.413	
	Fuxian County, Shaanxi, China	-0.563	
	Ansai county, China	-0.614	
	Ansai county, Shaanxi, China	-0.654	
	Ansai county, Shaanxi, China	-0.661	
	Ansai, Shaanxi, China	-0.844	
	Ansai county, China	-0.892	
	Tianshui city, Gansu, China	-1.393	
	Shaanxi, China	-1.406	
	Shaanxi, China	-1.459	
	Ansai county, Shaanxi, China	-1.503	
	Ansai county, Shaanxi, China	-1.973	
	Krasnoyarsk, Siberia	-5.383	
	Ansai County, northern Shaanxi, China	-0.588	
	Ansai County, northern Shaanxi, China	-0.623	
	Ansai County, northern Shaanxi, China	-0.730	
	Ansai County, northern Shaanxi, China	-0.812	
	Ansai County, northern Shaanxi, China	-1.379	
	Ansai County, northern Shaanxi, China	-2.049	
	Shenmu County, China	+0.229	
	Ansai, Shaanxi, China	+0.123	
	Shenmu County, China	+0.105	
	Shenmu County, China	+0.060	
	Ansai, Shaanxi, China	-0.170	
	Ansai, Shaanxi, China	-0.178	
	Ansai, Shaanxi, China	-0.225	
	Shaanxi, China	-0.528	
	Ansai, Shaanxi, China	-0.676	
	Shaanxi, China	-0.864	
	Shaanxi, China	-0.883	
	Ansai, Shaanxi, China	-0.925	
	Shaanxi, China	-1.353	
	Ansai county, China	-1.104	
	Guyuan, Ningxia autonomous region, China	-1.412	
	Guyuan, Ningxia autonomous region, China	-2.258	
	Ansai county, Shaanxi, China	-0.851	
	Ningxia, China	-1.265	
	Dingxi, Gansu, China	-1.345	

Habitat	Notes	Sediment/Soil Carbon Accumulation rates (tonne CO_2e ha^{-1} yr^{-1})	References
	Ansai county, China	-1.362	
	Ningxia, China	-1.688	
	Dingxi, Gansu, China	-1.977	
	Ansai County, China	-2.085	
	Shaanxi, China	-0.348	
	Ansai county, China	-0.751	
	Wangdonggou watershed, China	-0.030	
	Wangdonggou watershed, China	-0.183	
	Wangdonggou watershed, China	-0.437	
	Ansai County, China	+0.339	
	Ansai County, China	-0.506	
	Jianping County, Liaoning, China	-0.693	
	Jianping County, Liaoning, China	-0.760	
	Jianping County, Liaoning, China	-0.912	
	Tianshui city, Gansu, China	-1.218	
	Ansai county, Shaanxi, China	-1.298	
	Ansai county, China	-1.681	
	Ansai County, China	-1.753	
	Ansai County, China	-1.918	
	Datong, Qinghai, China	-4.454	
	Datong, Qinghai, China	-17.578	
Evergreen Forest	Shaanxi, China	-0.094	(Hou et al., 2020)
	Shaanxi, China	-0.095	
	Shaanxi, China	-0.564	
	Shaanxi, China	-0.079	
	Shaanxi, China	-0.107	
	Shaanxi, China	-0.893	
	Atlanta, USA	-0.086	
	Atlanta, USA	-0.125	
	Atlanta, USA	-0.954	
	Yongshou County, Shaanxi, China	-0.148	
	Yongshou County, Shaanxi, China	-0.334	
	Shaanxi, China	-0.755	
	Yongshou County, Shaanxi, China	-1.646	
	Araguás catchment, Central Pyrenees	-2.738	
	Araguás catchment, Central Pyrenees	-3.406	
	Shaanxi, China	-0.269	
	Shaanxi, China	-0.334	
	Shaanxi, China	-1.555	

Habitat	Notes	Sediment/Soil Carbon Accumulation rates (tonne CO_2e ha^{-1} yr^{-1})	References
	Perloja experiment site, southern Lithuania	0.000	
	Perloja experiment site, southern Lithuania	-0.008	
	Perloja experiment site, southern Lithuania	-0.432	
	Perloja Experimental Station of Lithuanian Institute of Agriculture	-0.506	
	Perloja Experimental Station of Lithuanian Institute of Agriculture	-0.526	
	Qinling Mountains, China	-0.969	
	Córdoba, Argentina	-3.024	
	Marondera, Zimbabwe, Africa	+1.301	
	Marondera, Zimbabwe, Africa	-0.001	
	Marondera, Zimbabwe, Africa	-0.112	
	Sichuan, China	-0.496	
	Sichuan, China	-2.582	
	Lvliang, Shanxi, China	+0.041	
	Lvliang, Shanxi, China	-0.522	
	Sac County Conservation District, Iowa, USA	+0.021	
	Negev Desert, Israel	-0.579	
	Negev Desert, Israel	-0.911	
	Sac County Conservation District, Iowa, USA	-0.986	
	La Pampa, Argentina	-1.343	
	Lublin, Poland	-0.066	
	Manica Province, Central Mozambique	-0.507	
	Manica Province, Central Mozambique	-1.187	
	Manica Province, Central Mozambique	-1.274	
	Manica Province, Central Mozambique	-1.392	
	Manica Province, Central Mozambique	-3.554	
	Manica Province, Central Mozambique	-3.724	
	Vallgorguina valley, Barcelona	-0.352	
	Vallgorguina valley, Barcelona	-0.915	
	Vallgorguina valley, Barcelona	-0.086	
	Vallgorguina valley, Barcelona	-0.543	
	Ituzaingo, Corrientes, Argentina	+1.373	
	Turkey	-0.319	
	Rio Grande do Sul, southern Brazil	+8.398	
	Rio Grande do Sul, southern Brazil	+3.551	

Habitat	Notes	Sediment/Soil Carbon Accumulation rates (tonne CO_2e ha^{-1} yr^{-1})	References
	Krasnoyarsk, Siberia	+1.994	
	Kanto Plain, central Japan	+0.576	
	Kanto Plain, central Japan	+0.437	
	Krasnoyarsk, Siberia	-0.127	
	Qinling Mountains, China	-0.436	
	Kanto Plain, central Japan	-0.483	
	Chandanpokpi, NE India	-0.508	
	Ansai, Shaanxi, China	-0.544	
	Ansai, Shaanxi, China	-0.664	
	Ansai, Shaanxi, China	-0.696	
	Chandanpokpi, NE India	-0.710	
	Chandanpokpi, NE India	-0.862	
	Gelawdios, Amhara National Regional State, North-central Ethiopia	-1.049	
	Uruguay	-1.162	
	La Plata, Argentina	-1.428	
	Gelawdios, Amhara National Regional State, North-central Ethiopia	-1.651	
	Gelawdios, Amhara National Regional State, North-central Ethiopia	-2.000	
	Krasnoyarsk, Siberia	-2.401	
	Buenos Aires, Argentina	-2.717	
	Krasnoyarsk, Siberia	-5.383	
	Vallgorguina valley, Barcelona	+0.027	
	Vallgorguina valley, Barcelona	-0.364	
	Shenmu County, China	+0.256	
	Sao Paulo, Brazil	-0.218	
	Sao Paulo, Brazil	+0.148	
	Shenmu County, China	+0.064	
	Shenmu County, China	+0.025	
	Sao Paulo, Brazil	-0.013	
	Chilimo-Gaji dry Afromontane forest, Ethiopia	-0.193	
	Chilimo-Gaji dry Afromontane forest, Ethiopia	-0.579	
	Chilimo-Gaji dry Afromontane forest, Ethiopia	-0.627	
	Chilimo-Gaji dry Afromontane forest, Ethiopia	-1.098	
	Chilimo-Gaji dry Afromontane forest, Ethiopia	-1.950	

Habitat	Notes	Sediment/Soil Carbon Accumulation rates (tonne CO_2e ha^{-1} yr^{-1})	References
	Chilimo-Gaji dry Afromontane forest, Ethiopia	-1.954	
	Chilimo-Gaji dry Afromontane forest, Ethiopia	-2.328	
	Chilimo-Gaji dry Afromontane forest, Ethiopia	-2.336	
	Chilimo-Gaji dry Afromontane forest, Ethiopia	-2.391	
	Chilimo-Gaji dry Afromontane forest, Ethiopia	-2.918	
	Chilimo-Gaji dry Afromontane forest, Ethiopia	-3.389	
	Chilimo-Gaji dry Afromontane forest, Ethiopia	-3.519	
	Chilimo-Gaji dry Afromontane forest, Ethiopia	-4.085	
	Chilimo-Gaji dry Afromontane forest, Ethiopia	-4.264	
	Chilimo-Gaji dry Afromontane forest, Ethiopia	-4.601	
	Chilimo-Gaji dry Afromontane forest, Ethiopia	-4.700	
	Chilimo-Gaji dry Afromontane forest, Ethiopia	-5.810	
	Chilimo-Gaji dry Afromontane forest, Ethiopia	-6.911	
	Sao Paulo, Brazil	+0.190	
	Sao Paulo, Brazil	+0.021	
	Sao Paulo, Brazil	-0.171	
	Datong, Qinghai, China	+7.069	
	Candelaria, Misiones, Argentina	+1.218	
	Kanto Plain, central Japan	+0.424	
	Kanto Plain, central Japan	+0.171	
	Kanto Plain, central Japan	-0.035	
	Dingxi, Gansu, China	-0.549	
	Dingxi, Gansu, China	-0.910	
	Uruguay	-1.314	
	Datong, Qinghai, China	-9.804	
	Shaanxi, China	-0.872	
	Shaanxi, China	-1.300	
	Shaanxi, China	-2.090	

Habitat	Notes	Sediment/Soil Carbon Accumulation rates (tonne CO_2e ha^{-1} yr^{-1})	References
	Puruki, New Zealand	+4.468	
	Tikitere, New Zealand	+2.553	
	Tikitere, New Zealand	+0.638	
	Vallgorguina valley, Barcelona	+0.110	
	Tikitere, New Zealand	-0.798	
	Vallgorguina valley, Barcelona	-0.987	
	Ecuador	+2.602	
	Vallgorguina valley, Barcelona	-0.596	
	Vallgorguina valley, Barcelona	-0.710	
	Belete Forest, Ethiopia	-1.277	
	Belete Forest, Ethiopia	-1.835	
	Belete Forest, Ethiopia	-2.626	
	Belete Forest, Ethiopia	-2.626	
	Belete Forest, Ethiopia	-3.527	
	Belete Forest, Ethiopia	-4.031	
	Belete Forest, Ethiopia	-4.520	
	Belete Forest, Ethiopia	-6.292	
	Belete Forest, Ethiopia	-7.122	
	Marondera, Zimbabwe, Africa	+6.014	
	Rotorua, New Zealand	+5.505	
	Palmerston North, New Zealand	+3.633	
	Marondera, Zimbabwe, Africa	+1.733	
	tropical Andes, southern Ecuador	+1.248	
	Okuku, New Zealand	+1.021	
	Okuku, New Zealand	+0.716	
	Uberlandia, Brazil	+0.679	
	Uberlandia, Brazil	+0.630	
	Marondera, Zimbabwe, Africa	+0.591	
	Chandanpokpi, NE India	+0.352	
	Uberlandia, Brazil	+0.217	
	Chandanpokpi, NE India	-0.576	
	Chandanpokpi, NE India	-0.935	
	Uruguay	-2.237	
Mixed Forest	Calculated by averaging a random subset of 103 evergreen forest and 103 deciduous forest values from the above Huo et al. 2020 database.	-0.973	(Hou et al., 2020)
Shrub/Scrub	Desert Shrubland	-0.10	(Zhou et al., 2011)
	Desert Shrubland	-0.13	
	Desert Shrubland	-2.00	

Habitat	Notes	Sediment/Soil Carbon Accumulation rates (tonne CO_2e ha^{-1} yr^{-1})	References
	Desert Shrubland	-2.50	
	Desert Shrubland	-0.44	
	Desert Shrubland	-0.23	
Herbaceous/Grassland	Grassland	-4.04	(Gebhart et al., 1994)
	Pasture/range land	-0.73	(Bruce et al., 1999)
	Grassland	-1.84	(Conant et al., 2001)
	Cropland to range land	-1.17	(Liebig et al., 2005)
	Eastern Washington state	-1.95	(Stockle et al., 2012)
	Grassland	-1.98	(Conant et al., 2001)
	Grassland	-0.73	(Yellajosula et al., 2020)
Hay/Pasture	Improved – Sub-Saharan Africa	-6.7	(Dondini et al., 2023)
	Improved – Central & South America	-5.8	
	Improved – Western Europe	-3.2	
	Improved – Oceania	-2.8	
	Improved – East Asia	-2.5	
	Improved – North America	-2.5	
	Improved – South Asia	-2.5	
	Improved – Eastern Europe	-2.5	
	Improved – West Asia & Northern Africa	-2.1	
	Improved – Russian Federation	-2.0	
	Unimproved – Central & South America	-3.5	
	Unimproved – South Asia	-2.9	
	Unimproved – Eastern Europe	-2.85	
	Unimproved – Sub-Saharan Africa	-2.7	
	Unimproved – Western Europe	-2.7	
	Unimproved – East Asia	-2.3	
	Unimproved – Oceania	-2.1	
	Unimproved – Russian Federation	-1.9	
	Unimproved – North America	-1.8	
	Unimproved – West Asia & Northern Africa	-1.5	
Cultivated Crops	Corn-soybean	-3.30	(West & Post, 2002)
	All crop systems	-0.55	
	mean with crop rotation	-0.73	
	Wheat	-1.87	
	All crop systems	-1.47	(Lal et al., 1999)
	Corn-soybean	-0.73	(West & Post, 2002)

Habitat	Notes	Sediment/Soil Carbon Accumulation rates (tonne CO_2e ha^{-1} yr^{-1})	References
Woody Wetlands	Fresh Forested Wetland	-6.0	(Scaroni, 2011)
	Fresh Forested Wetland	-12.0	
	Fresh Forested Wetland	-4.9	(Rybczyk et al., 2002)
	Fresh Forested Wetland	-12.5	(Hupp et al., 2019)
Emergent Herbaceous Wetlands	Fresh Marsh	-8.2	(Smith, DeLaune, and Patrick 1983)
	Fresh Marsh	-5.5	(Hatton et al., 1983)
	Fresh Marsh	-9.7	(Nyman et al. 2006)
	Fresh Marsh	-3.8	(DeLaune et al. 2013)
	Fresh Marsh	-2.2	(Piazza et al., 2011)
	Fresh Marsh	-7.6	(DeLaune et al. 2018)
	Fresh Marsh	-14.6	(Baustian et al., 2021)
	Fresh Marsh	-10.8	(Snedden 2021)
	Fresh Marsh	-8.3	(Nyman et al. 1990)
	Fresh Marsh	-3.0	
	Intermediate Marsh	-7.3	(Snedden 2021)
	Intermediate Marsh	-4.1	(Hatton et al., 1983)
	Intermediate Marsh	-5.6	(Baustian et al., 2021)
	Intermediate Marsh	-4.8	(Nyman et al. 1990)
	Intermediate Marsh	-10.9	(Foret 1997)
	Intermediate Marsh	-1.8	(Graham 2021)
	Intermediate Marsh	-8.6	(Foret 2001)
	Brackish Marsh	-2.8	(Engle, 2011)
	Brackish Marsh	-5.2	(Piazza et al., 2011)
	Brackish Marsh	-10.9	(Smith, DeLaune, and Patrick 1983)
	Brackish Marsh	-4.4	(Hatton et al., 1983)
	Brackish Marsh	-10.4	(Nyman et al. 2006)
	Brackish Marsh	-2.8	(DeLaune et al. 2013)
	Brackish Marsh	-15.1	(Baustian et al., 2021)
	Brackish Marsh	-6.7	(Engle, 2011)
	Brackish Marsh	-12.6	
	Brackish Marsh	-19.8	
	Brackish Marsh	-6.6	(Snedden 2021)
	Brackish Marsh	-3.9	(Graham 2021)

Habitat	Notes	Sediment/Soil Carbon Accumulation rates (tonne CO_2e ha^{-1} yr^{-1})	References
	Brackish Marsh	-7.0	(Nyman et al. 1990)
	Brackish Marsh	-12.4	(Cahoon, 1994; Ouyang & Lee, 2014)
	Brackish Marsh	-16.4	
	Brackish Marsh	-5.1	(Markewich et al., 1998; Ouyang & Lee, 2014)
	Brackish Marsh	-11.4	(Foret 1997)
	Brackish Marsh	-10.8	(Foret 2001)
	Brackish marsh	-10.0	(Wang et al. 2019)
	Saline Wetlands	-6.7	(Smith, DeLaune, and Patrick 1983)
	Saline Wetlands	-6.1	(Hatton et al., 1983)
	Saline Wetlands	-5.6	(Piazza et al., 2011)
	Saline Wetlands	-7.3	(Nyman et al. 2006)
	Saline Wetlands	-5.7	(Baustian et al., 2021)
	Saline Wetlands	-2.8	(Engle, 2011)
	Saline Wetlands	-6.7	
	Saline Wetlands	-12.6	
	Saline Wetlands	-19.8	
	Saline Wetlands	-5.8	(Snedden 2021)
	Saline Wetlands	-2.6	(Smith 2012; Abbott et al. 2019)
	Saline Wetlands	-2.1	
	Saline Wetlands	-3.9	
	Saline Wetlands	-2.6	(Chmura et al., 2003; Ouyang & Lee, 2014)
	Saline Wetlands	-3.4	
	Saline Wetlands	-10.0	(Wang et al. 2019)
	Saline Wetlands	-5.4	(Smith 2012; Abbott et al. 2019)
	Saline Wetlands	-5.4	
	Saline Wetlands	-5.6	
	Saline Wetlands	-4.2	
	Saline Wetlands	-3.6	
	Saline Wetlands	-2.9	
	Saline Wetlands	-7.8	(Nyman et al. 1990)

A.3 NON-CO_2 GREENHOUSE GAS (GHG) FLUX

Table A-3. Non-CO_2 greenhouse gas flux values obtained through literature reviews.

Habitat	Notes	N_2O/CH_4	GHG flux (tonne CO_2e ha^{-1} yr^{-1})	References
Open Water	Fresh	CH_4	+0.0035	(DeLaune et al. 1983)
	Fresh	N_2O	+0.1013	(Smith et al. 1983)
	Fresh	CH_4	+0.3559	(Wang et al. 2021)
	Saline	CH_4	+0.0003	(DeLaune et al. 1983)
	Saline	N_2O	+0.0298	(Smith et al. 1983)
Perennial Ice/Snow	CH_4 and N_2O flux through a Wyoming snowpack	$N_2O + CH_4$	+0.398	(Sommerfeld et al., 1993)
		$N_2O + CH_4$	+0.245	
		$N_2O + CH_4$	+0.384	
		$N_2O + CH_4$	+0.279	
		$N_2O + CH_4$	+0.237	
		$N_2O + CH_4$	+0.160	
		$N_2O + CH_4$	+0.094	
		$N_2O + CH_4$	+0.144	
Developed, Open Space	GHG assumed to be zero.	$N_2O + CH_4$	0.00	-
Developed, Low Intensity	GHG assumed to be zero.	$N_2O + CH_4$	0.00	-
Developed, Medium Intensity	GHG assumed to be zero.	$N_2O + CH_4$	0.00	-
Developed, High Intensity	GHG assumed to be zero.	$N_2O + CH_4$	0.00	-
Barren Land	GHG assumed to be zero.	$N_2O + CH_4$	0.00	-
Deciduous/Evergreen/ Mixed Forests	over-mature forest	$N_2O + CH_4$	+1.510	(Wu & Mu, 2019)
	Korean pine plantation	$N_2O + CH_4$	+0.390	
	hardwood forest	$N_2O + CH_4$	+0.220	
	Betula platyphylla forest	$N_2O + CH_4$	+0.080	
	Populous davidiana forest	$N_2O + CH_4$	+0.310	
	mixed deciduous forest	$N_2O + CH_4$	+0.370	
	Mongolian oak forest	$N_2O + CH_4$	+0.140	
	Old growth forest, Upland	$N_2O + CH_4$	-0.062	(Ullah & Moore, 2011)
	Old growth forest, Slope	$N_2O + CH_4$	+0.033	
	Old growth forest, Riparian	$N_2O + CH_4$	+0.328	
	Old growth forest, Hemlock	$N_2O + CH_4$	+0.493	
	Semi-managed Forest, Upland	$N_2O + CH_4$	+0.063	
	Semi-managed Forest, Slope	$N_2O + CH_4$	+0.043	
	mixed hardwood	$N_2O + CH_4$	-0.123	(Kim & Tanaka, 2003)
	mixed hardwood	$N_2O + CH_4$	-0.105	
	mixed hardwood	$N_2O + CH_4$	-0.098	
	mixed hardwood	$N_2O + CH_4$	-0.019	

Habitat	Notes	N_2O/CH_4	GHG flux (tonne CO_2e ha^{-1} yr^{-1})	References
	mixed hardwood	$N_2O + CH_4$	-0.093	
	mixed hardwood	$N_2O + CH_4$	-0.061	
	mixed hardwood	$N_2O + CH_4$	-0.012	
	Black spruce	$N_2O + CH_4$	-0.065	
	Black spruce	$N_2O + CH_4$	-0.041	
	Black spruce	$N_2O + CH_4$	-0.052	
	Black spruce	$N_2O + CH_4$	-0.001	
	Black spruce	$N_2O + CH_4$	+0.218	
	Black spruce	$N_2O + CH_4$	-0.022	
	Black spruce	$N_2O + CH_4$	-0.082	
	Black spruce	$N_2O + CH_4$	-0.019	
	Black spruce	$N_2O + CH_4$	-0.028	
	Black spruce	$N_2O + CH_4$	+0.026	
	Black spruce	$N_2O + CH_4$	-0.114	
	Black spruce	$N_2O + CH_4$	+0.032	
	Black spruce	CH_4	-0.050	
	Black spruce	CH_4	-0.035	
	Black spruce	CH_4	-0.026	
	Black spruce	$N_2O + CH_4$	-0.045	
	Black spruce	$N_2O + CH_4$	+0.006	
	Black spruce	$N_2O + CH_4$	-0.062	
	Drained spruce site with young trees	$N_2O + CH_4$	+0.302	(Arnold et al., 2005)
	Drained spruce site with young trees	$N_2O + CH_4$	+0.217	
	Drained spruce site with young trees	$N_2O + CH_4$	+0.248	
	Drained spruce site with old trees	$N_2O + CH_4$	+0.155	
	Drained spruce site with old trees	$N_2O + CH_4$	+0.278	
	Drained spruce site with old trees	$N_2O + CH_4$	+0.239	
	Drained spruce site with old trees	$N_2O + CH_4$	+0.224	
	Drained pine site	$N_2O + CH_4$	+0.208	
	Drained pine site	$N_2O + CH_4$	+0.492	
	Drained pine site	$N_2O + CH_4$	+0.377	
Shrub/Scrub	Clocaenog Shrubland	$N_2O + CH_4$	+0.035	(Carter et al., 2012)
	Clocaenog Shrubland	$N_2O + CH_4$	+0.017	
	Clocaenog Shrubland	$N_2O + CH_4$	+0.034	
	Mols Shrubland	$N_2O + CH_4$	-0.072	

Habitat	Notes	N_2O/CH_4	GHG flux (tonne CO_2e ha^{-1} yr^{-1})	References
	Mols Shrubland	$N_2O + CH_4$	-0.075	
	Mols Shrubland	$N_2O + CH_4$	-0.083	
	Brandbjerg Shrubland	$N_2O + CH_4$	-0.009	
	Brandbjerg Shrubland	$N_2O + CH_4$	-0.026	
	Brandbjerg Shrubland	$N_2O + CH_4$	-0.026	
	Oldebroek Shrubland	$N_2O + CH_4$	+0.012	
	Oldebroek Shrubland	$N_2O + CH_4$	-0.074	
	Oldebroek Shrubland	$N_2O + CH_4$	+0.001	
	Garraf Shrubland	$N_2O + CH_4$	-0.066	
	Garraf Shrubland	$N_2O + CH_4$	-0.078	
	Garraf Shrubland	$N_2O + CH_4$	-0.081	
Herbaceous/Grassland	Tallgrass prairie, KN	CH_4	-0.045	(Gebhart et al., 1994)
	Tallgrass prairie, KN	CH_4	-0.043	
	Tallgrass prairie, KN	CH_4	-0.103	
	Tallgrass prairie, KN	CH_4	-0.064	
	Tallgrass prairie, KN	CH_4	-0.205	
	Tallgrass prairie, TX	N_2O	+0.084	(Dowhower et al., 2020)
	Tallgrass prairie, TX	CH_4	+0.099	
	grasslands, Netherlands	CH_4	-0.020	(van den Pol-van Dasselaar et al., 1997)
	Natural grasslands	$N_2O + CH_4$	-0.026	(Kaye et al., 2004)
Hay/Pasture	Grazed Pasture	$N_2O + CH_4$	+0.034	(van Delden et al., 2018)
	Grazed Pasture	$N_2O + CH_4$	+0.030	
Cultivated Crops	Winter wheat-summer maize	CH_4	-0.004	(Wang et al. 2014)
	Winter wheat-summer maize	CH_4	-0.005	
	Winter wheat-summer maize	CH_4	-0.006	
	Winter wheat-summer maize	CH_4	-0.003	
	Winter wheat-summer maize	N_2O	+0.028	
	Winter wheat-summer maize	N_2O	+0.067	
	Winter wheat-summer maize	N_2O	+0.078	
	Winter wheat-summer maize	N_2O	+0.133	
Woody Wetlands	Fresh Forested Wetland	CH_4	+13.33	(Alford et al., 1997)
	Fresh Forested Wetland	CH_4	+19.71	(Lane et al., 2017)
	Fresh Forested Wetland	CH_4	-0.01	(Yu et al., 2008)
	Fresh Forested Wetland	CH_4	+0.46	
	Fresh Forested Wetland	CH_4	+45.6	
	Fresh Forested Wetland	N_2O	+0.13	
	Fresh Forested Wetland	N_2O	+3.39	
	Fresh Forested Wetland	N_2O	+29.6	
	Fresh Forested Wetland	N_2O	+0.13	(Scaroni, 2011)
	Fresh Forested Wetland	N_2O	+0.22	
	Fresh Forested Wetland	N_2O	+0.78	

Habitat	Notes	N_2O/CH_4	GHG flux (tonne CO_2e ha^{-1} yr^{-1})	References
	Fresh Forested Wetland	CH_4	+52.2	(Wang et al. 2021)
	Fresh Forested Wetland	CH_4	+3.94	
	Fresh Forested Wetland	N_2O	+2.58	(Lane et al., 2017)
Emergent Herbaceous Wetlands	Brackish Marsh	CH_4	+18.25	(DeLaune et al. 1983)
	Brackish Marsh	CH_4	+2.78	(Krauss et al., 2016)
	Brackish Marsh	CH_4	+12.40	
	Brackish Marsh	CH_4	+3.450	(Holm et al., 2016)
	Brackish Marsh	N_2O	+0.358	(Krauss et al., 2016)
	Brackish Marsh	N_2O	+0.143	(Smith, DeLaune, and Patrick Jr 1983)
	Brackish Marsh	CH_4	+2.850	(Lane et al., 2016)
	Brackish Marsh	N_2O	+0.033	
	Fresh Marsh	CH_4	+40.000	(DeLaune et al. 1983)
	Fresh Marsh	CH_4	+11.775	(Krauss et al., 2016)
	Fresh Marsh	CH_4	+22.975	
	Fresh Marsh	CH_4	+15.400	(Holm et al., 2016)
	Fresh Marsh	CH_4	+22.900	(Alford et al., 1997)
	Fresh Marsh	N_2O	+0.164	(Smith, DeLaune, and Patrick Jr 1983)
	Fresh Marsh	CH_4	+78.500	(Lane et al., 2016)
	Fresh Marsh	N_2O	+0.176	
	Fresh Marsh	CH_4	+119.56	(Lane et al., 2017)
	Fresh Marsh	N_2O	+0.151	
	Fresh Marsh	N_2O	-0.060	(Krauss et al., 2016)
	Saline Wetlands	CH_4	+1.075	(DeLaune et al. 1983)
	Saline Wetlands	N_2O	+0.092	(Smith, DeLaune, and Patrick Jr 1983)
	Saline Wetlands	CH_4	+1.970	(Lane et al., 2016)
	Saline Wetlands	N_2O	+0.066	

A.4 REFERENCES

Abbott, K. M., Elsey-Quirk, T., & DeLaune, R. D. (2019). Factors influencing blue carbon accumulation across a 32-year chronosequence of created coastal marshes. *Ecosphere*, *10*(8), e02828. https://doi.org/10/gn55xj

Alford, D. P., Delaune, R. D., & Lindau, C. W. (1997). Methane flux from Mississippi River deltaic plain wetlands. *Biogeochemistry*, *37*(3), 227–236. https://doi.org/10/bqvkjw

Anesio, A. M., Hodson, A. J., Fritz, A., Psenner, R., & Sattler, B. (2009). High microbial activity on glaciers: Importance to the global carbon cycle. *Global Change Biology*, *15*(4), 955–960. https://doi.org/10/fph2nj

Arnold, K. V., Weslien, P., Nilsson, M., Svensson, B. H., & Klemedtsson, L. (2005). Fluxes of CO2, CH4 and N2O from drained coniferous forests on organic soils. *Forest Ecology and Management*, *210*(1–3), 239–254. https://doi.org/10/ccnz3h

Baustian, M. M., Stagg, C. L., Perry, C. L., Moss, L., & Carruthers, T. (2021). Long-Term Carbon Sinks in Marsh Soils of the Mississippi River Deltaic Plain Are at Risk to Wetland Loss. *AGU Biogeosciences*, *126*. https://doi.org/10/grmtwt

Brantley, C. G., Day, J. W., Lane, R. R., Hyfield, E., Day, J. N., & Ko, J.-Y. (2008). Primary production, nutrient dynamics, and accretion of a coastal freshwater forested wetland assimilation system in Louisiana. *Ecological Engineering*, *34*(1), 7–22. https://doi.org/10/cvm8jc

Bruce, J. P., Frome, M., Haites, E., Janzen, H., Lal, R., & Paustian, K. (1999). Carbon sequestration in soils. *Journal of Soil and Water Conservation*, *54*(1), 382–389.

Cahoon, D. R. (1994). Recent accretion in two managed marsh impoundments in coastal Louisiana. *Ecological Applications*, *4*(1), 166. https://doi.org/10/cpnctx

Cardoch, L., Day, J. W., & Ibàñez, C. (2002). Net primary productivity as an indicator of sustainability in the EBRO and Mississippi Deltas. *Ecological Applications*, *12*(4), 1044–1055. https://doi.org/10/fvz4g2

Carter, M. S., Larsen, K. S., Emmett, B., Estiarte, M., Field, C., Leith, I. D., Lund, M., Meijide, A., Mills, R. T. E., Niinemets, Ü., Peñuelas, J., Portillo-Estrada, M., Schmidt, I. K., Selsted, M. B., Sheppard, L. J., Sowerby, A., Tietema, A., & Beier, C. (2012). Synthesizing greenhouse gas fluxes across nine European peatlands and shrublands – responses to climatic and environmental changes. *Biogeosciences*, *9*(10), 3739–3755. https://doi.org/10/f23kw4

Chmura, G. L., Anisfeld, S. C., Cahoon, D. R., & Lynch, J. C. (2003). Global Carbon Sequestration in Tidal, Saline Wetland Soils. *Global Biogeochemical Cycles*, *17*(4), 22-1-22–11. https://doi.org/10/fpgmg8

Conant, R. T., Paustian, K., & Elliott, E. T. (2001). Grassland management and conversion into grassland: Effects on soil carbon. *Ecological Applications*, *11*(2). https://doi.org/10/fg55bh

Conner, W. H. (1994). The Effect of salinity and waterlogging on growth and survival of baldcypress and Chinese tallow seedlings. *Journal of Coastal Research*, *10*(4), 1045–1049. JSTOR. https://www.jstor.org/stable/4298295

Conner, W. H., & Day, J. W. (1976). Productivity and composition of a baldcypress-water tupelo site and a bottomland hardwood site in a Louisiana swamp. *American Journal of Botany*, *63*(10), 1354–1364. https://doi.org/10.2307/2441844

Conner, W. H., & Day, J. W. (1987). *The Ecology of Barataria Basin, Louisiana: An Estuarine Profile*. National Wetlands Research Center, U.S. Fish and Wildlife Service, U.S. Department of the Interior.

Conner, W. H., Day, J. W., & Slater, W. R. (1993). Bottomland hardwood productivity: Case study in a rapidly subsiding, Louisiana, USA, watershed. *Wetlands Ecology and Management*, *2*(4), 189–197. https://doi.org/10/dmg6w2

Cramer, G. W., Day, J. W., & Conner, W. H. (1981). Productivity of four marsh sites surrounding Lake Pontchartrain, Louisiana. *American Midland Naturalist*, *106*(1), 65. https://doi.org/10.2307/2425135

Darby, F. A., & Turner, R. E. (2008). Below- and aboveground *Spartina alterniflora* Production in a Louisiana Salt Marsh. *Estuaries and Coasts*, *31*(1), 223–231. https://doi.org/10.1007/s12237-007-9014-7

Day, J. W. (1973). *Community structure and carbon budget of a salt marsh and shallow bay estuarine system in Louisiana*. Center for Wetland Resources, Louisiana State University.

Day, J. W., Butler, T., & Conner, W. (1977). *Productivity and nutrient export studies in a cypress swamp and lake system in Louisiana*. https://doi.org/10.1016/B978-0-12-751802-2.50026-6

Day, J. W., Jr., Lane, R., Moerschbaecher, M., DeLaune, R. D., Mendelssohn, I. A., Baustian, J. J., & Twilley, R. (2013). Vegetation and soil dynamics of a Louisiana estuary receiving pulsed Mississippi river water following Hurricane Katrina. *Estuaries and Coasts*, *36*, 665–682. https://doi.org/10.1007/s12237-012-9581-0

Day, J. W., Westphal, A., Pratt, R., Hyfield, E., Rybczyk, J., Paul Kemp, G., Day, J. N., & Marx, B. (2006). Effects of long-term municipal effluent discharge on the nutrient dynamics, productivity, and benthic community structure of a tidal freshwater forested wetland in Louisiana. *Ecological Engineering*, *27*(3), 242–257. https://doi.org/10.1016/j.ecoleng.2006.03.004

DeLaune, R. D., Kongchum, M., White, J. R., & Jugsujinda, A. (2013). Freshwater diversions as an ecosystem management tool for maintaining soil organic matter accretion in coastal marshes. *Catena*, *107*, 139–144. https://doi.org/10/f4x7v6

DeLaune, R. D., Sasser, C. E., Evers-Hebert, E., White, J. R., & Roberts, H. H. (2016). Influence of the Wax Lake Delta sediment diversion on aboveground plant productivity and carbon storage in deltaic island and mainland coastal marshes. *Estuarine, Coastal and Shelf Science*, *177*, 83–89. https://doi.org/10.1016/j.ecss.2016.05.010

Delaune, R. D., & Smith, C. J. (1984). Carbon cycle and the rate of vertical accumulation of peat in the Mississippi River deltaic plain. *Southeast. Geol.; (United States)*, *25:2*. https://www.osti.gov/biblio/5230563

DeLaune, R. D., Smith, C. J., & Patrick, W. H. (1983). Methane release from Gulf coast wetlands. *Tellus B: Chemical and Physical Meteorology*, *35*(1), 8–15. https://doi.org/10/gh4wht

DeLaune, R. D., White, J. R., Elsey-Quirk, T., Roberts, H. H., & Wang, D. Q. (2018). Differences in long-term vs short-term carbon and nitrogen sequestration in a coastal river delta wetland: Implications for global budgets. *Organic Geochemistry*, *123*, 67–73. https://doi.org/10.1016/j.orggeochem.2018.06.007

Dondini, M., Martin, M., Camillis, C., Uwizeye, A., Soussana, J.-F., Robinson, T., & Steinfeld, H. (2023). *Global assessment of soil carbon in grasslands-from current stock estimates to sequestration potential*. FAO. https://doi.org/10.4060/cc3981en

Dowhower, S. L., Teague, W. R., Casey, K. D., & Daniel, R. (2020). Soil greenhouse gas emissions as impacted by soil moisture and temperature under continuous and holistic planned grazing in native tallgrass prairie. *Agriculture, Ecosystems & Environment*, *287*, 106647. https://doi.org/10/gn54js

Edwards, B. L., Allen, S. T., Braud, D. H., & Keim, R. F. (2019). Stand density and carbon storage in cypress-tupelo wetland forests of the Mississippi River delta. *Forest Ecology and Management*, *441*, 106–114. https://doi.org/10.1016/j.foreco.2019.03.046

Edwards, K. R., & Mills, K. P. (2005). Aboveground and belowground productivity of *Spartina alterniflora* (smooth cordgrass) in natural and created Louisiana salt marshes. *Estuaries*, *28*(2), 252–265. https://doi.org/10.1007/BF02732859

Elder, J. F., & Cairns, D. J. (1982). *Production and Decomposition of Forest Litter Fall on the Apalachicola River Flood Plain, Florida*. U.S. Government Printing Office.

Engle, V. D. (2011). Estimating the provision of ecosystem services by Gulf of Mexico coastal wetlands. *Wetlands*, *31*(1), 179–193. https://doi.org/10.1007/s13157-010-0132-9

Feijtel, T. C., DeLaune, R. D., & Patrick Jr, W. H. (1985). Carbon flow in coastal Louisiana. Marine Ecology Progress Series. *Marine Ecology Progress Series. Oldendorf*, *24*(3), 255–260. http://www.int-res.com/articles/meps/24/m024p255.pdf

Flynn, K. M., Mendelssohn, I. A., & Wilsey, B. J. (1999). The effect of water level management on the soils and vegetation of two coastal Louisiana marshes. *Wetlands Ecology and Management*, *7*(4), 193–218. http://link.springer.com/article/10.1023/A:1008486500173

Foret, J. D. (1997). *Accretion, Sedimentation, and Nutrient Accumulation Rates as Influenced by Manipulations in Marsh Hydrology in the Chenier Plain, Louisiana* [Thesis]. University of Southwestern Louisiana.

Foret, J. D. (2001). *Nutrient Limitation of Tidal Marshes on the Chenier Plain, Louisiana* [Dissertation]. University of Louisiana at Lafayette.

Gebhart, D. L., Johnson, H. B., Mayeux, H. S., & Polley, H. W. (1994). The CRP increases soil organic carbon. *Journal of Soil and Water Conservation*, *49*(5), 488–492.

Graham, S. (2021). *Effects of Marsh Management in Coastal Marsh Impoundments on Marsh Vertical Accretion in the Face of Sea Level Rise.* [Master of Science, Louisiana State University, School of Renewable Natural Resources]. https://digitalcommons.lsu.edu/gradschool_theses/5298

Graham, S., & Mendelssohn, I. (2010). Multiple levels of nitrogen applied to an oligohaline marsh identify a plant community response sequence to eutrophication. *Marine Ecology Progress Series*, *417*, 73–82. https://doi.org/10/dj4tpv

Hatton, R. S., DeLaune, R. D., & Patrick, W. H. (1983). Sedimentation, accretion, and subsidence in marshes of Barataria Basin, Louisiana. *Limnology and Oceanography*, *28*(3), 494–502. https://doi.org/10.4319/lo.1983.28.3.0494

Hillmann, E. R., Rivera-Monroy, V. H., Nyman, J. A., & La Peyre, M. K. (2020). Estuarine Submerged Aquatic Vegetation Habitat Provides Organic Carbon Storage Across a Shifting Landscape. *Science of The Total Environment*, *717*, 137217. https://doi.org/10.1016/j.scitotenv.2020.137217

Hillmann, E. R., Shaffer, G. P., Wood, W. B., Day, J. W., Day, J., Mancuso, J., Lane, R. R., & Hunter, R. G. (2019). Above- and belowground response of baldcypress and water tupelo seedlings to variable rates of nitrogen loading: Mesocosm and field studies. *Ecological Engineering*, *137*, 1–6. https://doi.org/10.1016/j.ecoleng.2018.08.019

Hoeppner, S. S., Shaffer, G. P., & Perkins, T. E. (2008). Through droughts and hurricanes: Tree mortality, forest structure, and biomass production in a coastal swamp targeted for restoration in the Mississippi River Deltaic Plain. *Forest Ecology and Management*, *256*(5), 937–948. https://doi.org/10.1016/j.foreco.2008.05.040

Holm, G. O., Perez, B. C., McWhorter, D. E., Krauss, K. W., Johnson, D. J., Raynie, R. C., & Killebrew, C. J. (2016). Ecosystem Level Methane Fluxes from Tidal Freshwater and Brackish Marshes of the Mississippi River Delta: Implications for Coastal Wetland Carbon Projects. *Wetlands*, *36*, 401–413. https://doi.org/10/f8ptzg

Hopkinson, C. S., Gosselink, J. G., & Parrondo, R. T. (1978). Aboveground production of seven marsh plant species in coastal Louisiana. *Ecology*, *59*(4), 760–769. https://doi.org/10.2307/1938780

Hopkinson, C. S., Gosselink, J. G., & Parrondo, R. T. (1980). Production of coastal Louisiana marsh plants calculated from phenometric techniques. *Ecology*, *61*(5), 1091–1098. https://doi.org/10.2307/1936828

Hou, G., Delang, C. O., Lu, X., & Gao, L. (2020). A meta-analysis of changes in soil organic carbon stocks after afforestation with deciduous broadleaved, sempervirent broadleaved, and conifer tree species. *Annals of Forest Science*, *77*(4), 92. https://doi.org/10/gq7f8z

Hupp, C. R., Kroes, D. E., Noe, G. B., Schenk, E. R., & Day, R. H. (2019). Sediment trapping and carbon sequestration in floodplains of the lower Atchafalaya Basin, LA: Allochthonous versus autochthonous carbon sources. *Journal of Geophysical Research: Biogeosciences*, *124*(3), 663–677. https://doi.org/10.1029/2018JG004533

Kaswadji, R. F., Gosselink, J. G., & Turner, R. E. (1990). Estimation of primary production using five different methods in a *Spartina alterniflora* salt marsh. *Wetlands Ecology and Management*, *1*(2). https://doi.org/10.1007/BF00177280

Kaye, J. P., Burke, I. C., Mosier, A. R., & Pablo Guerschman, J. (2004). Methane and Nitrous Oxide Fluxes from Urban Soils to the Atmosphere. *Ecological Applications*, *14*(4), 975–981. https://doi.org/10/dftj9f

Kim, Y., & Tanaka, N. (2003). Effect of forest fire on the fluxes of CO_2, CH_4 and N_2O in boreal forest soils, interior Alaska. *Journal of Geophysical Research: Atmospheres*, *108*(D1). https://doi.org/10/c4zwc4

Kirby, C. J., & Gosselink, J. G. (1976). Primary production in a Louisiana Gulf Coast *Spartina alterniflora* marsh. *Ecology*, *57*(5), 1052–1059. https://doi.org/10.2307/1941070

Krauss, K. W., Holm, G. O., Perez, B. C., McWhorter, D. E., Cormier, N., Moss, R. F., Johnson, D. J., Neubauer, S. C., & Raynie, R. C. (2016). Component greenhouse gas fluxes and radiative balance from two deltaic marshes in Louisiana: Pairing chamber techniques and eddy covariance. *Journal of Geophysical Research: Biogeosciences*, *121*(6), 1503–1521. https://doi.org/10/grpfpm

Lal, R., Follett, R. F., Kimble, J., & Cole, C. V. (1999). Managing U.S. cropland to sequester carbon in soil. *Journal of Soil and Water Conservation*, *54*(1), 374–381. https://www.jswconline.org/content/54/1/374

Lane, R. R., Mack, S. K., Day, J. W., DeLaune, R. D., Madison, M. J., & Precht, P. R. (2016). Fate of soil organic carbon during wetland loss. *Wetlands*, *36*(6), 1167–1181. https://doi.org/10.1007/s13157-016-0834-8

Lane, R. R., Mack, S. K., Day, J. W., Kempka, R., & Brady, L. J. (2017). Carbon sequestration at a forested wetland receiving treated municipal effluent. *Wetlands*, *37*(5), 861–873. https://doi.org/10/gb4skr

Liebig, M. A., Morgan, J. A., Reeder, J. D., Ellert, B. H., Gollany, H. T., & Schuman, G. E. (2005). Greenhouse gas contributions and mitigation potential of agricultural practices in northwestern USA and western Canada. *Soil and Tillage Research*, *83*(1), 25–52. https://doi.org/10/cfspgn

Markewich, W., Britsch, L. D., Buell, G. R., Dillon, D. L., Fraticelli, C. M., Fries, T. L., Markewich, H. W., Mcgeehin, J. P., Pracht, J. B., Robbins, J. A., Samuel, B. M., & Wrenn, J. H. (1998). *Carbon Storage and Late Holocene Chronostratigraphy of a Mississippi River Deltaic Marsh, St. Bernard Parish, Louisiana* (Open-File Report 98–36; Mississippi Basin Carbon Project Process Studies, p. 66). U.S. Geological Survey. https://pubs.usgs.gov/of/1998/0036/report.pdf

Megonigal, J. P., Conner, W. H., Kroeger, S., & Sharitz, R. R. (1997). Aboveground production in southeastern floodplain forests: A test of the subsidy–stress hypothesis. *Ecology*, *78*(2), 370–384. https://doi.org/10.1890/0012-9658(1997)078[0370:APISFF]2.0.CO;2

Middleton, B. A., & McKee, K. L. (2004). Use of a latitudinal gradient in bald cypress (*Taxodium distichum*) production to examine physiological controls of biotic boundaries and potential responses to environmental change. *Global Ecology and Biogeography*, *13*, 247–258. https://doi.org/10/fmhmc9

Murray, F., Baldi, G., von Bernard, T., Viglizzo, E. F., & Jobbágy, E. G. (2016). Productive performance of alternative land covers along aridity gradients: Ecological, agronomic and economic perspectives. *Agricultural Systems*, *149*, 20–29. https://doi.org/10/f89q2r

Nyman, J. A., Delaune, R. D., & Patrick, W. H. (1990). Wetland soil formation in the rapidly subsiding Mississippi River Deltaic Plain: Mineral and organic matter relationships. *Estuarine, Coastal and Shelf Science*, *31*(1), 57–69. https://doi.org/10/dhx9q2

Nyman, J. A., DeLaune, R. D., Pezeshki, S. R., & Patrick, W. H., Jr. (1995). Organic matter fluxes and marsh stability in a rapidly submerging estuarine marsh. *Estuaries*, *18*(1B), 207–218. https://doi.org/10/dknpj9

Nyman, J. A., Walters, R. J., Delaune, R. D., & Patrick Jr, W. H. (2006). Marsh vertical accretion via vegetative growth. *Estuarine, Coastal and Shelf Science*, *69*, 370–380. https://doi.org/10/d3wjmw

Ouyang, X., & Lee, S. Y. (2014). Updated Estimates of Carbon Accumulation Rates in Coastal Marsh Sediments. *Biogeosciences*, *11*(18), 5057–5071. https://doi.org/10/f6kbg6

Pezeshki, S. R., & DeLaune, R. D. (1991). A comparative study of above-ground productivity of dominant U.S. Gulf Coast marsh species. *Journal of Vegetation Science*, *2*(3), 331–338. https://doi.org/10/fttvvw

Pham, H. T. (2014). *The rate and process of mangrove forest expansion on above- and belowground carbon relations in coastal Louisiana* [Dissertation]. North Carolina Agricultural and Technical State University.

Piazza, S. C., Steyer, G. D., Cretini, K. F., Sasser, C. E., Visser, J. M., Holm, G. O., Sharp, L. A., Evers, D. E., & Meriwether, J. R. (2011). *Geomorphic and Ecological Effects of Hurricanes Katrina and Rita on Coastal Louisiana Marsh Communities* (Open-File Report 2011–1094; p. 126). U.S. Geological Survey.

Reinsch, S., Koller, E., Sowerby, A., De Dato, G., Estiarte, M., Guidolotti, G., Kovács-Láng, E., Kröel-Dulay, G., Lellei-Kovács, E., Larsen, K. S., Liberati, D., Peñuelas, J., Ransijn, J., Robinson, D. A., Schmidt, I. K., Smith, A. R., Tietema, A., Dukes, J. S., Beier, C., & Emmett, B. A. (2017). Shrubland primary production and soil respiration diverge along European climate gradient. *Scientific Reports*, *7*(1), 43952. https://doi.org/10/f9tmxs

Rybczyk, J. M., Day, J. W., & Conner, W. H. (2002). The impact of wastewater effluent on accretion and decomposition in a subsiding forested wetland. *Wetlands*, *22*(1), 18–32. https://doi.org/10/bwvmc3

Sasser, C. E., Evers-Hebert, E., Holm, G. O., Milan, B., Sasser, J. B., Peterson, E. F., & DeLaune, R. D. (2018). Relationships of marsh soil strength to belowground vegetation biomass in Louisiana coastal marshes. *Wetlands*, *38*(2), 401–409. https://doi.org/10.1007/s13157-017-0977-2

Sasser, C. E., & Gosselink, J. G. (1984). Vegetation and primary production in a floating freshwater marsh in Louisiana. *Aquatic Botany*, *20*(3), 245–255. https://doi.org/10.1016/0304-3770(84)90090-1

Scaroni, A. E. (2011). *The effect of habitat change on nutrient removal in the Atchafalaya River Basin, Louisiana* [Dissertation]. Louisiana State University.

Shaffer, G., Day, J., Kandalepas, D., Wood, W., Hunter, R., Lane, R., & Hillmann, E. (2016). Decline of the Maurepas Swamp, Pontchartrain Basin, Louisiana, and approaches to restoration. *Water*, *8*(3), 101. https://doi.org/10.3390/w8030101

Shaffer, G. P., Wood, W. B., Hoeppner, S. S., Perkins, T. E., Zoller, J., & Kandalepas, D. (2009). Degradation of baldcypress–water tupelo swamp to marsh and open water in Southeastern Louisiana, U.S.A.: An irreversible trajectory? *Journal of Coastal Research*, *10054*, 152–165. https://doi.org/10/cpz4ds

Smith, C. J., DeLaune, R. D., & Patrick Jr, W. H. (1983). Carbon dioxide emission and carbon accumulation in coastal wetlands. *Estuarine, Coastal and Shelf Science*, *17*, 21–29. https://doi.org/10/ffk8tt

Smith, C. J., DeLaune, R. D., & Patrick, W. H. (1983). Nitrous oxide emission from Gulf Coast wetlands. *Geochimica et Cosmochimica Acta*, *47*(10), 1805–1814. https://doi.org/10/fvxsvc

Smith, K. (2012). *Paleoecological study of coastal marsh in the Chenier Plain, Louisiana: Investigating the diatom composition of hurricane-deposited sediments and a diatom-based quantitative reconstruction of sea-level characteristics* [Dissertation, University of Florida]. https://www.proquest.com/openview/5161101a3cc36613372c30be59609871/1?pq-origsite=gscholar&cbl=18750

Snedden, G. (2021). *Soil properties and soil radioisotope activity across Breton Sound basin wetlands (2008-2013)* [Data release]. U.S. Geological Survey. https://doi.org/10.5066/P9XWAXOT

Snedden, G. A., Cretini, K., & Patton, B. (2015). Inundation and salinity impacts to above- and belowground productivity in *Spartina patens* and *Spartina alterniflora* in the Mississippi River Deltaic Plain: Implications for using river diversions as restoration tools. *Ecological Engineering*, *81*, 133–139. https://doi.org/10/f7fmwz

Sommerfeld, R., Mosier, A., & Musselman, R. (1993). CO2, CH4 and N2O flux through a Wyoming snowpack and implications for global budgets. *Nature*, *361*(6408), 140–142. https://doi.org/10/bgjq5d

Stagg, C. L., & Mendelssohn, I. A. (2011). Controls on resilience and stability in a sediment-subsidized salt marsh. *Ecological Applications*, *21*(5), 1731–1744. https://doi.org/10/dsqjqs

Stagg, C. L., Schoolmaster, D. R., Piazza, S. C., Snedden, G., Steyer, G. D., Fischenich, C. J., & McComas, R. W. (2016). A landscape-scale assessment of above- and belowground primary production in coastal wetlands: Implications for climate change-induced community shifts. *Estuaries and Coasts*. https://doi.org/10/f94nbz

Stockle, C., Higgins, S., Kemanian, A., Nelson, R., Huggins, D., Marcos, J., & Collins, H. (2012). Carbon storage and nitrous oxide emissions of cropping systems in eastern Washington: A simulation study. *Journal of Soil and Water Conservation*, *67*(5), 365–377. https://doi.org/10/f4mm2p

Stow, C. A., De Laune, R. D., & Patrick, W. H. (1985). Nutrient fluxes in a eutrophic coastal Louisiana freshwater lake. *Environmental Management*, *9*(3), 243–251. https://doi.org/10/dqsggm

Sun, Y., Chang, J., & Fang, J. (2023). Above- and belowground net-primary productivity: A field-based global database of grasslands. *Ecology*, *104*(2), e3904. https://doi.org/10/gs7wm9

Ullah, S., & Moore, T. R. (2011). Biogeochemical controls on methane, nitrous oxide, and carbon dioxide fluxes from deciduous forest soils in eastern Canada. *Journal of Geophysical Research*, *116*(G3), G03010. https://doi.org/10/cj45dz

van Delden, L., Rowlings, D. W., Scheer, C., De Rosa, D., & Grace, P. R. (2018). Effect of urbanization on soil methane and nitrous oxide fluxes in subtropical Australia. *Global Change Biology*, *24*(12), 5695–5707. https://doi.org/10/gtktmp

van den Pol-van Dasselaar, A., van Beusichem, M. L., & Oenema, O. (1997). Effects of grassland management on the emission of methane from intensively managed grasslands on peat soil. *Plant and Soil*, *189*(1), 1–9. https://doi.org/10/crw7rs

Wang, D., White, J. R., Delaune, R. D., Yu, Z., & Hu, Y. (2021). Peripheral freshwater deltaic wetlands are hotspots of methane flux in the coastal zone. *Science of The Total Environment*, *775*, 145784. https://doi.org/10.1016/j.scitotenv.2021.145784

Wang, F., Lu, X., Sanders, C. J., & Tang, J. (2019). Tidal wetland resilience to sea level rise increases their carbon sequestration capacity in United States. *Nature Communications*, *10*(1), 5434. https://doi.org/10/gjjpsz

Wang, Y., Hu, C., Ming, H., Oenema, O., Schaefer, D. A., Dong, W., Zhang, Y., & Li, X. (2014). Methane, Carbon Dioxide and Nitrous Oxide Fluxes in Soil Profile under a Winter Wheat-Summer Maize Rotation in the North China Plain. *PLoS ONE*, *9*(6), e98445. https://doi.org/10/f6bfdd

West, T. O., & Post, W. M. (2002). Soil Organic Carbon Sequestration Rates by Tillage and Crop Rotation: A Global Data Analysis. *Soil Science Society of America Journal*, *66*(6), 1930–1946. https://doi.org/10/dnzmfx

White, D. A., & Simmons, M. J. (1988). Productivity of the marshes at the mouth of the Pearl River, Louisiana. *Castanea*, *53*(3), 215–224. https://www.jstor.org/stable/4033568

White, D. A., Weiss, T. E., Trapani, J. M., & Thien, L. B. (1978). Productivity and decomposition of the dominant salt marsh plants in Louisiana. *Ecology*, *59*(4), 751. https://doi.org/10.2307/1938779

Wu, B., & Mu, C. (2019). Effects on Greenhouse Gas (CH4, CO2, N2O) Emissions of Conversion from Over-Mature Forest to Secondary Forest and Korean Pine Plantation in Northeast China. *Forests*, *10*(9), 788. https://doi.org/10/gs8b37

Yellajosula, G., Cihacek, L., Faller, T., & Schauer, C. (2020). Soil Carbon Change Due to Land Conversion to Grassland in a Semi-Arid Environment. *Soil Systems*, *4*(3), 43. https://doi.org/10/gs8b35

Yu, K., Faulkner, S. P., & Baldwin, M. J. (2008). Effect of hydrological conditions on nitrous oxide, methane, and carbon dioxide dynamics in a bottomland hardwood forest and its implication for soil carbon sequestration. *Global Change Biology*, *14*(4), 798–812. https://doi.org/10/dtgjf6

Zhou, Z.-Y., Li, F.-R., Chen, S.-K., Zhang, H.-R., & Li, G. (2011). Dynamics of vegetation and soil carbon and nitrogen accumulation over 26 years under controlled grazing in a desert shrubland. *Plant and Soil*, *341*(1), 257–268. https://doi.org/10/fc7jt3

APPENDIX B. SUPPLEMENTAL ANNUAL NET PRIMARY PRODUCTIVITY (ANPP) ESTIMATION FOR FOREST HABITATS

Land use/land cover (LULC) maps with a 10 m resolution for years 2017 to 2022, derived from European Space Agency (ESA) Sentinel-2 imagery data, were used to identify forest habitats areas within each DoD facility. For Scott Air Force Base (AFB) and Fort Moore, the forest habitat area remained relatively stable from 2017 to 2022. Conversely, at Tyndall AFB (Figure B-1), there was a notable decrease in forest cover in 2019, and the forest area had not recovered by 2022. The forest loss at Tyndall AFB was a consequence of Hurricane Michael in 2018. These data are displayed in Figure B-1, Figure B-2, and Figure B-3.

The National Forest Carbon Monitoring System (NFCMS) (https://doi.org/10.3334/ORNLDAAC/1829) provides data on aboveground woody biomass (AGB) and coarse woody debris (CWD). Using this data, an estimate of forest ANPP was derived by measuring the increase in AGB and CWD between the years 2000 and 2010, and then dividing the total increase by the number of years (10), therefore assuming a constant linear rate of change per year. Negative net AGB values were excluded since they indicate the removal or reduction of forest trees due to various disturbances, such as fire, harvest, or deforestation. The same criterion was applied to the calculation of CWD. Derived ANPP rates were plotted across forest habitat maps on each DoD facility spanning from 2017 to 2022 (Figure B-4, Figure B-5, and Figure B-6) and used to estimate forest ANPP specifically within each site's forested habitats during the specified time frame (Table B-1).

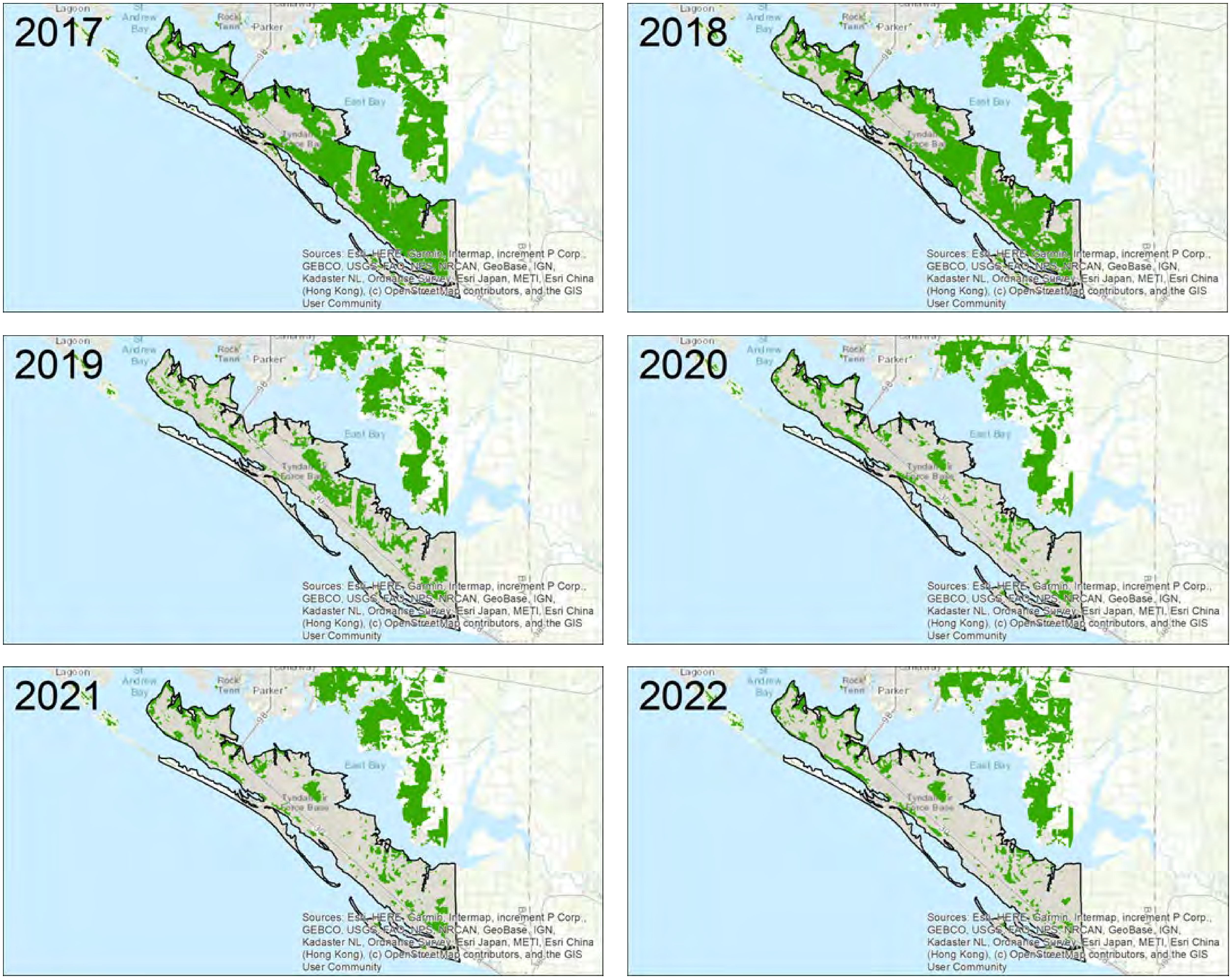

Figure B-1. Forest habitat change at the Tyndall AFB from 2017 to 2022. Green represents forest. Black polygon line indicates Tyndall AFB area. Note the large reduction in forest habitat seen between 2018 and 2019 due to Hurricane Michael, a Category 5 hurricane which made landfall near Tyndall AFB on October 10, 2018.

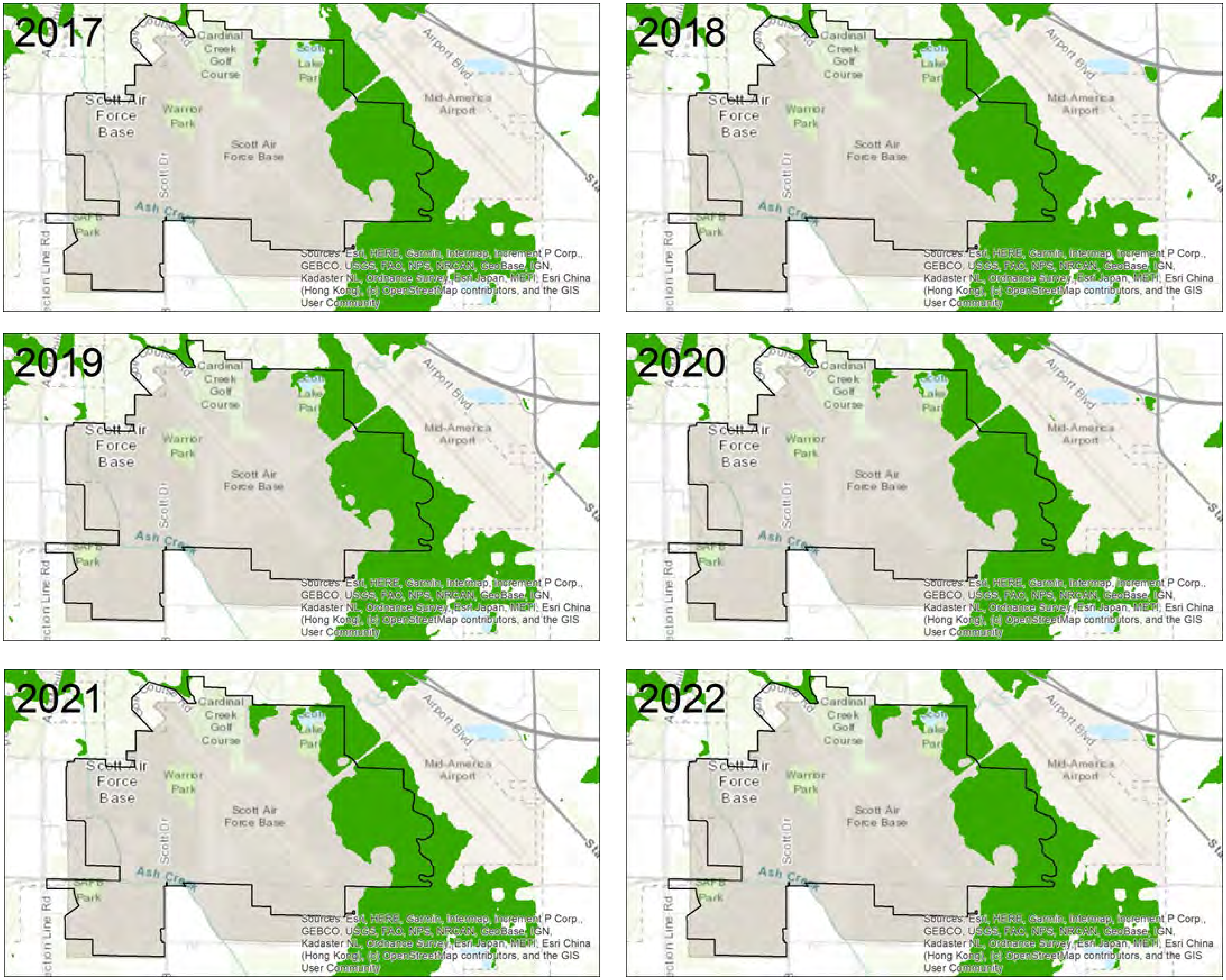

Figure B-2. Forest habitat change at the Scott AFB from 2017 to 2022. Green represents forest. Black polygon line indicates Tyndall AFB area.

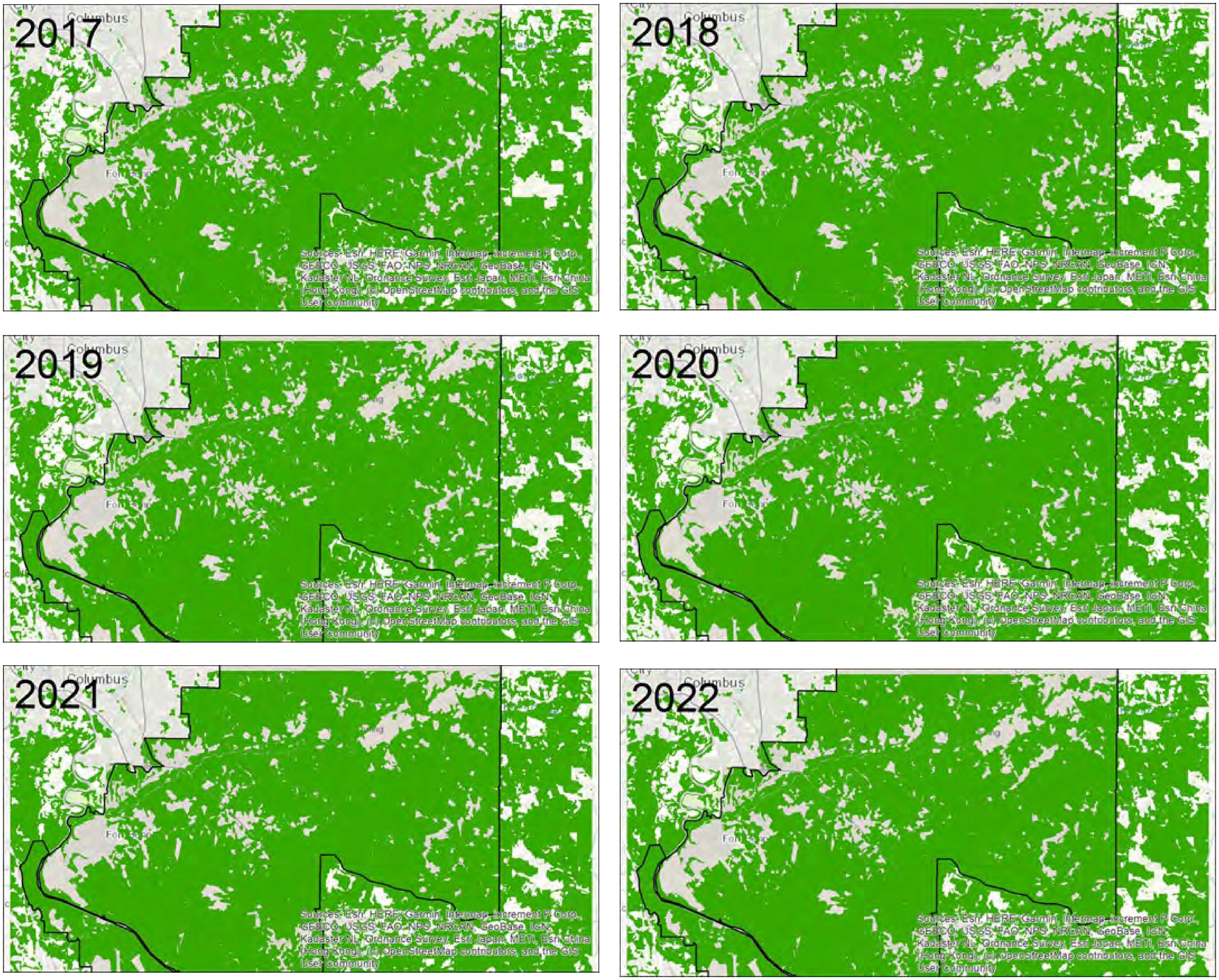

Figure B-3. Forest habitat change at Fort Moore from 2017 to 2022. Green represents forest. Black polygon line indicates Tyndall AFB area.

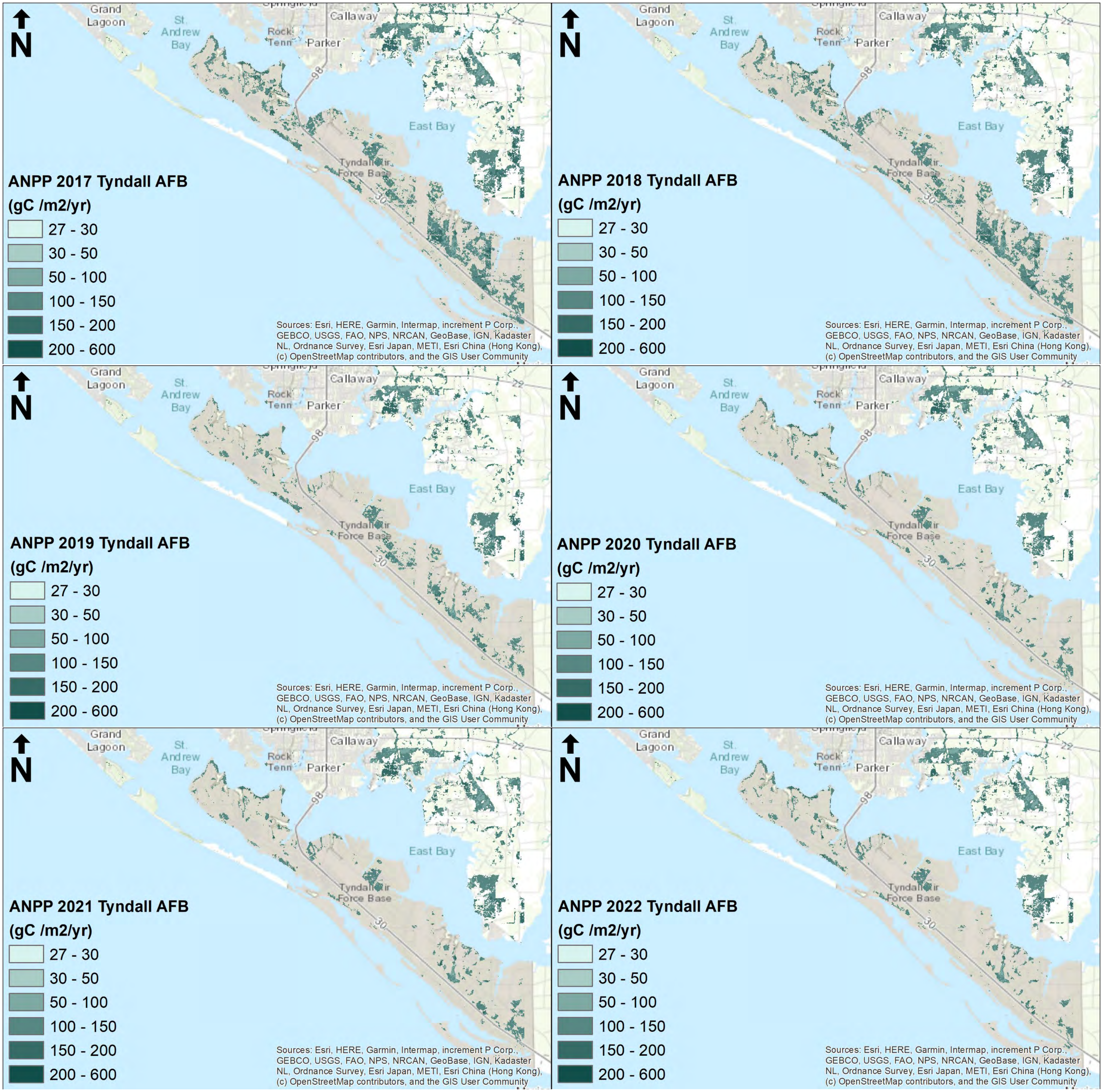

Figure B-4. Estimated ANPP (gC m^{-2} yr^{-1}) values in forest habitats surrounding Tyndall AFB from 2017 to 2022

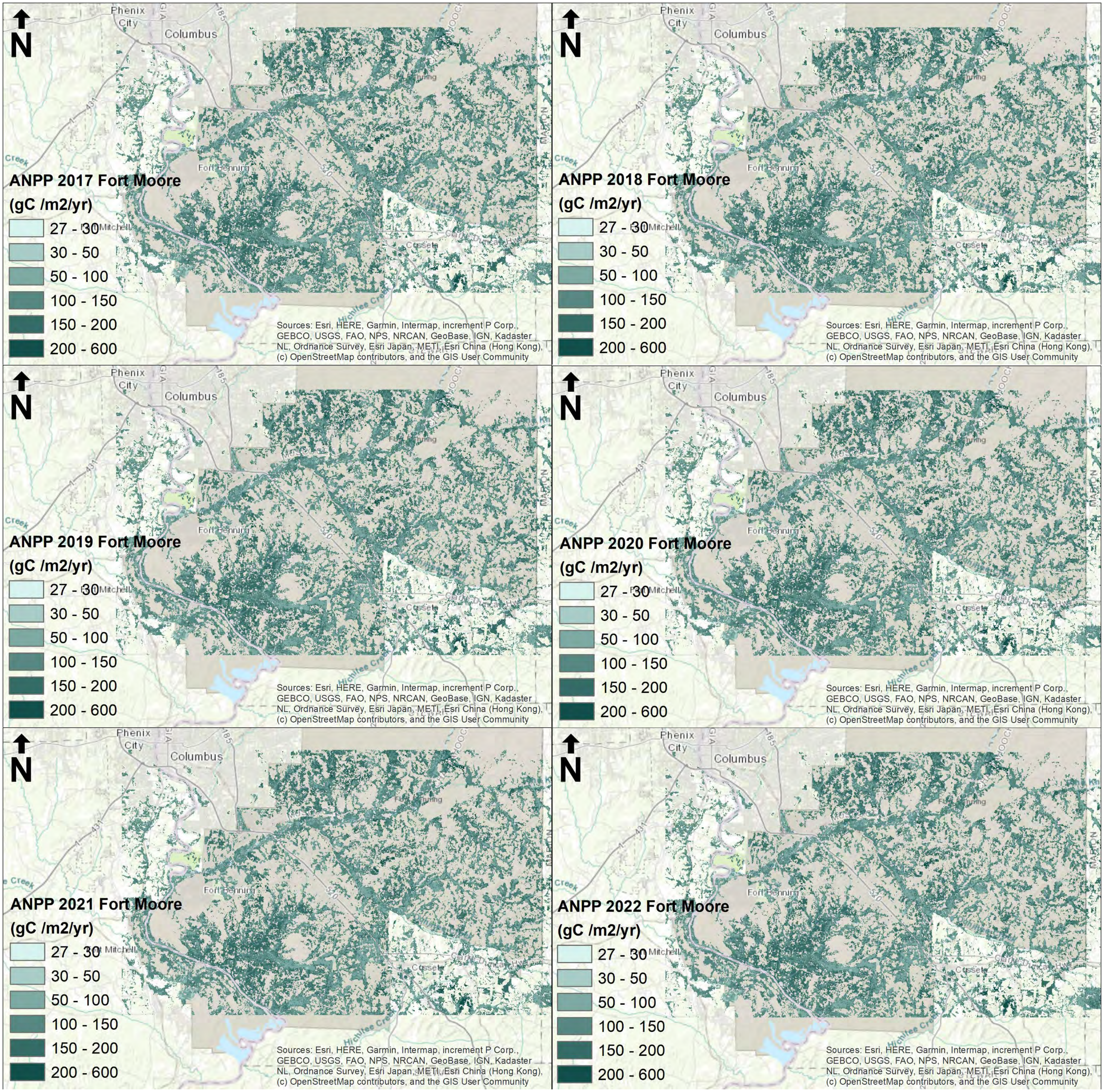

Figure B-5. Estimated ANPP (gC m^{-2} yr^{-1}) values in forest habitats surrounding Fort Moore from 2017 to 2022.

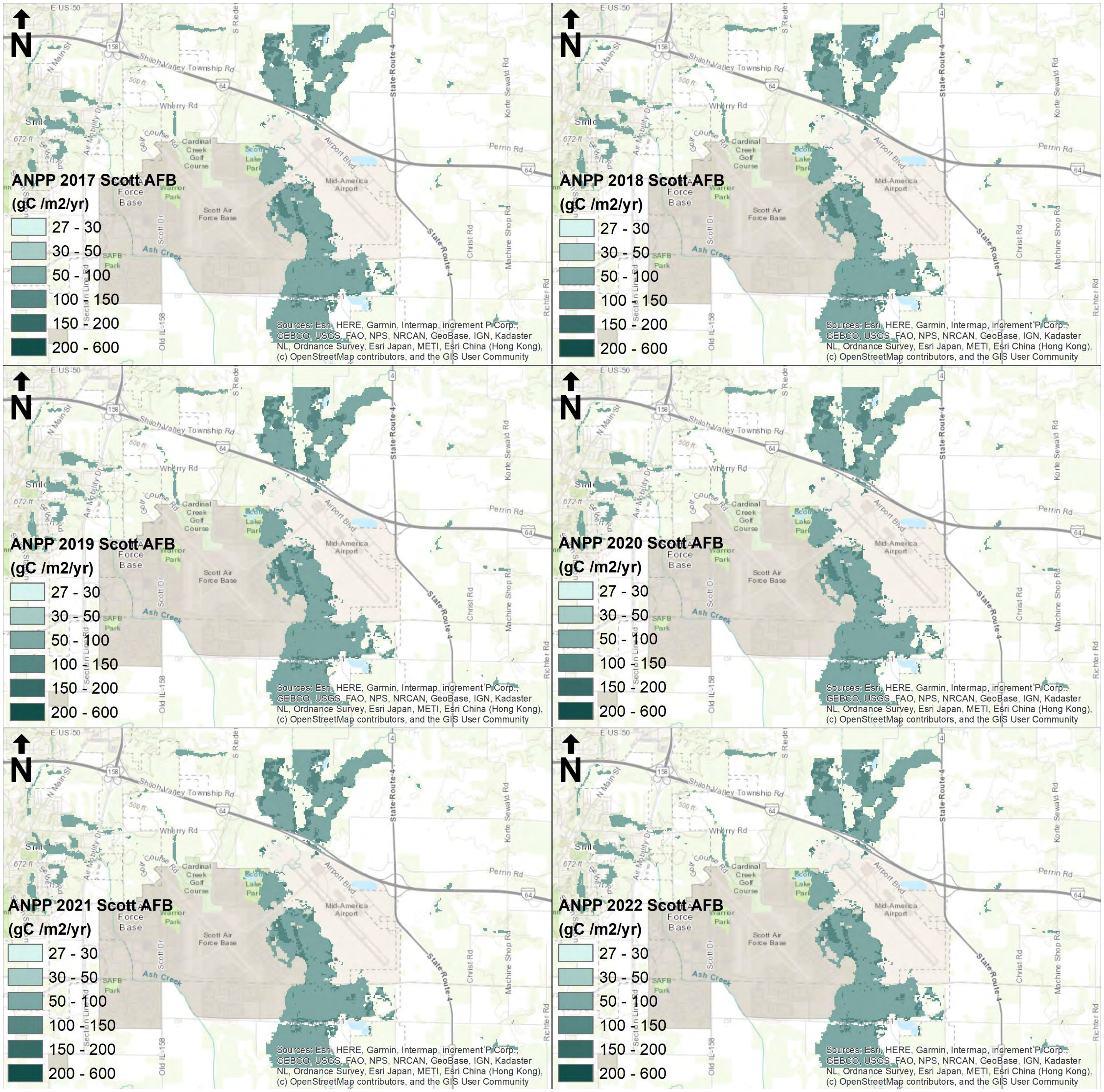

Figure B-6. Estimated ANPP (gC m^{-2} yr^{-1}) values in forest habitats surrounding Scott AFB from 2017 to 2022

Table B-1. Estimated aboveground net primary productivity (ANPP) of forests in three sites.

Sites	Dominant Tree	Year	Area (ha)	ANPP (tonne CO_2e ha^{-1} yr^{-1})			
				Mean	STD	SE	% Uncertainty
Tyndall AFB	Loblolly/Shortleaf Pine	2017	5,317	-4.84	0.91	0.00	0.1%
		2018	5,018	-4.82	0.91	0.00	0.1%
		2019	3,108	-4.87	0.89	0.00	0.1%
		2020	3,156	-4.80	0.90	0.00	0.1%
		2021	3,162	-4.81	0.90	0.00	0.1%
		2022	3,038	-4.78	0.91	0.00	0.1%
Scott AFB	Elm/Ash/Cottonwood	2017	1,294	-2.90	0.65	0.01	0.2%
		2018	1,331	-2.91	0.64	0.01	0.2%
		2019	1,314	-2.91	0.64	0.01	0.2%
		2020	1,314	-2.90	0.64	0.01	0.2%
		2021	1,326	-2.91	0.64	0.01	0.2%
		2022	1,315	-2.90	0.64	0.01	0.2%
Fort Moore	Loblolly/Shortlear Pine	2017	39,063	-4.80	1.27	0.00	0.0%
		2018	39,391	-4.80	1.27	0.00	0.0%
		2019	39,430	-4.80	1.27	0.00	0.0%
		2020	39,426	-4.80	1.27	0.00	0.0%
		2021	39,561	-4.82	1.28	0.00	0.0%
		2022	39,259	-4.82	1.29	0.00	0.0%

APPENDIX C. NATIONAL LAND COVER DATABASE CLASSIFICATIONS

The National Land Cover Database (NLCD) is a comprehensive land cover dataset that provides information on land use and land cover across the U.S. The NLCD is updated every 2-to-3 years and is considered the definitive land cover database for the country. The NLCD habitat classifications for Scott AFB, Fort Moore, and Tyndall AFB from 2001 to 2021 are contained in this appendix. The NLCD habitat classifications provide information on the types of habitats present in these areas, including grasslands, forests, wetlands, and developed areas.

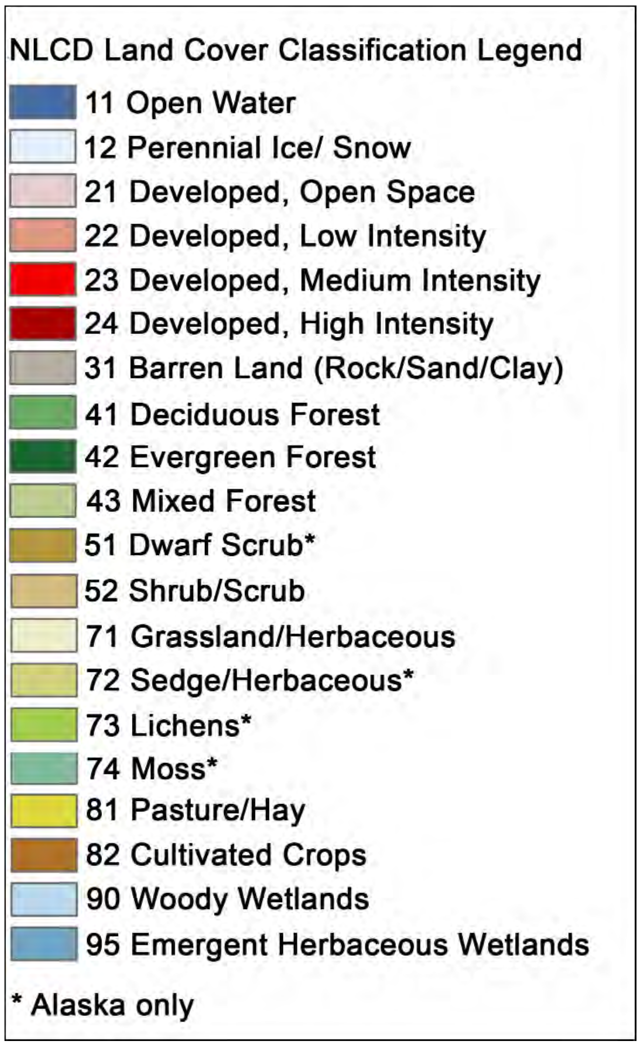

Figure C-1. NLCD class legend

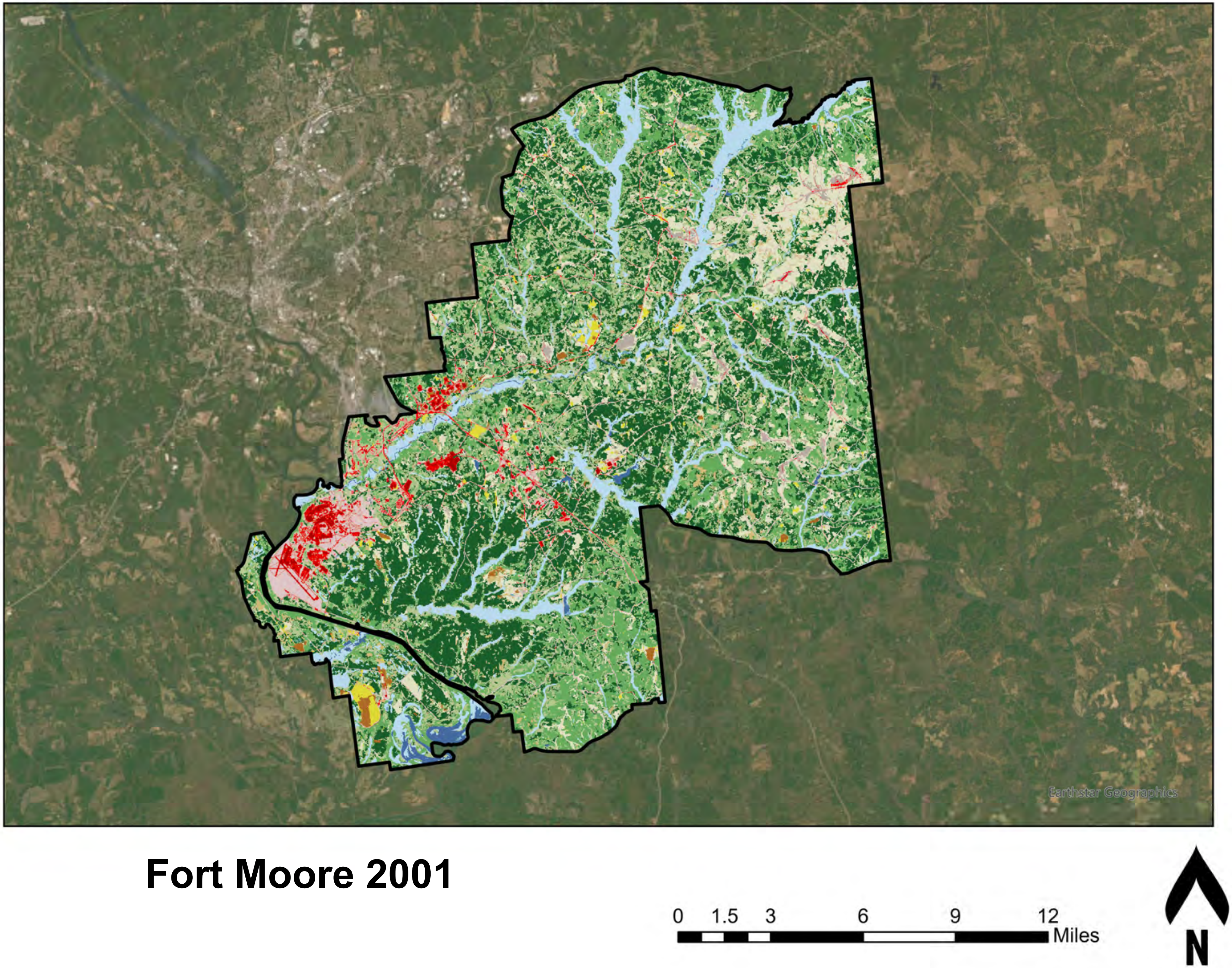

Fort Moore 2001

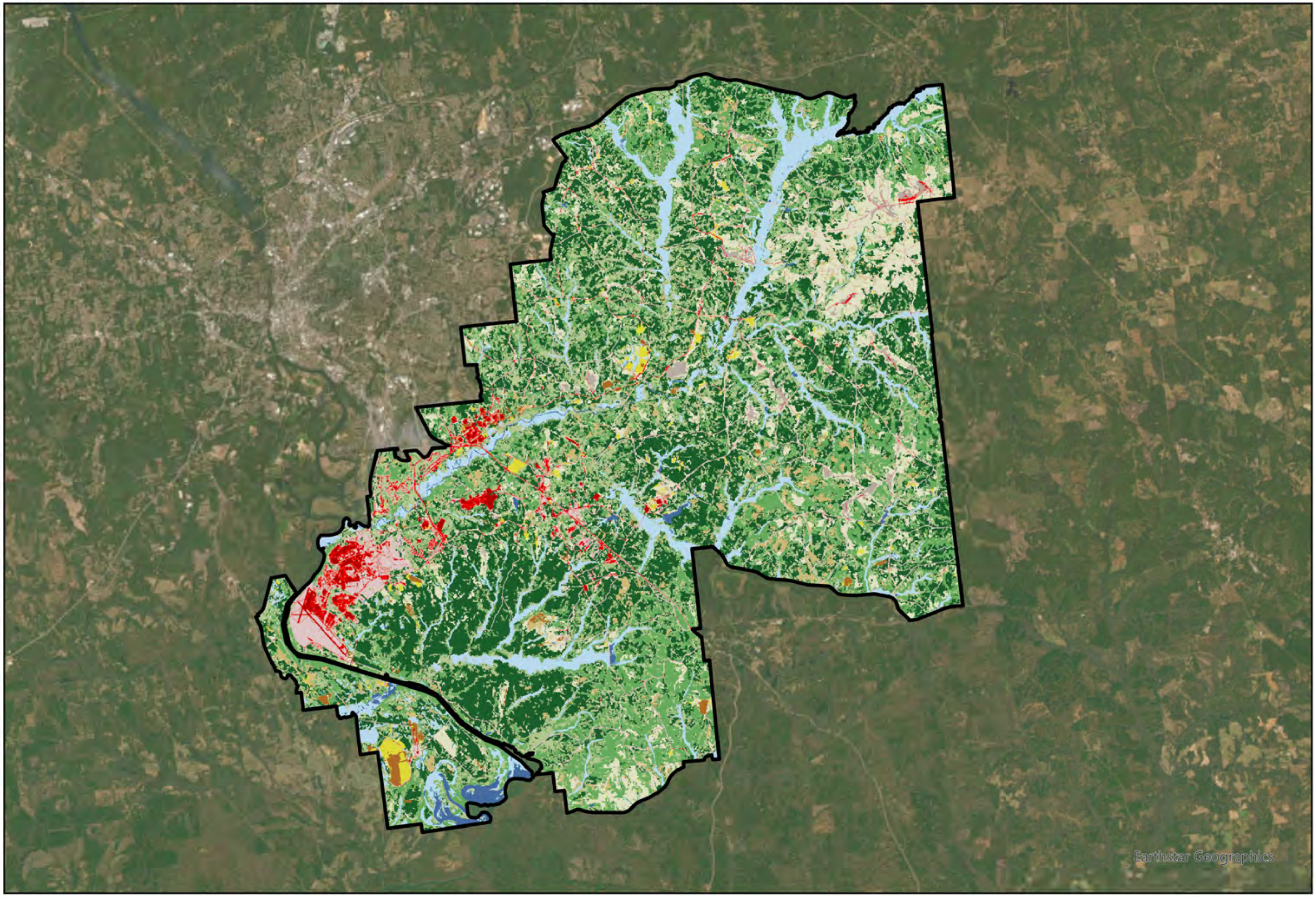

Fort Moore 2004

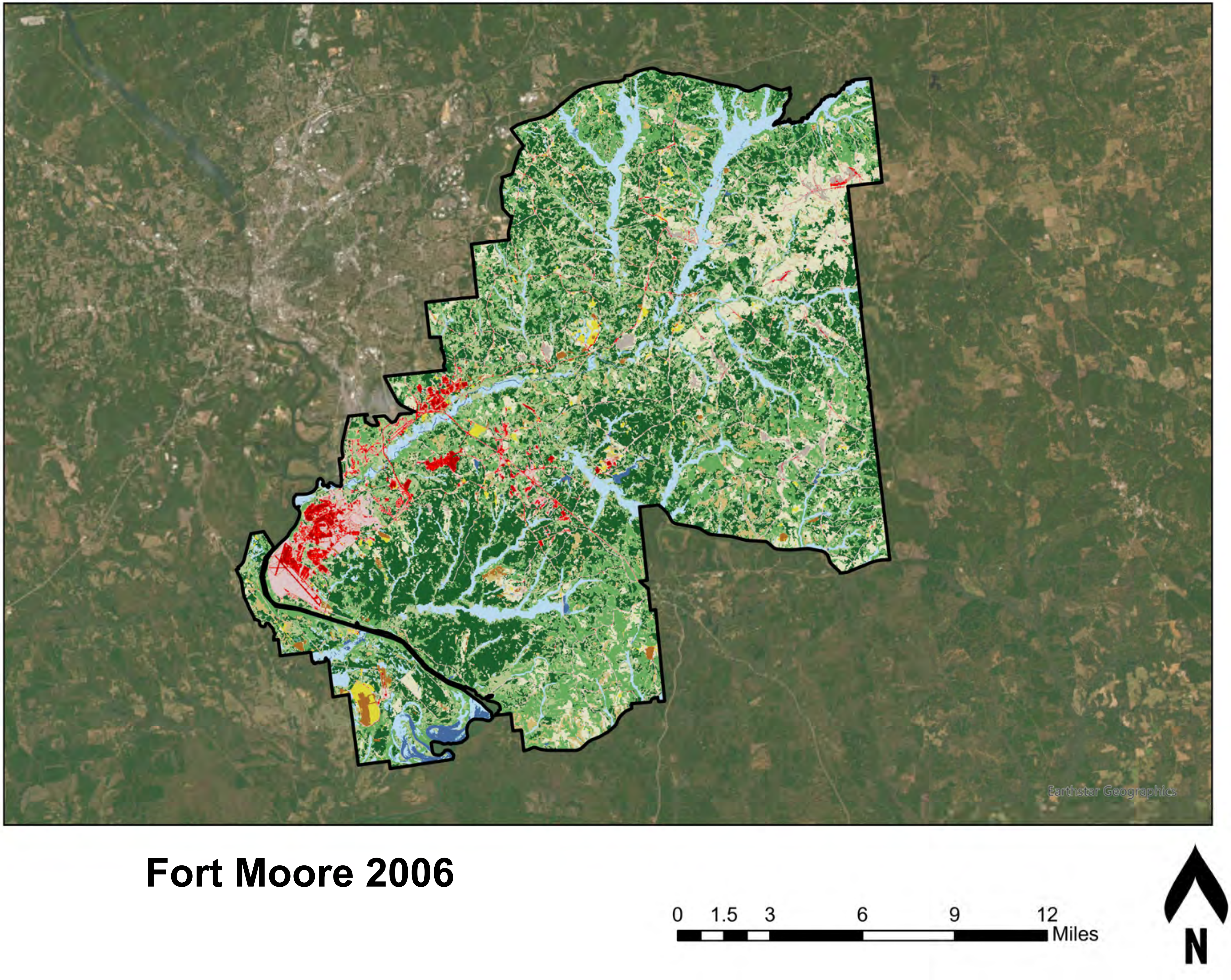

Fort Moore 2006

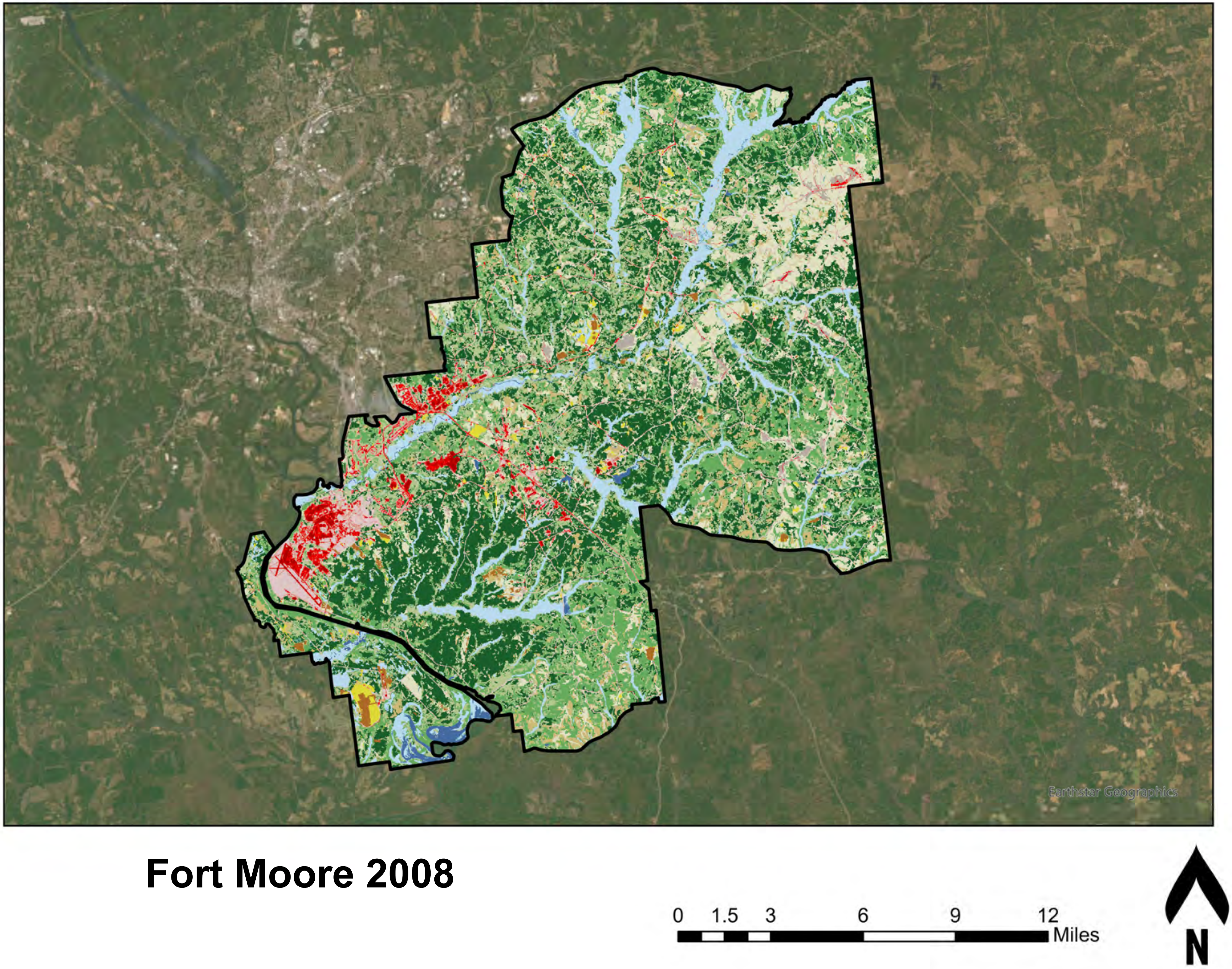

Fort Moore 2008

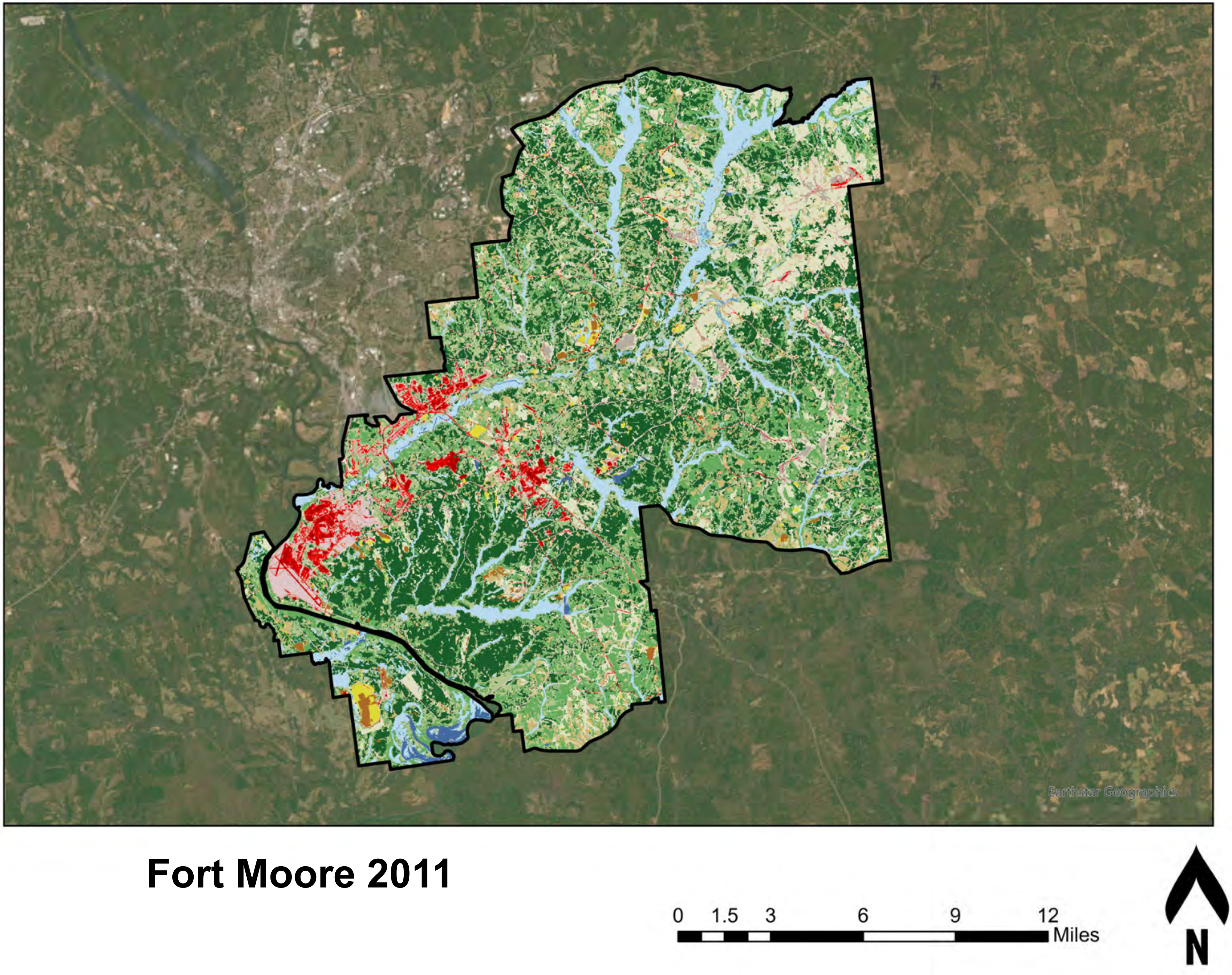

Fort Moore 2011

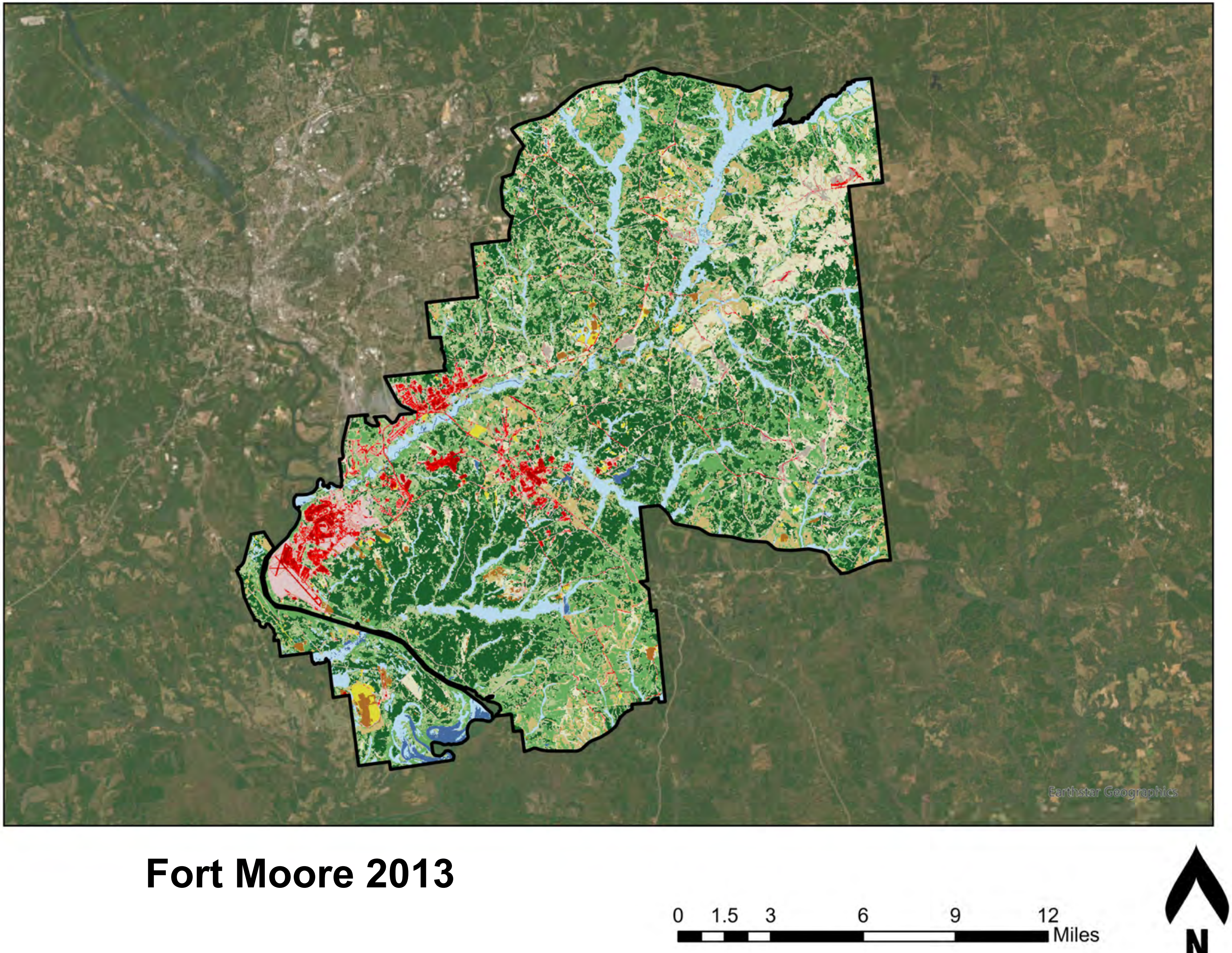

Fort Moore 2013

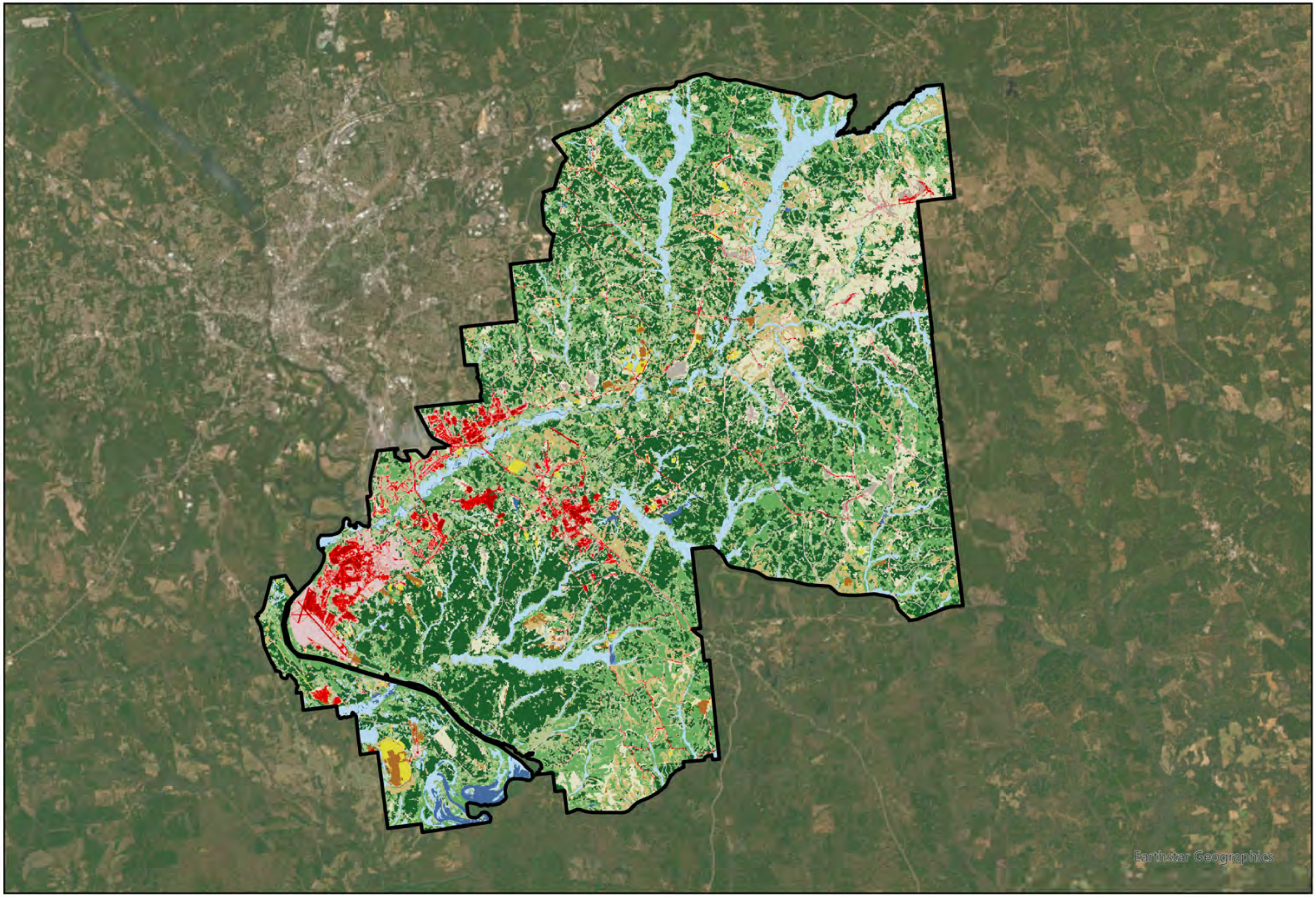

Fort Moore 2016

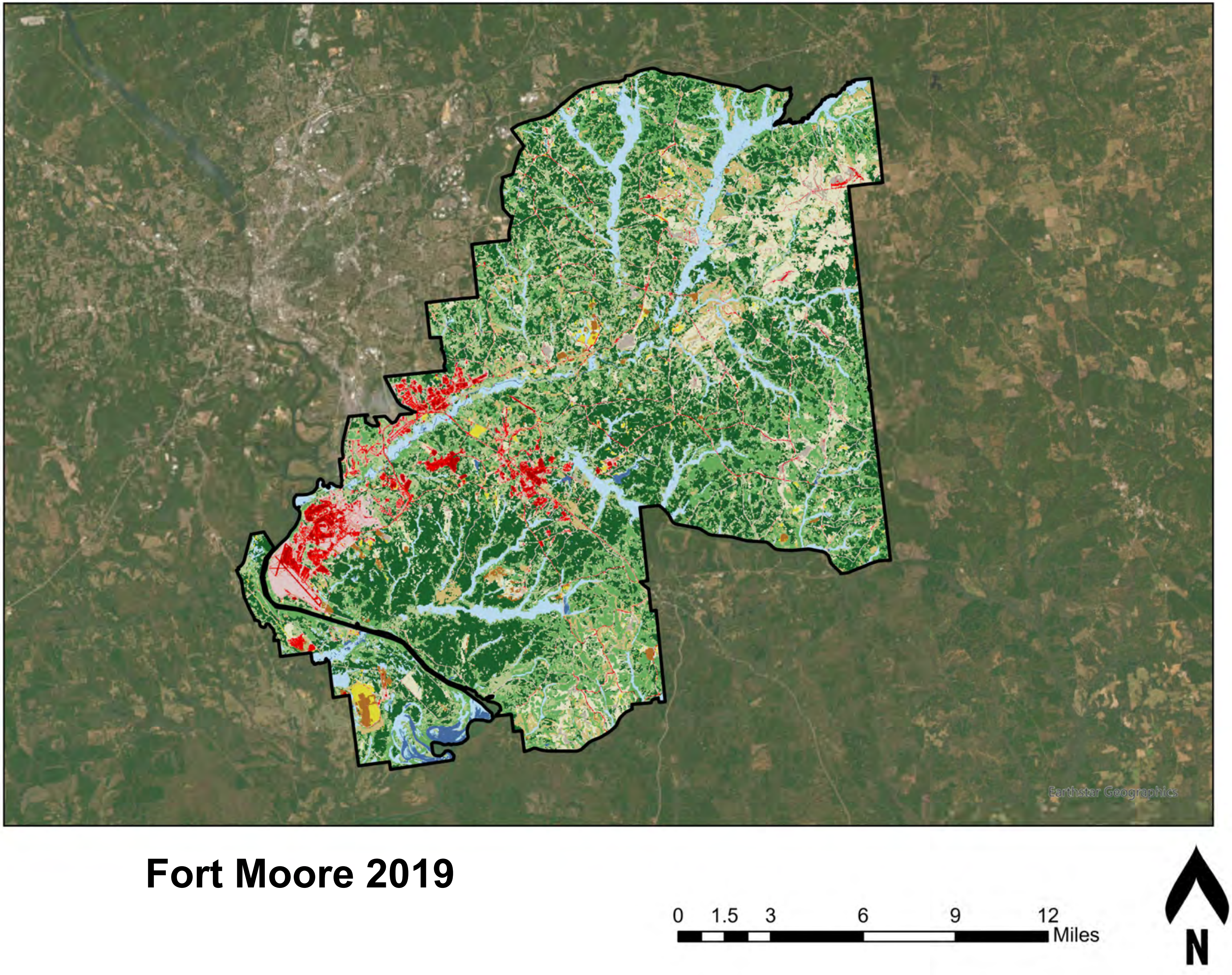

Fort Moore 2019

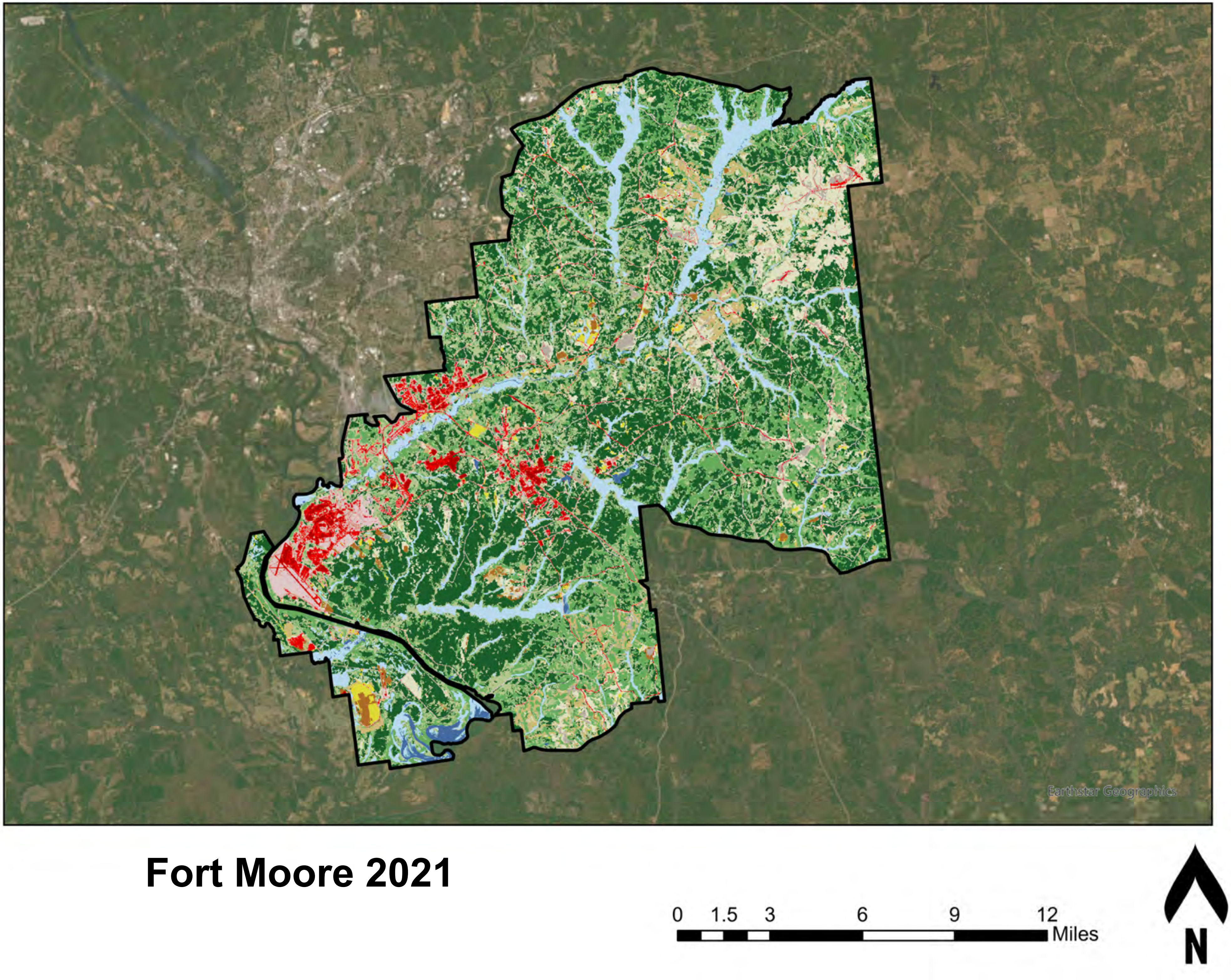

Fort Moore 2021

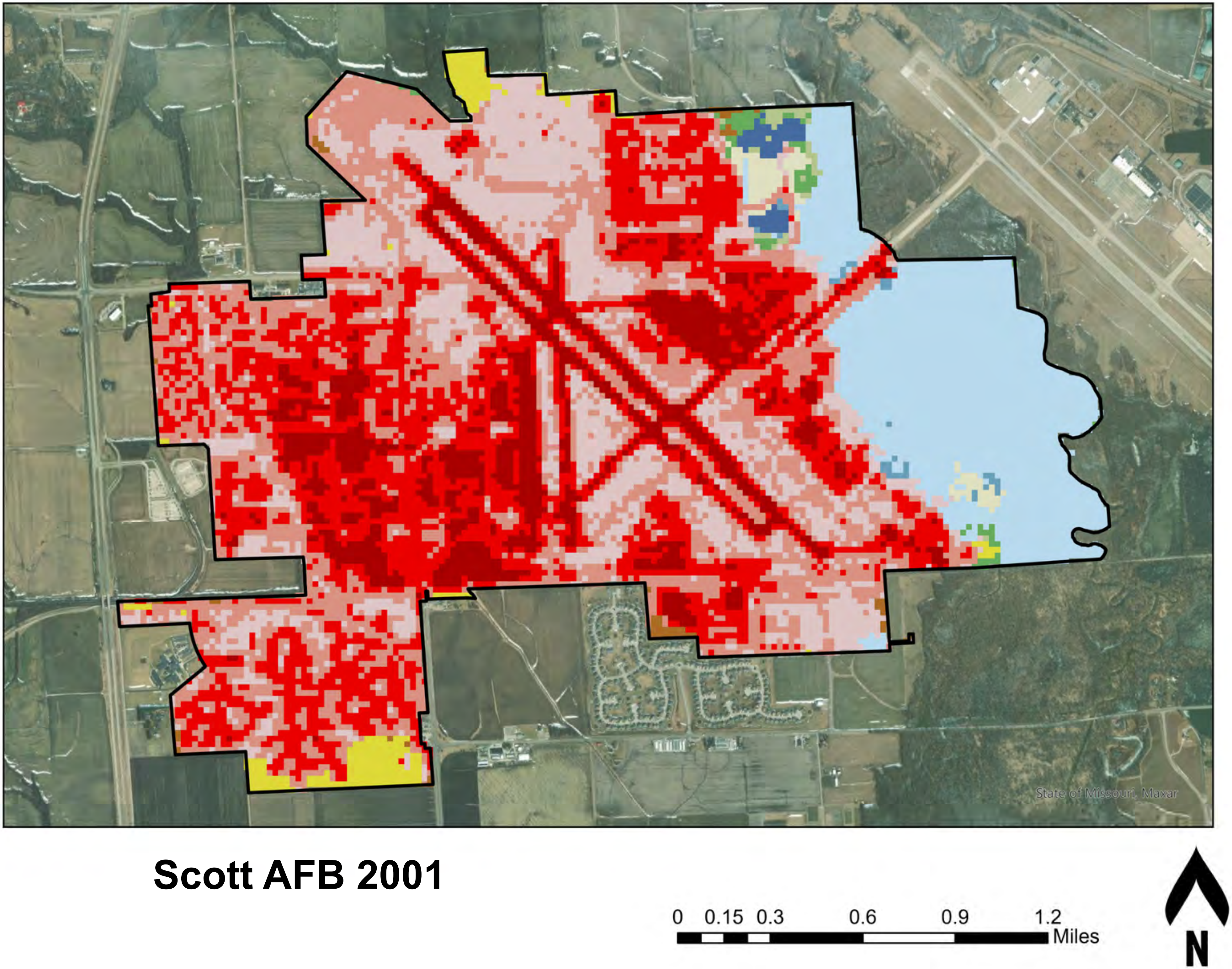

Scott AFB 2001

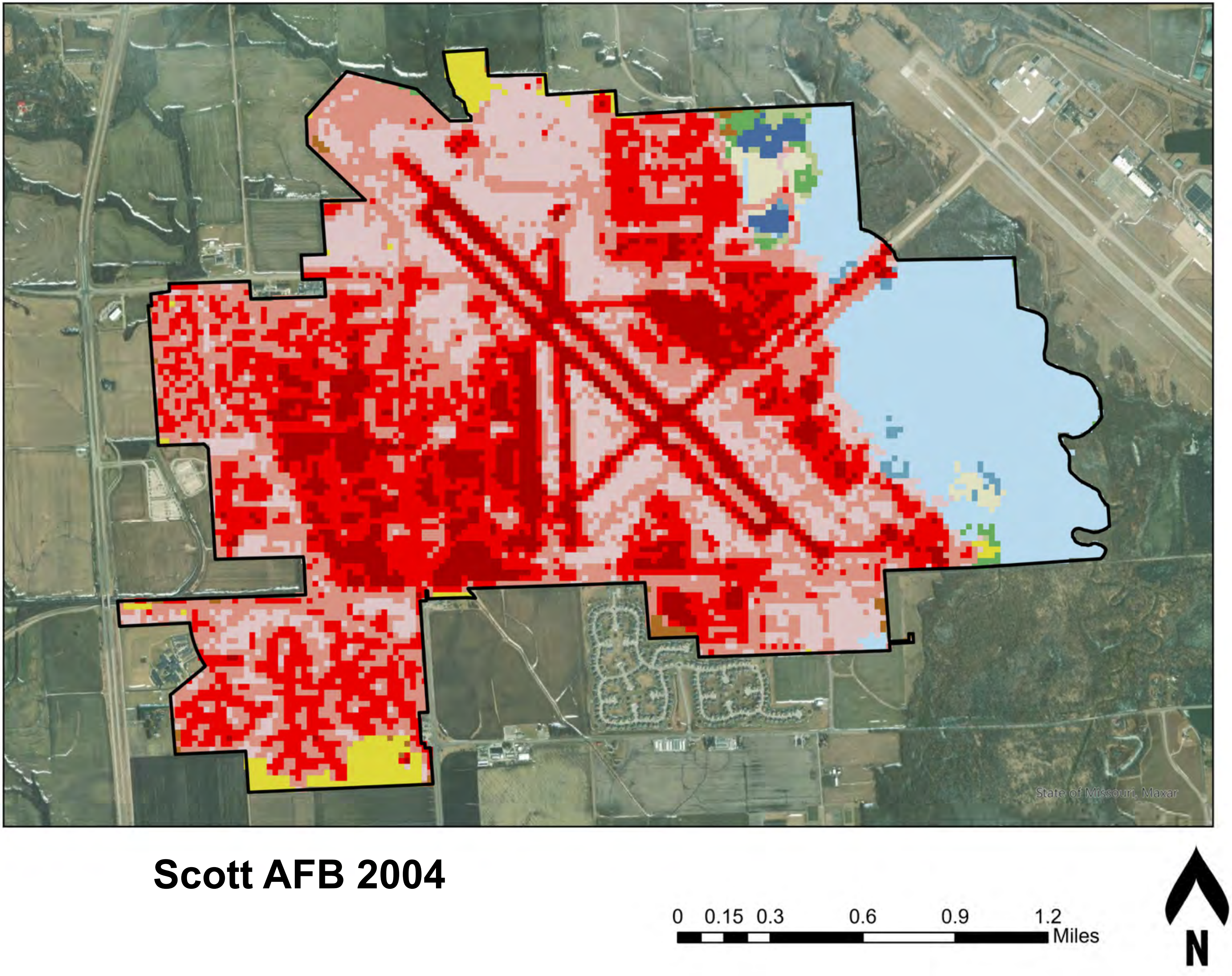

Scott AFB 2004

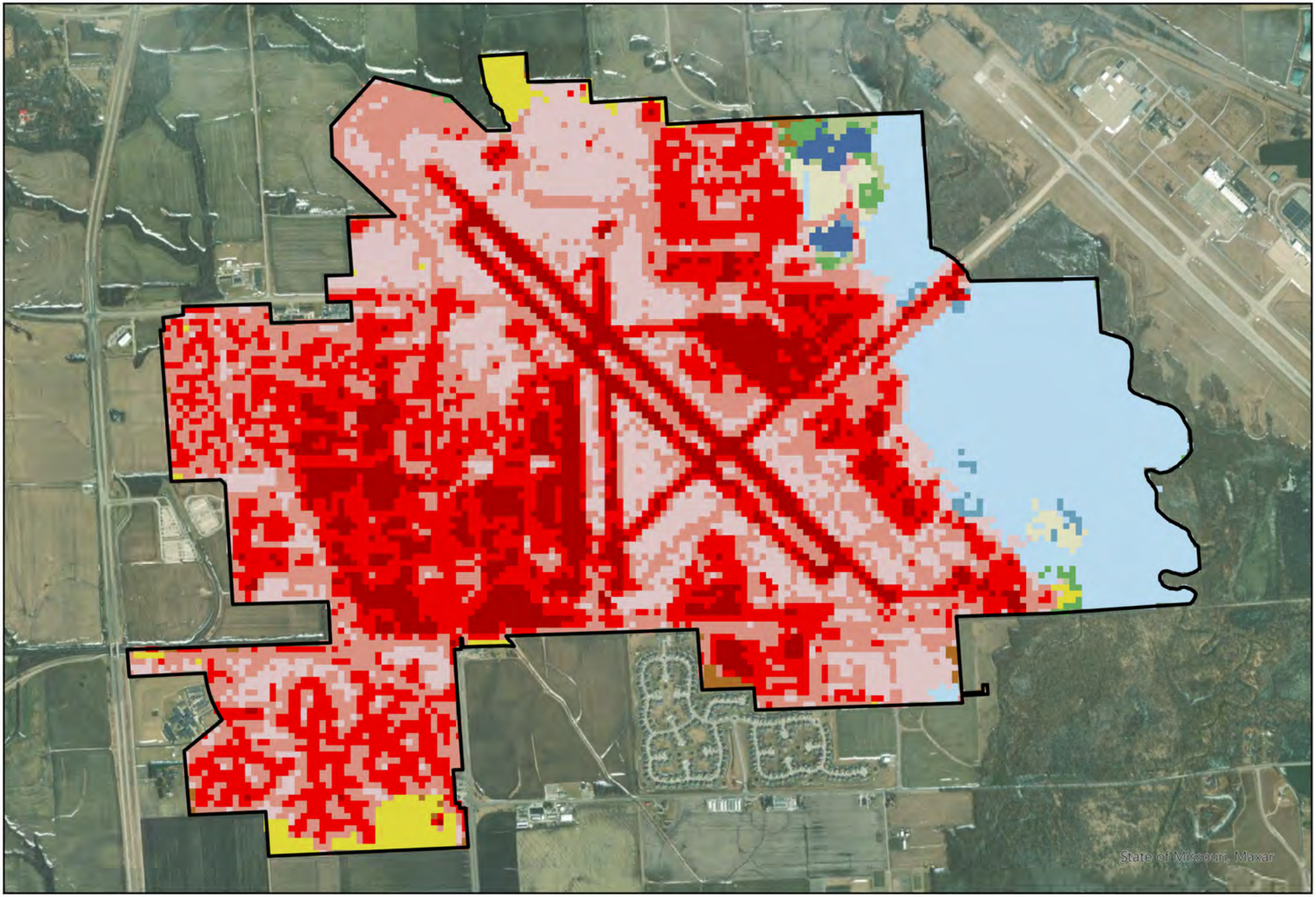

Scott AFB 2006

0 0.15 0.3 0.6 0.9 1.2
Miles

N

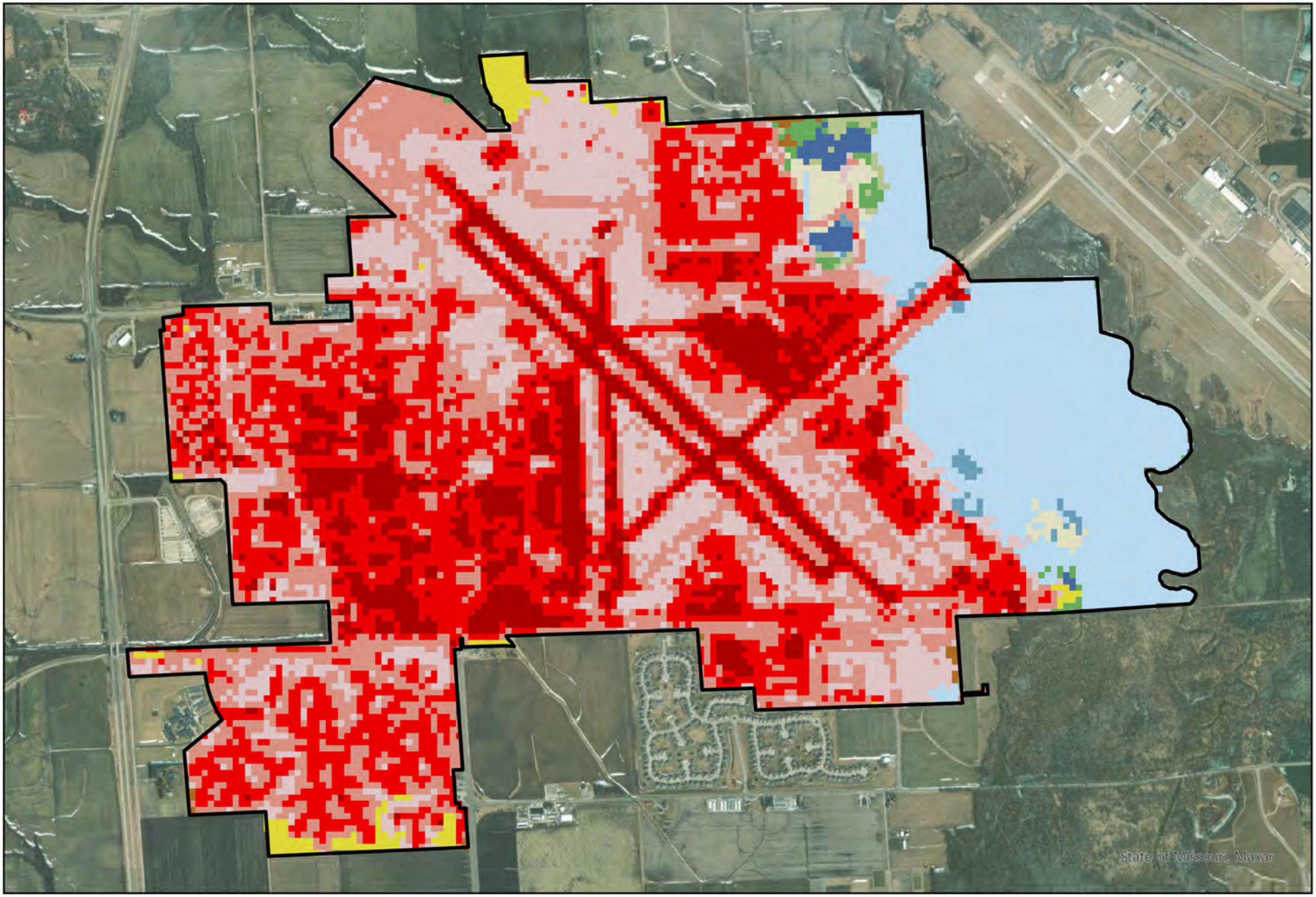

Scott AFB 2008

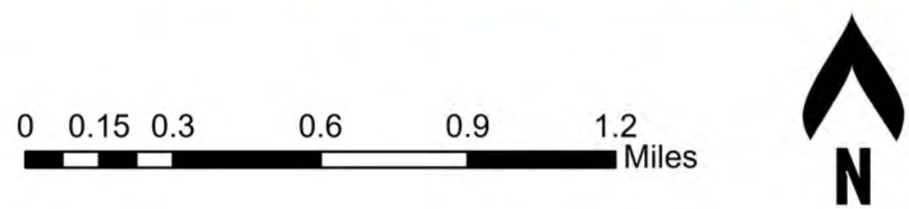

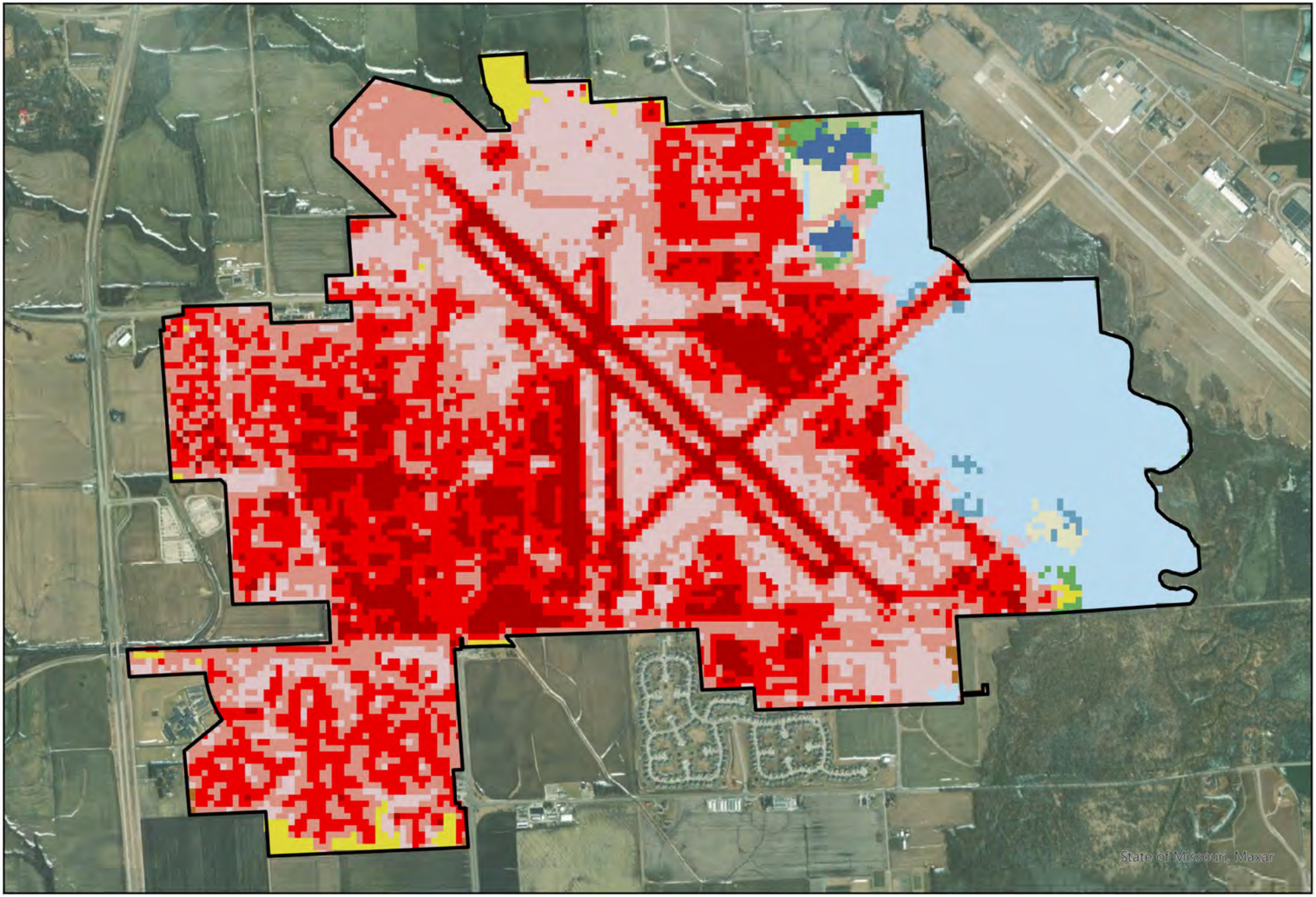

Scott AFB 2011

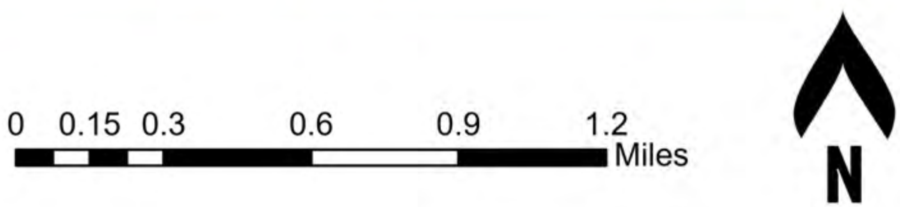

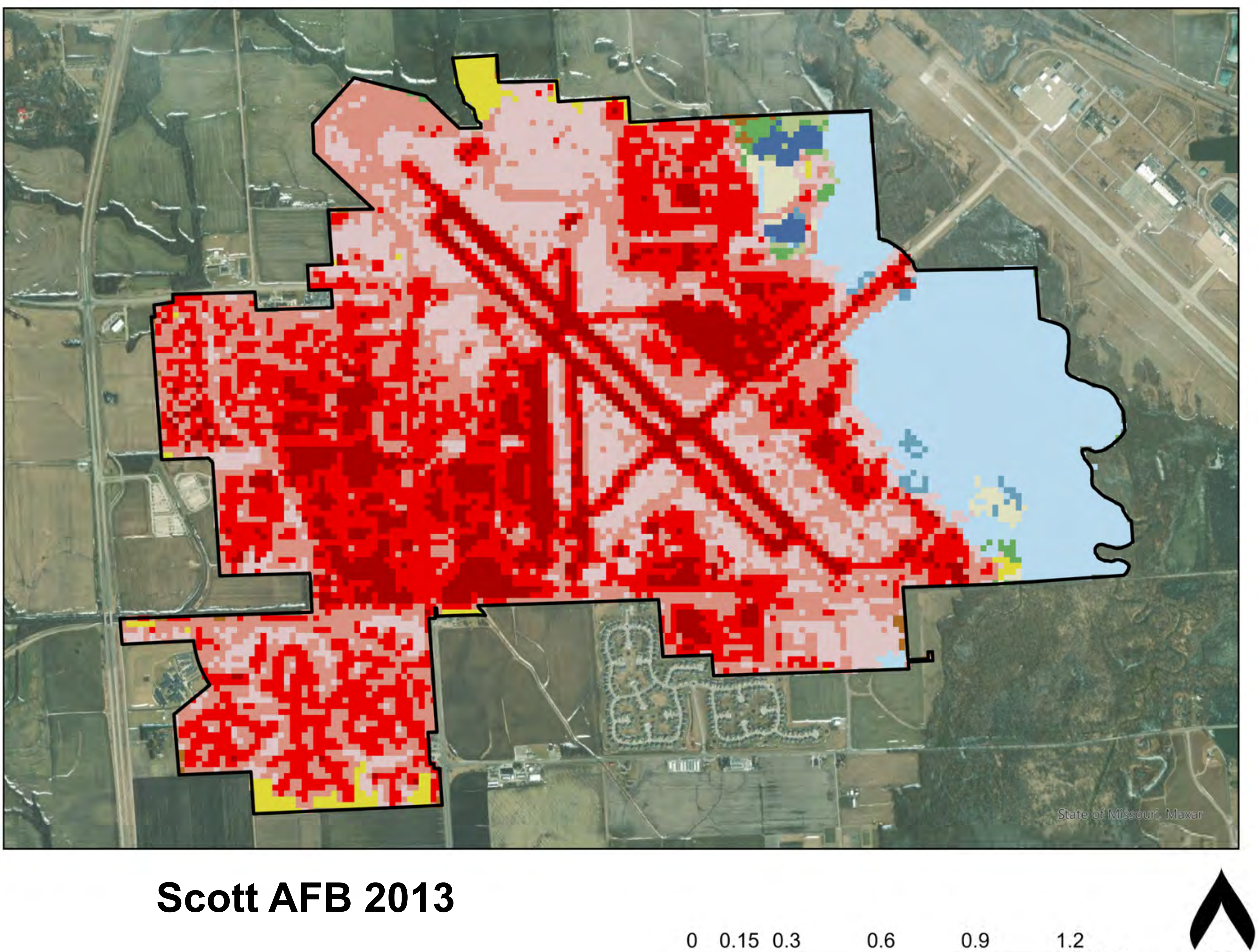

Scott AFB 2013

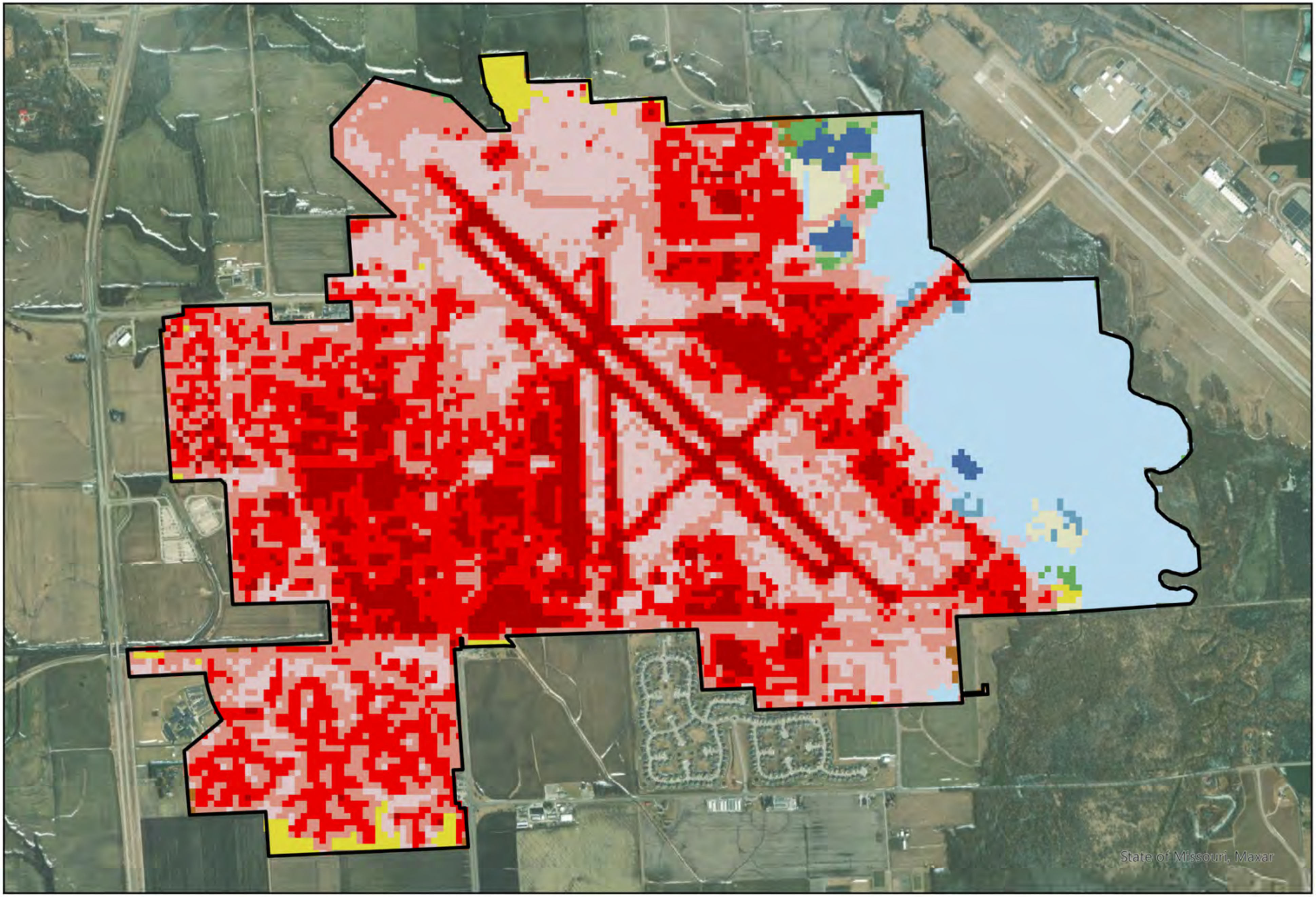

Scott AFB 2016

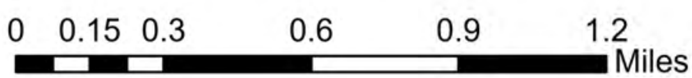

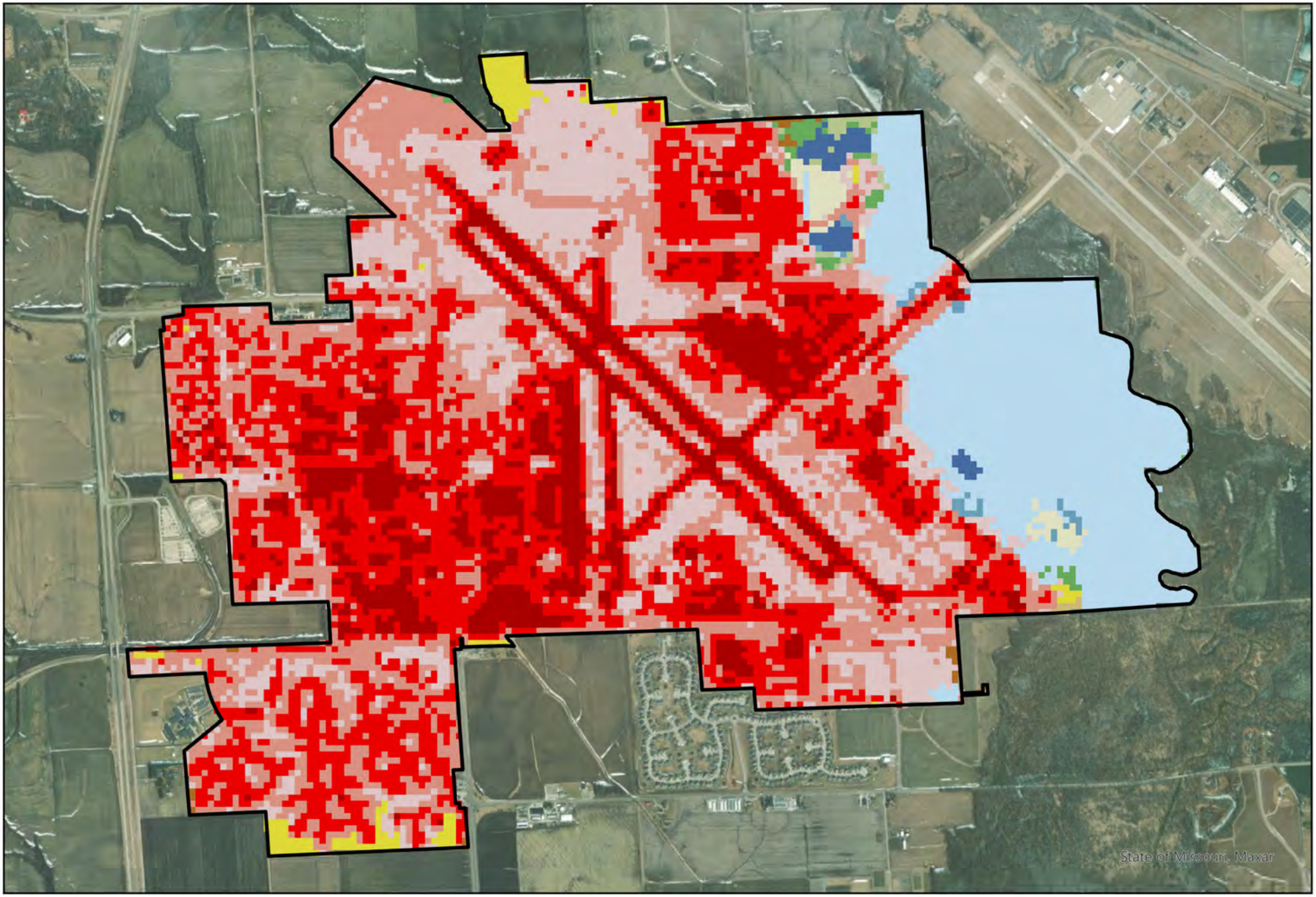

Scott AFB 2019

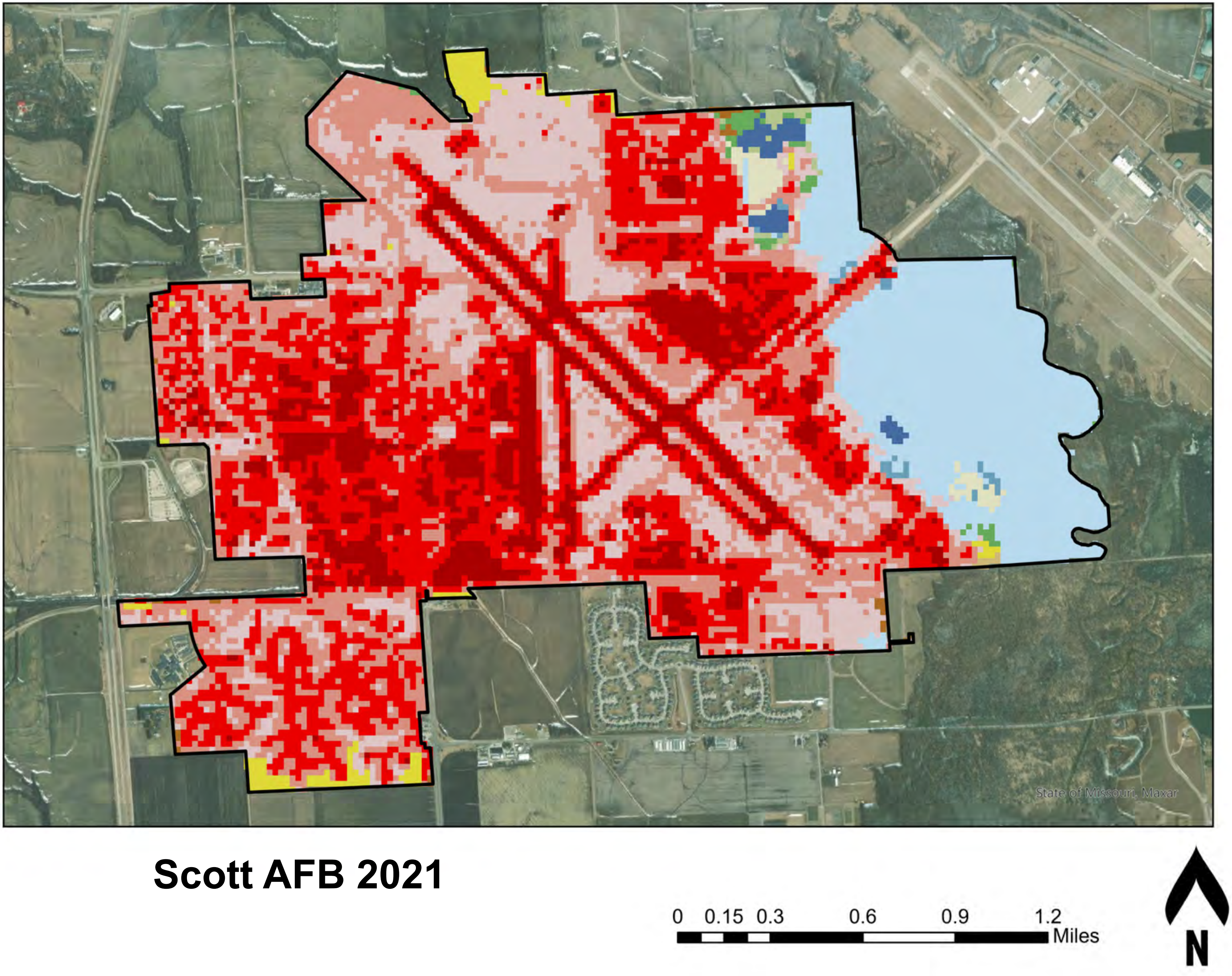

Scott AFB 2021

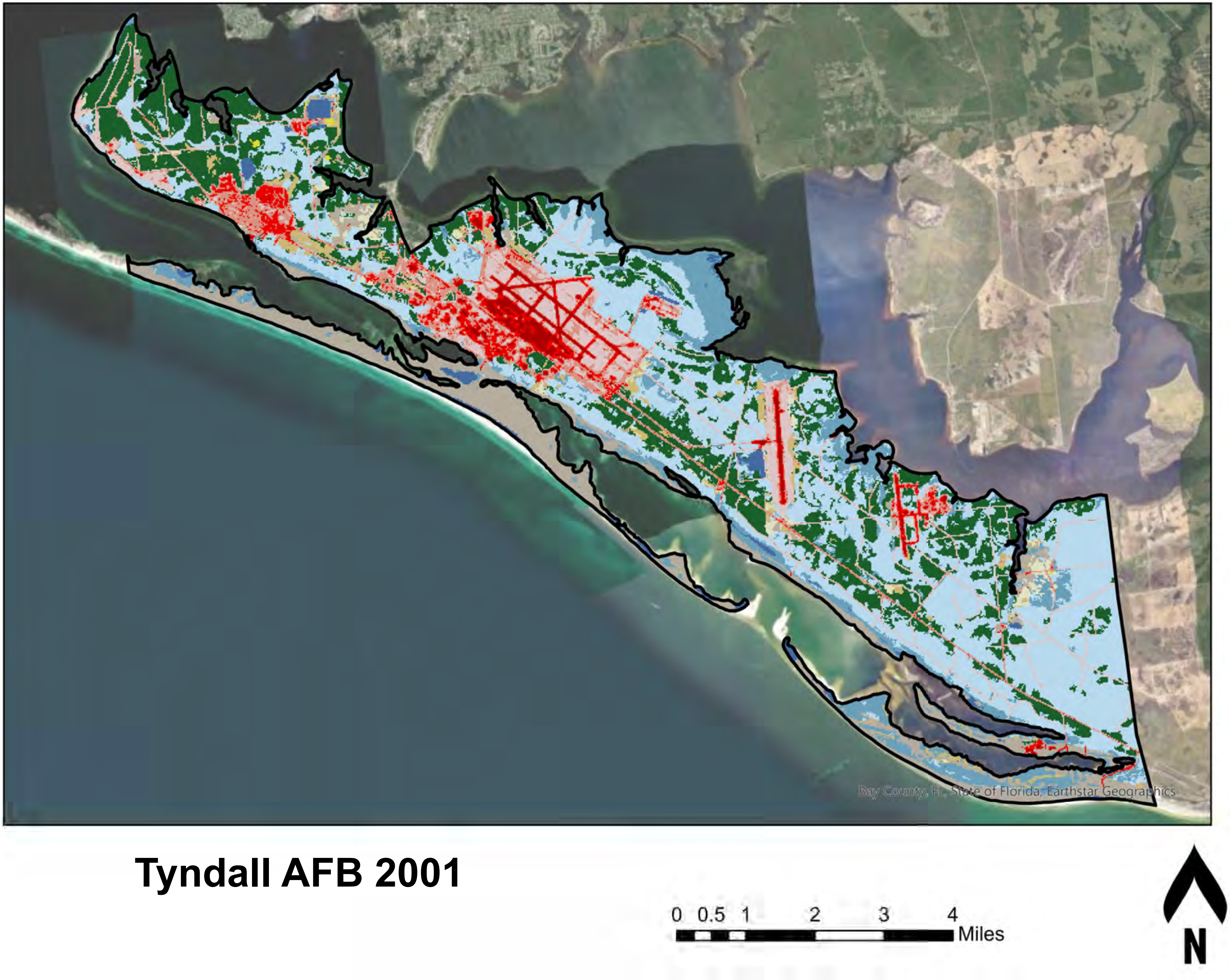

Tyndall AFB 2001

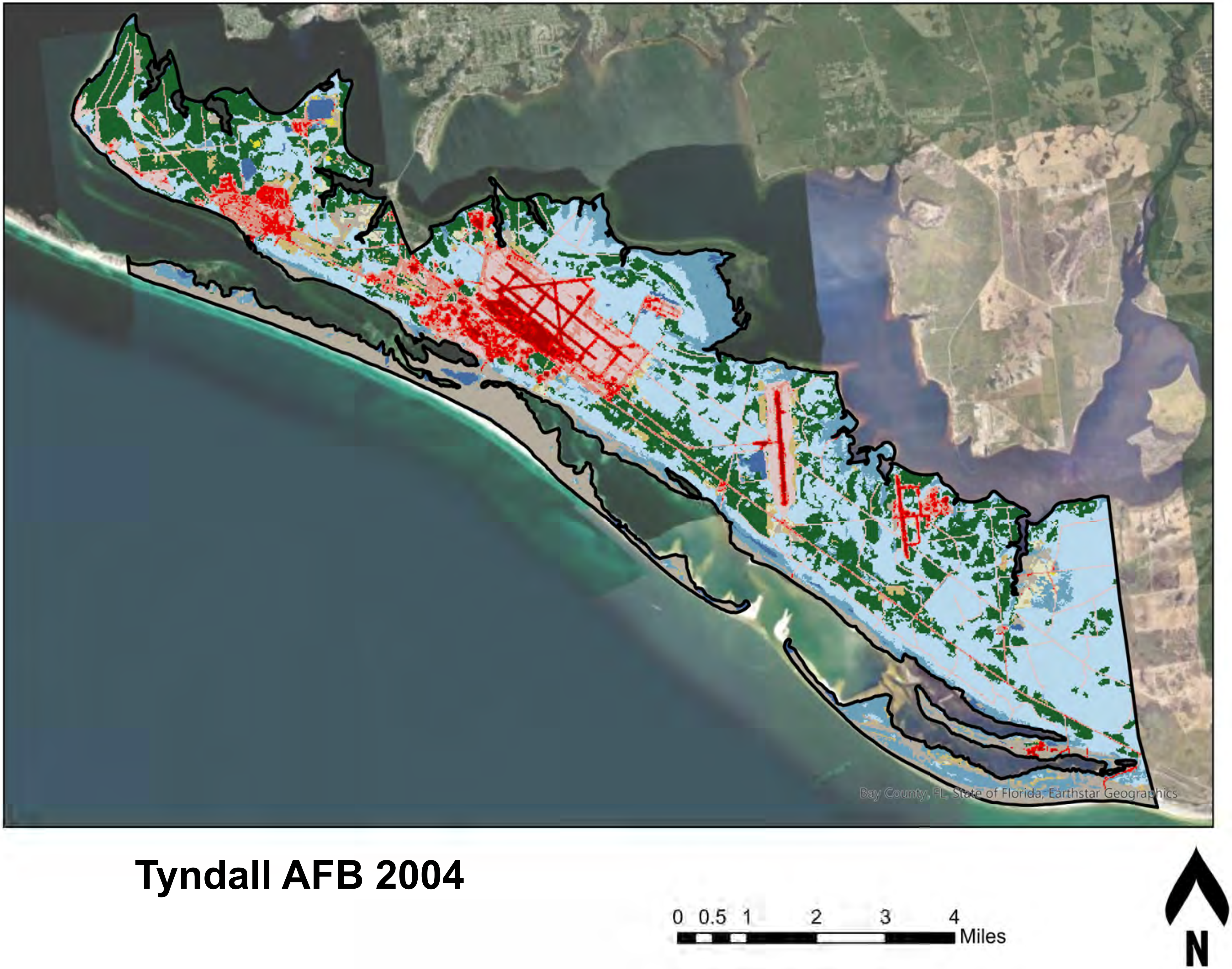

Tyndall AFB 2004

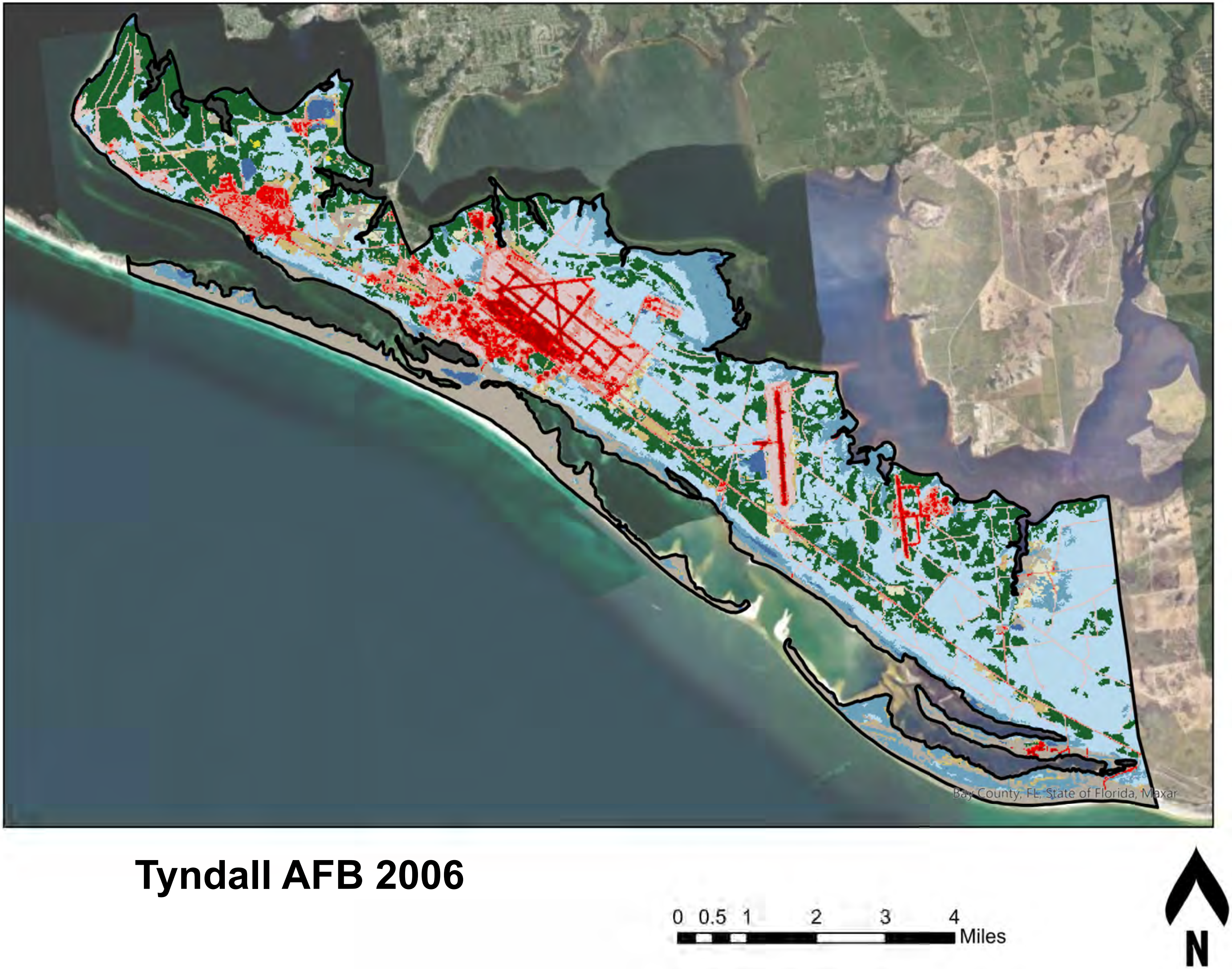

Tyndall AFB 2006

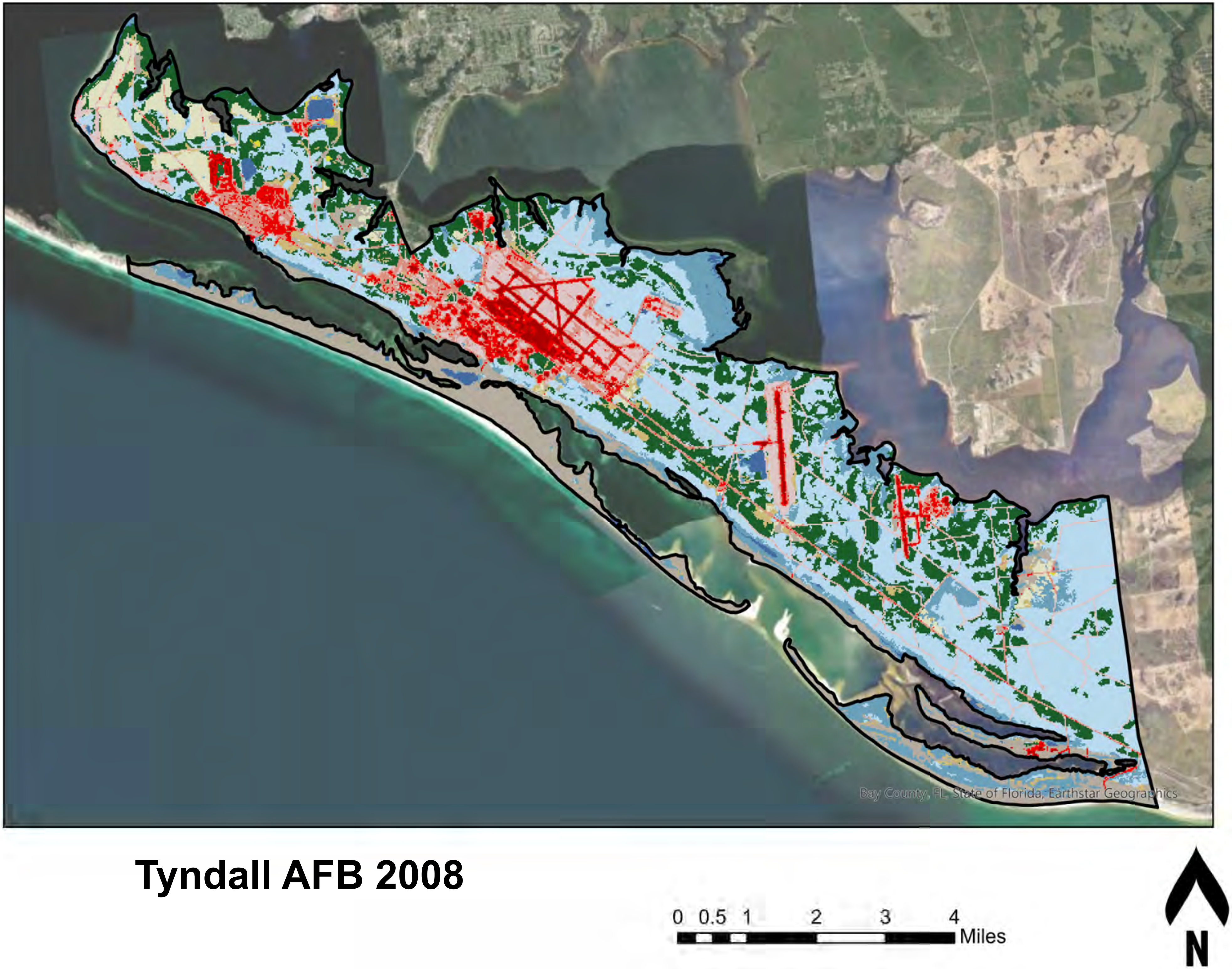

Tyndall AFB 2008

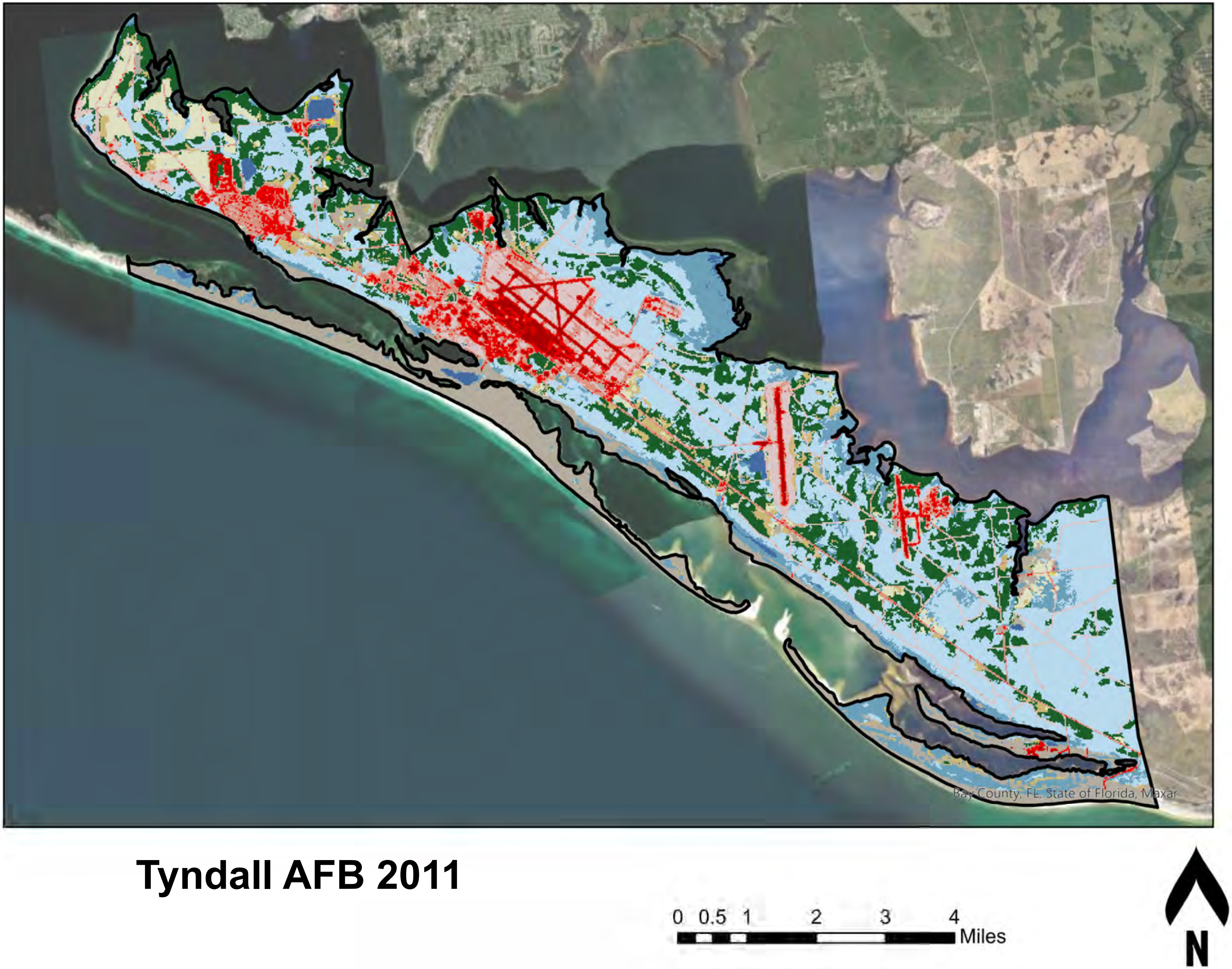

Tyndall AFB 2011

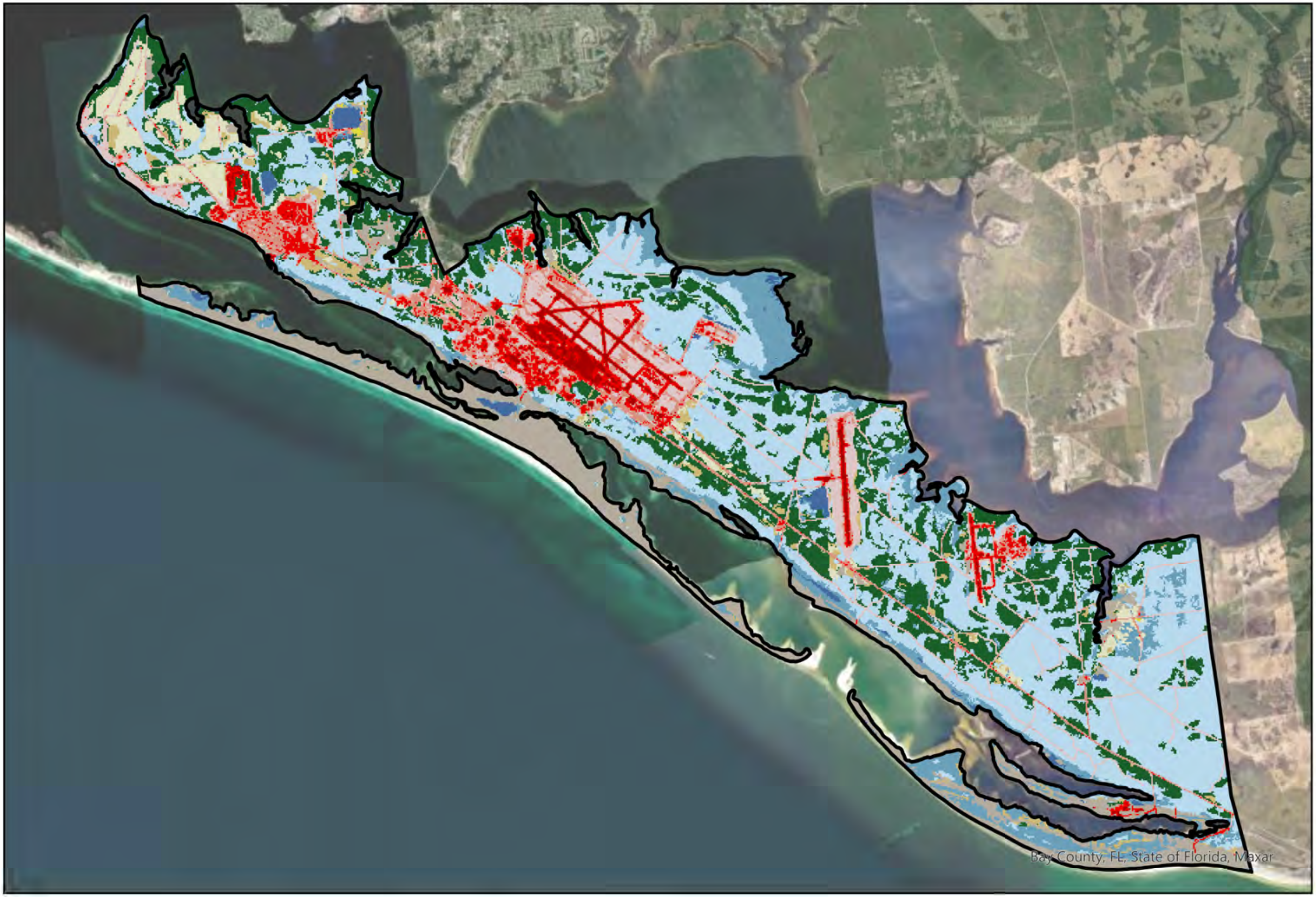

Tyndall AFB 2013

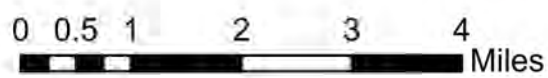

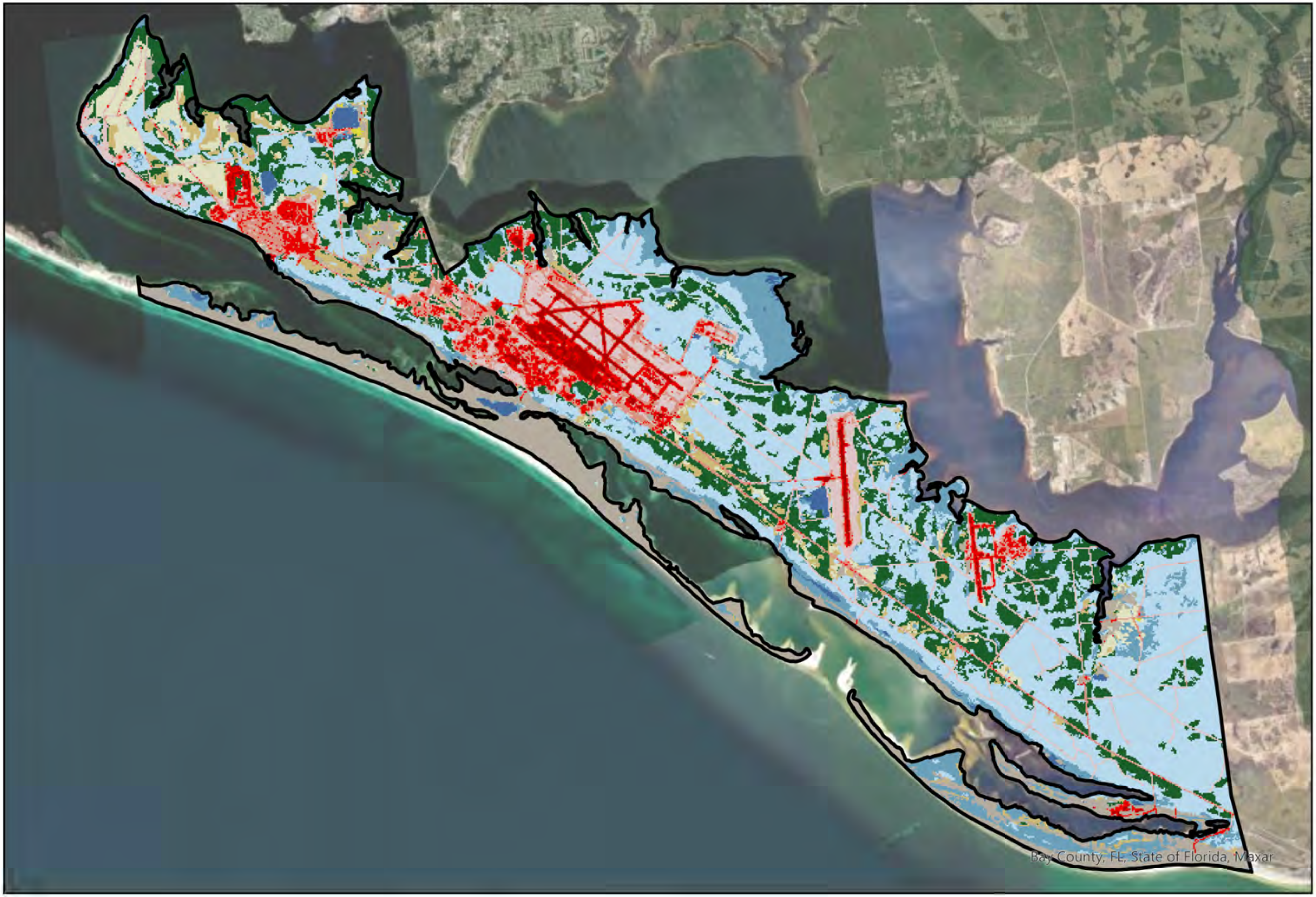

Tyndall AFB 2016

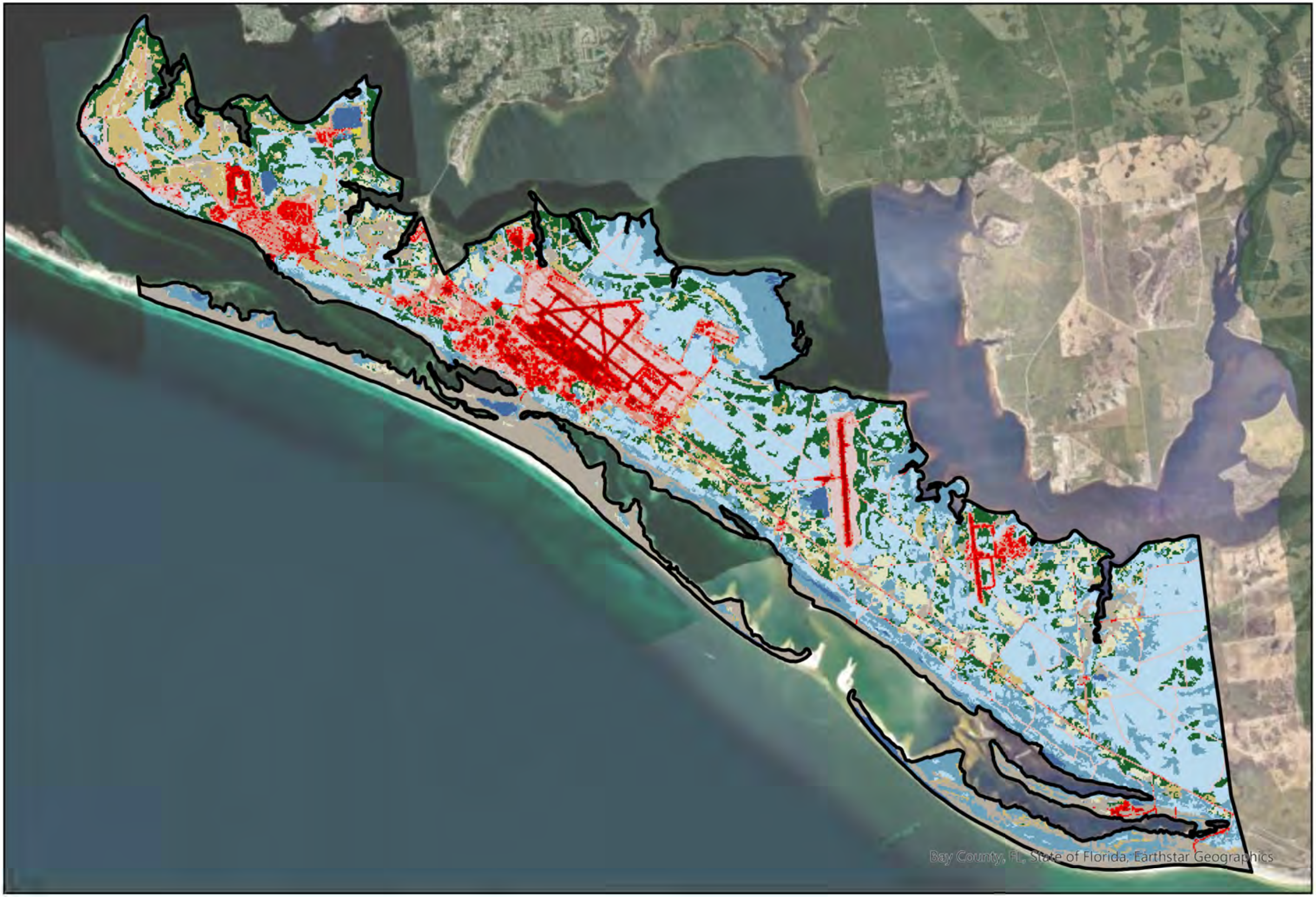

Tyndall AFB 2019

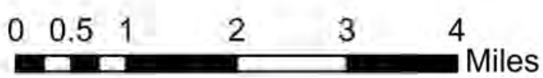

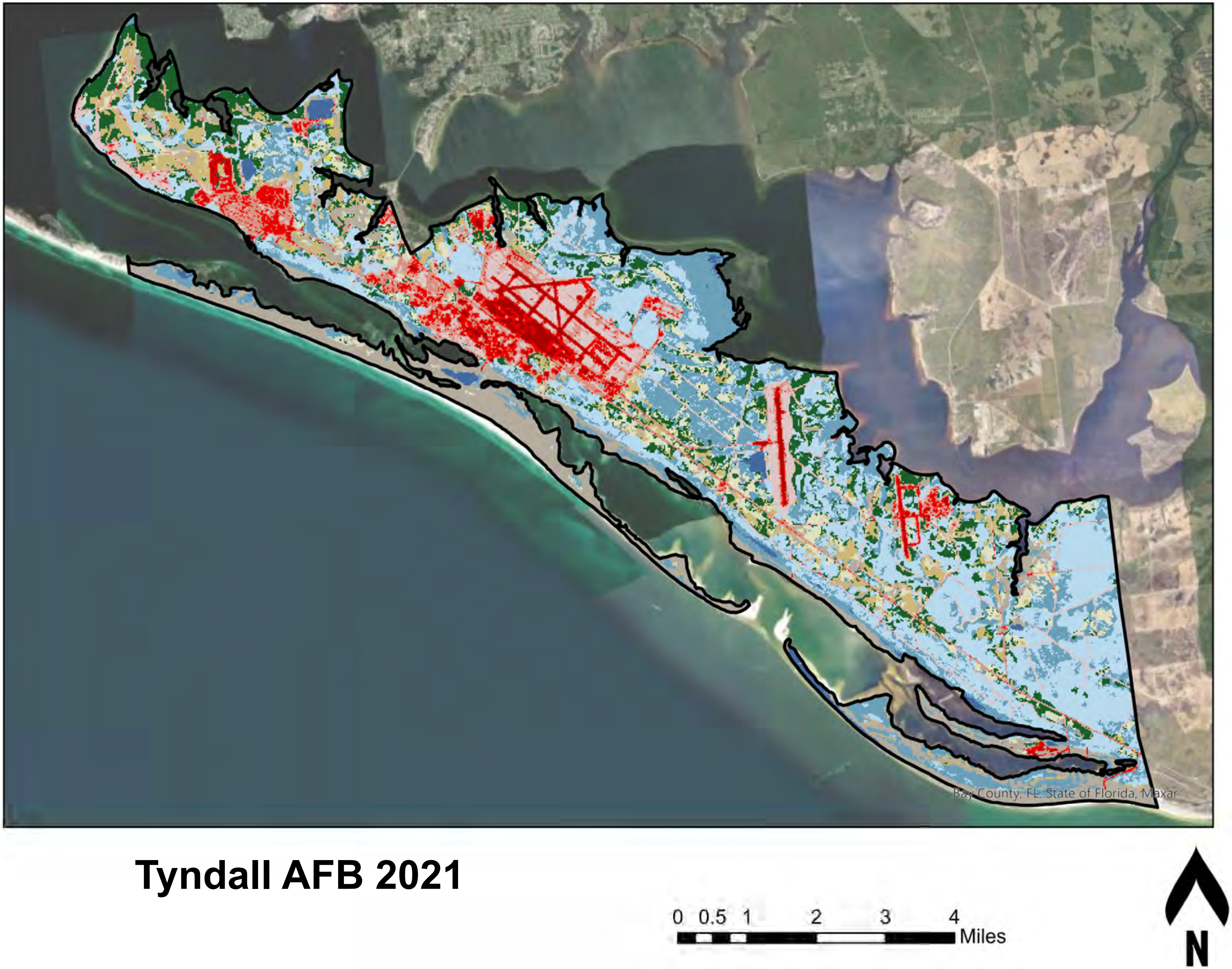

Tyndall AFB 2021

THE WATER INSTITUTE

1110 RIVER ROAD S., SUITE 200
BATON ROUGE, LA 70802

(225) 448-2813
WWW.THEWATERINSTITUTE.ORG